UNIVERSIDADE FEDERAL DO RIO GRANDE DO SUL - UFRGS

CENTRO ESTADUAL DE PESQUISAS EM SENSORIAMENTO REMOTO E METEOROLOGIA - CEPSRM

PROGRAMA DE PÓS-GRADUAÇÃO EM SENSORIAMENTO REMOTO

AVALIAÇÃO ANALÍTICA INTEGRADA DE PM_1 E NANOPARTÍCULAS ATMOSFÉRICAS

ISMAEL LUÍS SCHNEIDER

Porto Alegre – RS

2016

Ismael Luís Schneider

AVALIAÇÃO ANALÍTICA INTEGRADA DE PM_1 E NANOPARTÍCULAS ATMOSFÉRICAS

Orientadora: Profa. Dra. Elba Calesso Teixeira

Co-orientador: Prof. Dr. Luis Felipe Silva Oliveira

Banca Examinadora: Dra. Claudineia Brazil Saldanha (Faculdade Dom Bosco)

Dra. Dayana Milena Agudelo-Castañeda (Universidad de la Costa)

Dra. Silvia Beatriz Alves Rolim (PPGSR – UFRGS)

Tese submetida ao Programa de Pós-Graduação em Sensoriamento Remoto da Universidade Federal do Rio Grande do Sul, como requisito parcial para obtenção do grau de Doutor em Sensoriamento Remoto, linha de pesquisa Ciências Atmosféricas.

Porto Alegre – RS

2016

Aprovada pela Banca Examinadora em cumprimento ao requisito exigido para obtenção do Título de Doutor em Sensoriamento Remoto.

_____

Profa. Dra. Elba Calesso Teixeira (UFRGS/FEPAM)

Orientadora

_____

Prof. Dr. Luis Felipe Silva Oliveira

Coorientador

_____

Dra. Claudineia Brazil Saldanha

_____

Dra. Dayana Milena Agudelo-Castañeda

_____

Dra. Silvia Beatriz Alves Rolim

Aluno: Ismael Luís Schneider

Porto Alegre

2016

A toda minha família,

em especial aos meus pais

Ari e Ivanisse Schneider.

AGRADECIMENTOS

À Universidade Federal do Rio Grande do Sul (UFRGS) e ao Centro Estadual de Pesquisas em Sensoriamento Remoto e Meteorologia (CEPSRM) pelo ensino de qualidade e pela estrutura disponibilizada, sem a qual não seria possível a realização desta pesquisa.

À minha orientadora Profa. Dra. Elba Calesso Teixeira pelo auxílio e incentivo em todas as etapas do Doutorado e pela grandiosa dedicação nas orientações.

À Coordenação de Aperfeiçoamento de Pessoal de Nível Superior (CAPES), pela oportunidade de bolsa de pós-graduação, auxílio financeiro indispensável para a realização deste trabalho.

À Fundação Estadual de Proteção Ambiental do Estado do Rio Grande do Sul (FEPAM) por viabilizar a realização deste estudo através da disponibilização da infraestrutura necessária.

Aos funcionários do Programa Qualidade do Ar da FEPAM pelo apoio no desenvolvimento deste trabalho.

Aos Bolsistas de Iniciação Científica do Departamento de Pesquisas e Análises Laboratoriais da FEPAM pelo grande apoio e colaboração na pesquisa.

Aos colegas e professores do Programa de Pós-Graduação em Sensoriamento Remoto.

À minha família e amigos pela compreensão da minha ausência em alguns momentos, bem como pelo incentivo para a realização do Doutorado.

Enfim, a todos que de alguma maneira me ajudaram durante a realização deste trabalho.

Resumo

As nanopartículas atmosféricas podem causar diversos efeitos à saúde já que durante a inalação podem penetrar mais profundamente no sistema respiratório humano, atingindo inclusive os alvéolos e a corrente sanguínea, e, desta forma, aumentar os efeitos toxicológicos prejudiciais. Estas partículas podem ser emitidas diretamente para a atmosfera (partículas primárias) ou ser formadas por conversão gás-partícula (partículas secundárias). Durante a última década, estudos têm sido realizados para uma melhor compreensão sobre as concentrações de nanopartículas, avaliando sua emissão, formação, dispersão, exposição e os efeitos à saúde. No entanto, poucos estudos foram realizados no Brasil e desta forma ainda há pouca informação em relação a esta temática. A Região Metropolitana de Porto Alegre - RMPA (Brasil) possui forte tráfego veicular, cerca de 1,8 milhões de veículos e, apesar das fontes móveis impactarem fortemente a qualidade do ar nesta região e ser a principal fonte de nanopartículas, não há estudos que avaliem em profundidade os níveis deste importante poluente ambiental. Desta forma, no presente estudo foram avaliadas as concentrações de nanopartículas em diferentes pontos da RMPA. Além disso, foram avaliadas as concentrações ambientais de partículas <1 μm (MP_1) e metais associados, bem como foram identificadas e quantificadas as contribuições de fontes utilizando o modelo receptor *Positive Matrix Factorization* (PMF). Em adição, foi realizada uma análise das assinaturas espectrais no infravermelho de nitro-hidrocarbonetos policíclicos aromáticos (nitro-HPAs) associados ao MP_1. Este grupo de compostos orgânicos possui uma ampla distribuição no ambiente e, por possuírem propriedades mutagênicas e carcinogênicas, seus riscos ambientais foram calculados. Desta forma, considerando os resultados obtidos, verificou-se uma forte contribuição antropogênica dos poluentes avaliados na RMPA. Esta degradação da qualidade do ar está em geral associada ao tráfego veicular, especialmente no que se refere aos níveis de nanopartículas e nitro-HPAs associados ao MP_1. Além disso, as emissões industriais, a queima de carvão, biomassa e óleo combustível, bem como a queima de combustíveis veiculares apresentaram forte influência nos níveis de metais observados em MP_1.

Palavras-chave: Qualidade do Ar, Nanopartículas, Material Particulado Atmosférico, Espectrometria de Infravermelho, nitro-Hidrocarbonetos Policíclicos Aromáticos, Metais.

Abstract

Atmospheric nanoparticles can cause health effects, as during inhalation penetrate more deeply into the human respiratory system, including the alveoli and reaching the bloodstream, and thereby increase the damaging toxicological effects. These particles can be emitted directly to the atmosphere (primary particles) or be formed by gas-to-particle conversion (secondary particle). Over the last decade, studies have been conducted for a better understanding of the nanoparticles, assessing the emission, formation, dispersion, exposure and health effects. However, few studies have been conducted in Brazil and thus there is little information regarding this subject. The Metropolitan Area of Porto Alegre - MAPA (Brazil) has a strong vehicular traffic, about 1.8 million vehicles and, despite mobile sources strongly impact the air quality in this region and be the main source of nanoparticles, there are no studies that evaluate in depth the levels of this important environmental pollutant. Thus, considering this knowledge gap, the present study evaluated the nanoparticle concentrations in different sites of the MAPA. In addition, environmental concentrations of particles <1 μm (MP_1) and associated metals were evaluated and the sources were identified and quantified using the receptor model Positive Matrix Factorization (PMF). In addition, an analysis of the infrared spectral signatures of nitro polycyclic aromatic hydrocarbons (nitro-PAHs) associated with PM_1 was performed. This group of organic compounds has a wide distribution in the environment, and because they have mutagenic and carcinogenic properties, their environmental risks were calculated. Thus, considering the obtained results, a strong anthropogenic contribution of the evaluated pollutants in the MAPA was observed. This degradation of the air quality in general is associated with vehicular traffic, especially regarding the levels of nanoparticles and nitro-PAHs associated with PM_1. In addition, industrial emissions, coal, biomass and fuel oil combustion, as well as vehicle fuels combustion had a strong influence on the metal levels observed in PM_1.

Keywords: Air Quality, Nanoparticles, Atmospheric Particulate Matter, Infrared Spectrometry, nitro-Polycyclic Aromatic Hydrocarbons, Metals.

APRESENTAÇÃO DA ESTRUTURA DA TESE

Esta Tese de Doutorado, intitulada "**AVALIAÇÃO ANALÍTICA INTEGRADA DE PM1 E NANOPARTÍCULAS ATMOSFÉRICAS"**, foi desenvolvida entre Junho de 2012 e Junho de 2016 no Centro Estadual de Pesquisas em Sensoriamento Remoto e Meteorologia da Universidade Federal do Rio Grande do Sul (UFRGS) em colaboração com a Fundação Estadual de Proteção Ambiental do Rio Grande do Sul Henrique Luiz Roessler - RS (FEPAM-RS).

A Tese está distribuída da seguinte maneira:

- Capítulo I: Aspectos introdutórios

Trata sobre os aspectos introdutórios, objetivos, revisão bibliográfica, materiais e métodos.

- Capítulo II, III, IV, V: Resultados na forma de artigos científicos publicados ou submetidos para publicação.

Capítulo II. Artigo publicado intitulado "Atmospheric particle number concentration and size distribution in a traffic-impacted area", autores: Schneider, I. L.; Teixeira, E. C.; Silva, L. F. O.; Wiegand, F.. Publicado na Atmospheric Pollution Research, 6, 877-885, 2015.

Capítulo III. Artigo publicado intitulado "FTIR analysis and evaluation of carcinogenic and mutagenic risks of nitro-polycyclic aromatic hydrocarbons in $PM_{1.0}$", autores: Schneider, I. L.; Teixeira, E. C.; Agudelo-Castañeda, D. M.; Silva E Silva, G.; Balzaretti, N.; Braga, M. F.; Oliveira, L. F. S.. Publicado na Science of the Total Environment, 541, 1151-1160, 2016.

Capítulo IV. Artigo intitulado "Chemical characterization and source apportionment of PM1 in a metropolitan area of Brazil", autores: Schneider, I. L.; Teixeira, E. C.; Silva, L. F. O.; Agudelo-Castañeda, D. M.; Landim, A.A.; Querol, X.. Submetido a Atmospheric Environment, *under review*. As correções solicitadas pelos revisores já foram submetidos.

Capítulo V. Resumo de Congresso intitulado "Nanoparticles assessment in Sapiranga city, Southern Brazil", autores: Schneider, I. L.; Teixeira, E. C.; Oliveira, L. F. S.; Vargas, M. D.; Krecl, P.; Gidhagen, L. Publicado nos Anais do 10th International Conference on Air Quality - Science and Application, 2016.

- Capitulo VI: Considerações finais

Apresenta as conclusões, considerações finais e recomendações para futuras pesquisas.

- ANEXOS:

Resumos de artigos publicados em periódicos como co-autor ou trabalhos publicados em anais de eventos.

LISTA DE FIGURAS

SUMÁRIO

1. ASPECTOS INTRODUTÓRIOS

A poluição atmosférica é um dos problemas ambientais de maior preocupação e, devido à crescente urbanização, provavelmente vai se tornar cada vez mais importante no futuro (Dall'Osto *et al.*, 2012). A qualidade do ar, tipicamente expressa em termos de poluentes que causam efeitos adversos à saúde humana e ao meio ambiente, inclui poluentes gasosos (ozônio, óxidos de nitrogênio, monóxido de carbono, entre outros) e material particulado atmosférico. Este material particulado é um dos poluentes-chave em ambientes urbanos, e vários estudos tem focado nas frações com menores tamanhos de partículas, especialmente as nanopartículas.

As nanopartículas atmosféricas, especialmente aquelas <300 nm, podem ter origem natural ou serem resultantes de atividades antropogênicas, principalmente originadas por emissões veiculares (Kumar *et al.*, 2010). As partículas emitidas por motores diesel possuem tamanho de 20-130 nm (Kittelson, 1998; Morawska *et al.*, 1998a; Harris e Maricq, 2001; Ristovski *et al.*, 2006) e por motores a gasolina tamanho de 20-60 nm (Harris e Maricq, 2001; Ristovski *et al.*, 2006). Desta forma, em áreas urbanas, o continuo crescimento de fontes móveis, especialmente veículos movidos a gasolina e diesel, tem acarretado preocupação devido seu grande impacto na qualidade do ar (Colvile *et al.*, 2001; Shi *et al.*, 2001; Wahlin *et al.*, 2001; Johansson *et al.*, 2007; Keogh *et al.*, 2009; Teixeira *et al.*, 2011).

Além disso, estas nanopartículas podem ser muito prejudiciais para o organismo humano, pois durante a inalação possuem a capacidade de penetrarem mais profundamente no sistema respiratório humano e, desta forma, aumentam os seus efeitos toxicológicos prejudiciais. Por apresentarem uma maior área superficial por unidade de volume do que as partículas maiores observa-se um aumento na capacidade de compostos orgânicos se adsorverem, alguns dos quais são potencialmente cancerígenos (USEPA, 2002; Donaldson *et al.*, 2005; Kumar *et al.*, 2010). Vários estudos tem apontado a associação destas partículas com o aumento de

doenças respiratórias e cardiovasculares, tanto agudas como crônicas, bem como de mortalidade (Katsouyanni *et al.*, 2001; Peters *et al.*, 2001; Hoek *et al.*, 2002; Pekkanen *et al.*, 2002; Pope *et al.*, 2002).

Portanto, o efeito à saúde humana é um dos motivos pelo qual vários autores têm reportado a importância de controlar as nanopartículas atmosféricas, já que a estas partículas têm sido atribuídos diversos efeitos adversos (Murr e Garza, 2009). Além deste efeito, a visibilidade urbana (Horvath, 1994) e a influência climática (IPCC, 2007; Strawa *et al.*, 2010), bem como a sua influência sobre a química da atmosfera, através da sua composição e reatividade química (Kulmala *et al.*, 2004), são alterações provocadas pelas nanopartículas.

A atual legislação sobre a qualidade do ar concentra-se apenas sobre a massa total de MP_{10} e $MP_{2,5}$ (a massa das partículas com um diâmetro aerodinâmico inferior a 10 ou 2,5 μm, respectivamente), e relativamente pouca atenção tem sido dada a outros parâmetros, tais como a composição química ou a concentração em número de nanopartículas (Pey *et al.*, 2008). Para resolver este problema, foi criado o UNECE-GRPE *Particulate Measurement Program* (PMP), focado em criar uma regulamentação das emissões de nanopartículas dos veículos, propiciando uma ampla redução das emissões de partículas provenientes de fontes móveis (Mohr e Lehmann, 2003; Morawska *et al.*, 2008). Com base na recomendação do PMP, a Comissão Europeia adicionou um limite de número de partículas nos seus padrões de emissões Euro 5/6 para veículos comerciais ligeiros. No entanto, somente as partículas sólidas são contadas, com o material volátil sendo removido da amostra. Entretanto, quando consideradas normas que especifiquem padrões para qualidade do ar, as nanopartículas atmosféricas ainda não são reguladas para qualquer megalópole em desenvolvimento ou desenvolvida (Kumar *et al.*, 2011; Young *et al.*, 2012).

As nanopartículas atmosféricas, especialmente as oriundas de emissões veiculares, podem ser divididas em duas grandes categorias, dependendo da sua formação. Elas podem ser formadas no motor ou no tubo de escape (partículas primárias) ou ser formadas na atmosfera, através do processo de conversão gás-partícula (partículas secundárias).

As partículas primárias, emitidas diretamente a partir do motor do veículo, são principalmente aglomerados de material carbonoso de fase sólida variando em tamanho de 30 a 500 nm. Podem conter cinzas metálicas e hidrocarbonetos adsorvidos ou condensados e compostos de enxofre, e, em geral, são derivadas de aditivos de óleo de lubrificação e de desgaste do motor (Morawska *et al.*, 2008).

As partículas secundárias se formam à medida que os gases quentes de escape são expelidos a partir do tubo de escape de um veículo, arrefecem e condensam para formar um grande número de partículas muito pequenas no ar. Elas são voláteis e consistem principalmente de hidrocarbonetos e de ácido sulfúrico hidratado. Geralmente com tamanho abaixo de 30 nm, compondo o modo nucleação, são observadas próximas de rodovias com intenso tráfego veicular, especialmente com grande fração de veículos pesados a diesel (Charron e Harrison, 2003; Sturm *et al.*, 2003; Gramotnev e Ristovski, 2004; Zhu *et al.*, 2004; Rosenbohmet *et al.*, 2005; Westerdahl *et al.*, 2005; Ntziachristos *et al.*, 2007).

1.1. Concentrações em número de partículas

As concentrações de nanopartículas são muito afetadas pelas condições ambientais e dependem fortemente das intensidades de emissão, proximidade das fontes e condições meteorológicas. Em geral, as maiores concentrações em número ocorrem em áreas com alto tráfego veicular e regiões urbanas, onde também se observa o maior efeito sobre a saúde humana (Buseck e Adachi, 2008). Nas áreas rurais, as fontes naturais dominam, embora fontes antropogênicas também possam ser significativas (Seinfeld e Pandis 2006).

No estudo de Morawska *et al.* (2008) são apresentados os níveis de concentração de partículas para oito diferentes categorias, de acordo com o local de medição. A Figura 1 apresenta uma comparação das concentrações médias para estes diferentes ambientes. As maiores concentrações são observadas em túneis e rodovias, enquanto as menores concentrações são apontadas para áreas rurais e regiões de *background* limpo.

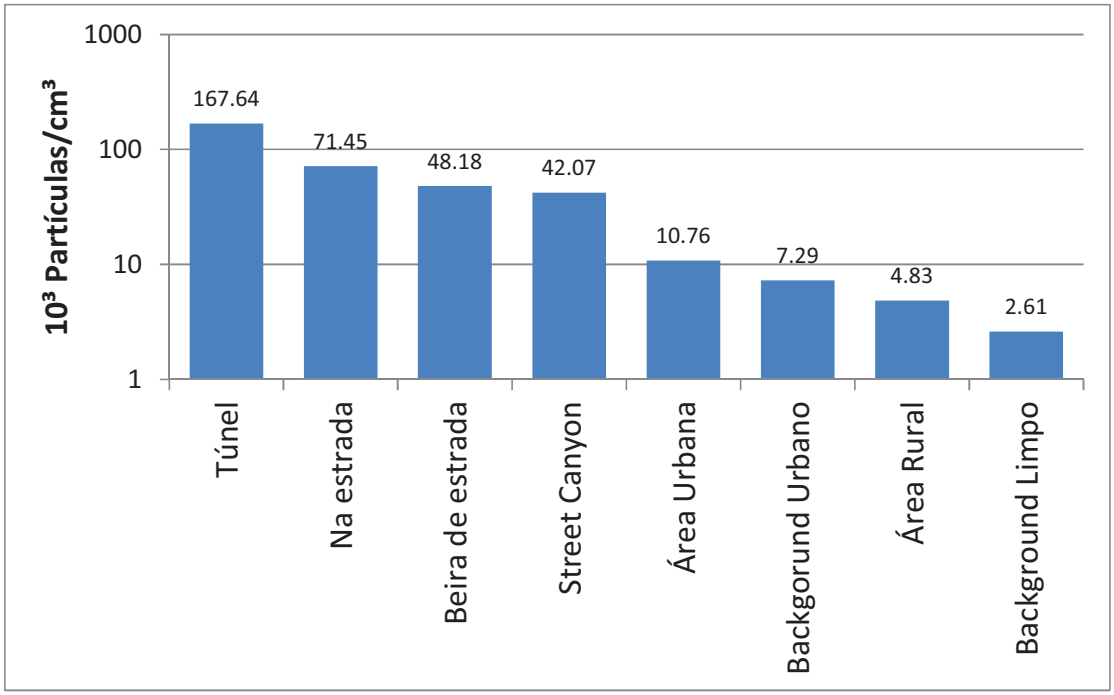

Figura 1. Concentrações médias do número de partículas para diferentes ambientes. (FONTE: Adaptado de Morawska et al. (2008))

Kumar *et al.* (2014) analisaram dados da concentração total de nanopartículas medidas em 40 diferentes locais em ambientes de beira de estrada em várias cidades no mundo. Na Tabela 1 é possível observar as concentrações em alguns dos locais apontados. Neste estudo destacam que as concentrações médias para cidades europeias são inferiores às cidades asiáticas, com médias de 3.15 ± 1.60 x 10^4 partículas/cm^3 e 11.7 ± 10.4 x 10^4 partículas/cm^3, respectivamente. Além disso, o estudo aponta, em termos absolutos, grandes diferenças na comparação de dados médios da concentração de nanopartículas nos diferentes locais avaliados, embora estas variações sejam menores para as cidades europeias em comparação com cidades asiáticas ou americanas.

Essa grande variabilidade nas concentrações de nanopartículas apontadas por Kumar *et al.* (2014), além das características dos diferentes locais avaliados, pode ser decorrente de outros fatores. Diferenças no intervalo de tamanho de partículas considerado em cada estudo (Kumar *et al.*, 2009a), distância do local de medição da estrada de e configurações topográficas (Fujitani *et al.*, 2012; Zhu *et al.*, 2002),

influências sazonais (Buonanno *et al.*, 2013; Fujitani *et al.*, 2012; Pirjola *et al.*, 2006; Sabaliauskas *et al.*, 2012). A variabilidade observada também pode ser atribuída a fatores como o volume de tráfego, tipo de combustível, morfologia urbana, clima, condições de dispersão específicas para local de amostragem e incerteza nos dados medidos (por exemplo, a coleta e manipulação dos dados) e erros mecânicos (por exemplo, erros de calibração do instrumento), que são difíceis de generalizar (Kumar *et al.*, 2014). Por isso, é difícil realizar uma comparação abrangente das propriedades modais das partículas de aerossol, porque há um número limitado de estudos dedicado à sua estrutura modal, diferentes técnicas instrumentais são empregadas, interpretação e análise de dados, etc. (Hussein *et al.*, 2005).

Tabela 1. Concentrações médias de nanopartículas atmosféricas reportadas em outros estudos

Cidade (País)	Concentração (#/cm^3)	Intervalo de Tamanho (nm)	Fonte
Cingapura	1.59E+04	6-220	Betha et al. (2013)
Brisbane (Austrália)	1.74E+04	15-700	Mejia et al. (2008)
Berlim (Alemanha)	2.80E+04	10-500	Birmili et al. (2009)
Raleigh (EUA)	3.00E+04	20-1000	Hagler et al. (2009)
Cambridge (Reino Unido)	3.02E+04	10-2500	Kumar et al. (2008)
Toronto (Canadá)	3.39E+04	20-1000	Beckerman et al. (2008)
Alameda (Santiago; Chile)	3.63E+04	10-702	Gramsch et al. (2009)
Santiago (Chile)	3.63E+04	10-700	Gramsch et al. (2009)
Dresda (Alemanha)	3.67E+04	3-800	Birmili et al. (2013)
Roma (Itália)	4.68E+04	10+	Paatero et al. (2005)
Barcelona (Espanha)	5.93E+04	10+	Paatero et al. (2005)
Corpus Christi (EUA)	6.60E+04	6-220	Wang et al. (2008)
Nova Iorque (EUA)	6.68E+04	8-294	Bae et al. (2010)
Londres (Reino Unido)	7.84E+04	10+	Putaud et al. (2010)
Kowoloon (Hong Kong)	8.97E+04	5-3000	Tsang et al. (2008)
Xangai (China)	1.20E+05	10-448	Li et al. (2007)
Hsinchu (Taiwan)	1.35E+05	5-200	Chen et al. (2010)
Delhi (Índia)	2.90E+05	10-1000	Apte et al. (2011)

* Adaptado de Kumar *et al.* (2014)

1.2. Distribuição em tamanho das nanopartículas

No que se refere ao intervalo de tamanho das nanopartículas, elas normalmente são discutidas em termos de modos (ou seja, nucleação, Aitken e

acumulação). Cada modo possui fontes, faixa de tamanho, mecanismos de formação, composição química e vias de deposição distintos (Hinds, 1999). Na Figura 2, a curva sólida reflete a concentração em número de partículas, correspondendo a soma das partículas nos diferentes modos. Além disso, é possível observar o esquema de distribuição para a área superficial, a massa e o volume das partículas de aerossol.

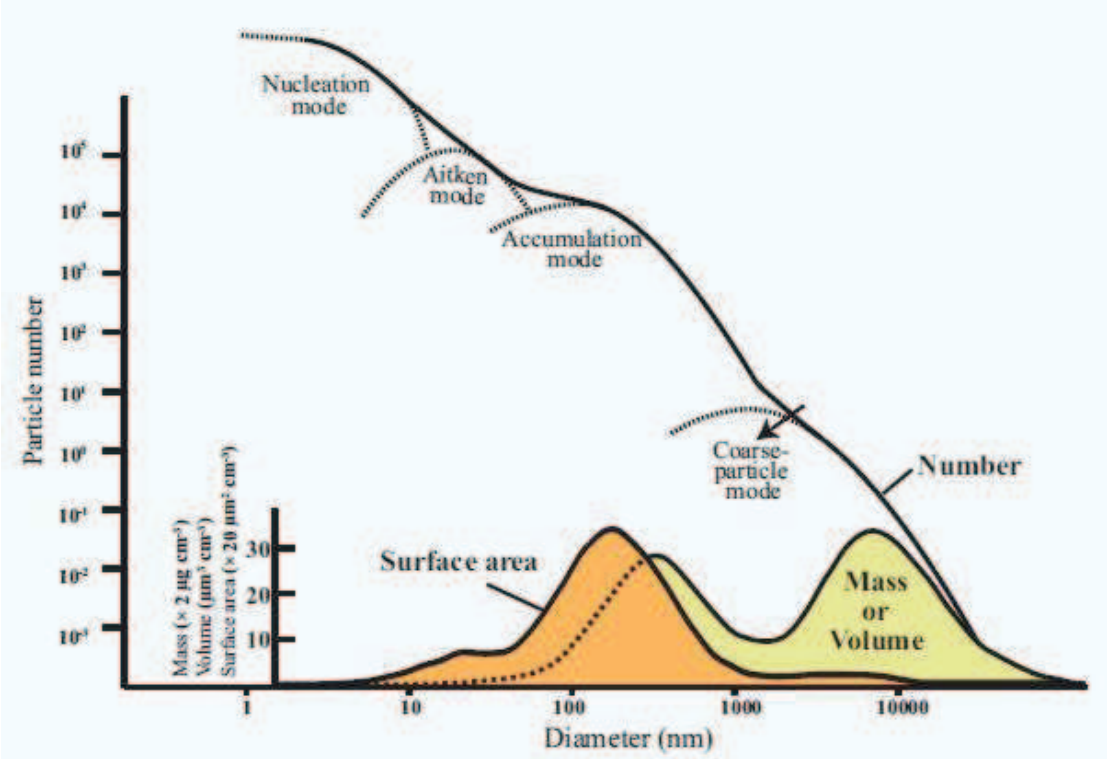

Figura 2. Esquema da distribuição de tamanho de partículas de aerossol para vários parâmetros (Número, N; massa, M; volume, V; área superficial, S) numa amostra atmosférica idealizada, em conjunto com as ilustrações de seus mecanismos de formação. (FONTE: Adaptado de Buseck e Adachi (2008))

1.2.1. Modo nucleação

As partículas do modo nucleação são aquelas <30 nm e que não estão presentes nas emissões primárias de escape, mas que são formadas através de nucleação (conversão gás-partícula) na atmosfera após arrefecimento rápido e diluição das emissões quando a proporção de saturação de compostos gasosos de baixa volatilidade (isto é, ácido sulfúrico) atinge um máximo (Charron e Harrison, 2003; Kittelson *et al.*, 2006a). A maioria destas partículas compreendem sulfatos,

nitratos e compostos orgânicos (Seinfeld e Pandis, 2006). Estas partículas são tipicamente gotículas de líquido compostas principalmente por componentes facilmente voláteis derivados de combustível não queimado e óleo lubrificante (isto é, a fração solvente orgânica) (Lingard *et al.*, 2006; Sakurai *et al.*, 2003; Wehner *et al.*, 2004).

Como pode ser observado na Figura 2, o maior número de partículas está neste intervalo de tamanho. Estas partículas são importantes para a formação e o crescimento de partículas maiores (Buseck e Adachi, 2008). A sua razão superfície volume é elevada, mas a sua área superficial total e volume são pequenas em relação aos outros grupos de tamanho.

As partículas do modo nucleação são encontradas em elevadas concentrações em número perto de fontes. As colisões umas com as outras e com partículas maiores, pertencentes aos outros modos, fazem com que o seu tempo de vida atmosférico seja relativamente curto. A deposição seca, liquefação, ou crescimento através de condensação são os outros mecanismos de remoção dominantes (Hinds, 1999).

1.2.2. Modo Aitken

O modo Aitken é uma fração de sobreposição (tipicamente definida como o intervalo 30-100 nm) dos modos nucleação e acumulação (Seinfeld e Pandis, 2006). As partículas deste modo surgem a partir do crescimento ou coagulação das partículas do modo nucleação, bem como pela produção em grande número de fontes de combustão primária, tais como os veículos (Kulmala *et al.*, 2004). Estas partículas são essencialmente compostas por um núcleo de fuligem/cinzas com uma camada externa de material volatizável (Lingard *et al.*, 2006).

1.2.3. Modo acumulação

As partículas do modo acumulação (aquelas entre 100 e 1000 nm) são aglomerados carbonosos (fuligem e/ou cinzas) (Kumar *et al.*, 2010). Elas provêm principalmente da combustão de combustível e óleo lubrificante de veículos movidos com motor a diesel ou movidos a gasolina com injeção direta (Graskow *et al.*, 1998;

Wehner *et al.*, 2009), bem como pela coagulação das partículas do modo nucleação (Hinds, 1999). A maioria destas partículas é formada na câmara de combustão (ou pouco depois) com matéria orgânica condensada associada (Kittelson *et al.*, 2006b). Estas partículas não são removidas de forma eficiente por difusão ou deposição, já que se coagulam muito lentamente, mas *rainout* ou *washout* são mecanismos de remoção eficazes (Hinds, 1999). Assim, eles tendem a ter relativamente longos tempos de vida atmosféricos (tipicamente de dias ou semanas) e, portanto, podem viajar por distâncias muito longas na atmosfera (Anastasio e Martin, 2001). Mais importante, as partículas neste modo são de tamanhos comparáveis com os comprimentos de onda da luz visível e, portanto, responsáveis por grande parte do problema de comprometimento da visibilidade provocado pelo homem em muitas áreas urbanas (Seinfeld e Pandis, 2006).

1.3. Influência dos parâmetros meteorológicos

Outros fatores importantes que devem ser considerados em estudos que envolvem a avaliação de nanopartículas atmosféricas são as variáveis meteorológicas e a sazonalidade, que afetam a distribuição de tamanho e concentração destas partículas. Por um lado, estes fatores ambientais afetam a estabilidade da camada limite, e, por outro, os ventos fortes podem produzir concentrações mais baixas (Kumar *et al.*, 2008a,b) ou mais altas por processos de ressuspensão para partículas maiores que 100 nm (Charron e Harrison, 2003). Certos autores reportam (He e Dhaniyala, 2012) que a concentração do número de partículas e a taxa de tamanho das partículas decaem com a velocidade e a direção do vento. Por exemplo, quando as direções de vento são paralelas a uma rodovia, as partículas ultrafinas da autoestrada são menos dispersas do que quando os ventos são perpendiculares à autoestrada (Reponen *et al.*, 2003). Sob condições de baixa velocidade do vento, a turbulência produzida pelo tráfego é o processo dominante na diluição de partículas emitidas no nível da rua (Vachon *et al.*, 2002; Di Sabatino *et al.*, 2003; Solazzo *et al.*, 2007) e as concentrações de nanopartículas atmosféricas em cada faixa de tamanho nos regimes de baixa velocidade do vento são independentes da velocidade do vento (Kumar *et al.*, 2008). Já em condições de velocidade do vento superiores, a turbulência produzida

pelo vento é o processo dominante na diluição de partículas emitidas no nível da rua (Britter e Hanna, 2003; Kastner-Klein *et al.*, 2004).

Temperatura e umidade relativa comumente exibem uma anti-correlação, com o aumento da temperatura durante o dia acompanhada por uma diminuição da umidade relativa. Em geral, ambos os parâmetros desempenham um papel importante na concentração em número de nanopartículas (Ruuskanen *et al.*, 2001; Charron e Harrison, 2003; Jamriska *et al.*, 2008, Morawska *et al.*, 2008). Charron e Harrison (2003) mostraram que as partículas no modo nucleação em um ambiente de beira de estrada atingiram um pico durante a madrugada mostrando uma associação inversa com a temperatura do ar. Isso ocorre porque uma diminuição na temperatura do ar ambiente aumenta a relação de supersaturação (Hinds, 1999), resultando assim em um aumento das partículas de modo nucleação. Do mesmo modo, temperaturas menores aumentam a condensação sobre partículas já formadas, causando o seu crescimento.

Isso ocorre porque nessas condições o alto teor de umidade relativa do ar contribui para a formação de novas partículas (modo nucleação) e também partículas de crescimento (modo nucleação e partículas primárias). Em ambos os casos, isto leva a alterações na distribuição de tamanho de partícula. Um aumento da taxa de formação de partículas do modo nucleação para maiores umidades relativas foi relatado, por exemplo, por Abdul-Khalek e Kittelson (1999), Mathis *et al.* (2004) e Kim *et al.* (2002). Em geral, maior teor de água na atmosfera favorece a nucleação binária homogênea de ácido sulfúrico e água (Easter e Peters, 1994), enquanto a nucleação ternária, envolvendo amônia (Korhonen *et al.*, 1999), de forma semelhante à nucleação de compostos orgânicos, é independente da umidade relativa (Morawska *et al.*, 2008).

O número e a distribuição de tamanho destas partículas na atmosfera também podem alterar-se rapidamente devido à influência de processos de transformação, tais como a coagulação e a condensação, e da turbulência que resulta em mistura e diluição (Kumar *et al.*, 2011). Isto pode ser visto nos gases de escape dos automóveis, por exemplo, onde a concentração elevada das partículas recém formadas na combustão resulta na coagulação imediata de muitas dessas partículas. Portanto, o tamanho das nanopartículas depende da multiplicidade de fontes, dos processos e dos

materiais que conduzem à sua formação. No entanto, o conhecimento complexo destes processos ainda apresenta lacunas e necessita de muitos estudos.

1.4. Espectroscopia no infravermelho

Devido à sua maior área superficial, como acima destacado, as nanopartículas atmosféricas podem adsorver diversos poluentes, que pelo seu tamanho podem ser inalados através do trato respiratório do ser humano e afetar negativamente a saúde. Alguns destes poluentes incluem Nitro-Hidrocarbonetos Policíclicos Aromáticos (nHPAs). Estes compostos são reconhecidos como carcinogênicos e estão associados principalmente com o material particulado e as suas maiores concentrações apresentam-se na fração respirável (Di Filippo *et al.*, 2010; Sienra *et al.*, 2005). Estes compostos são membros de uma classe de contaminantes ambientais encontrados em material particulado atmosférico, podendo a atividade mutagênica e carcinogênica destes compostos serem significativas e uma ameaça à saúde humana. Portanto, existe um interesse crescente na determinação da estrutura e reatividade destes compostos carcinogênicos/genotóxicos.

Estes compostos orgânicos em geral são determinados através de cromatografia gasosa (Dallarosa *et al.*, 2005a,2005b; Teixeira *et al.*, 2012), porém esta técnica apresenta diversas desvantagens. Além de exigir uma quantidade relativamente grande de massa de aerossol, os procedimentos de extração química e derivatização para detectar os compostos são complexos, além de não ser possível detectar moléculas muito grandes (Yu *et al.*, 1998). No entanto, uma técnica alternativa para determinar estes contaminantes é a espectroscopia. Entre as vantagens do emprego da espectroscopia estão a sua capacidade de detectar os compostos em pequenas quantidades, sem preparação da amostra e uso de reagentes químicos (técnica não destrutiva); a instrumentação pode estar no local de amostragem, o que elimina as perdas ou transformações durante o transporte, congelamento e armazenamento; realizar medições praticamente em tempo real (Allen *et al.*, 1994; Marshall *et al.*, 1994; Coury e Dillner, 2008; Navarta *et al.*, 2008).

A espectroscopia de infravermelho, também chamada de espectroscopia vibracional, mede diferentes tipos de vibrações entre átomos de acordo com as suas

ligações atômicas. Quando a ligação absorve energia, ela sofre alterações e, ao retornar ao estado original, libera essa energia, que então é detectada pelo espectrômetro. Os espectros vibracionais fornecem uma caracterização completa do estado eletrônico fundamental, do modo vibracional, bem como permitem observar a interação molecular, mudanças na estrutura e reatividade molecular.

Existem dois tipos de vibrações moleculares: estiramentos e deformações angulares. Os estiramentos podem ser simétricos ou assimétricos e são caracterizados pelas deformações que ocorrem ao longo do eixo de ligação que resultam em um contínuo alogamento e encurtamento da distância interatômica da ligação (Figura 3). As vibrações de deformação angular correspondem ao movimento de um grupo de átomos em relação ao resto da molécula, sem que as posições relativas dos átomos do grupo se alterem. Essas deformações recebem a denominação de deformação angular simétrica e assimétrica no plano e deformação angular simétrica e assimétrica fora do plano (Figura 4).

Figura 3. Estiramento Simétrico (a), Estiramento Assimétrico (b)

.

Figura 4. Deformação angular simétrica no plano (a); Deformação angular assimétrica no plano (b)

.

Estudos realizados por Coury e Dillner (2008) desenvolveram uma técnica de espectroscopia de infravermelho para a identificação e a quantificação de grupos funcionais orgânicos em amostras de partículas atmosféricas, ou seja, grupos funcionais aromáticos e grupos funcionais C-H. No entanto, poucos estudos tem sido realizados na identificação de grupos funcionais de n-HPAs por infravermelho, dentre os quais se citam Carrasco-Flores *et al.* (2005) e Onchoke e Parks (2011).

Assim, apesar de ser muito recente, a metodologia desenvolvida para a identificação de grupos funcionais de n-HPAs por infravermelho permite visualizar as bandas correspondentes aos grupos funcionais de interesse nos espectros gerados, e estes podem então ser comparados com dados da literatura. Outra técnica analítica não destrutiva que pode ser utilizada para caracterizar a natureza vibracional das amostras é a espectroscopia Raman. Esta técnica utiliza um laser para provocar na amostra o chamado "efeito Raman", de modo que fatores como a estrutura cristalográfica, a simetria e a composição química da amostra definam os níveis de energia vibracional que são característicos do arranjo atômico na estrutura.

Além da espectroscopia de infravermelho fornecer informações sobre as estruturas moleculares de partículas de aerossóis, existe a possibilidade de distinguir os isômeros dos compostos orgânicos de modo que o risco potencial destes diferentes isômeros possa ser avaliado. A posição de grupos, por exemplo, ligações nitro ligados ao sistema de anel aromático em n-HPAs pode influenciar fortemente na atividade mutagênica. As diferenças significativas nas propriedades mutagênicas entre os vários isômeros de nitro Benzo(a)Pireno (BaP) (os isoômeros 1 e 3 são mais tóxicos do que o isômero 6), por exemplo, estão relacionadas com a sua estrutura e correlacionadas entre espectros vibracionais e atividades biológicas, podendo, consequentemente, prever a toxicidade de nitro-HPAs.

1.5. Metais pesados em Material Particulado <1 µm (MP_1)

O material particulado atmosférico é uma mistura complexa de carbono elementar e orgânico, amônio, nitratos, sulfatos, elementos-traço e água. Com origem natural ou antropogênica, estes elementos podem ser emitidos diretamente para a atmosfera ou ser formados na atmosfera a partir de gases precursores (Aldabe *et al.*, 2011). Desta forma, o estudo da concentração de partículas, seus tamanhos e composição química é essencial para elucidar as fontes de aerossol e os processos associados com a sua formação (Wang *et al.*, 2003; Cheng *et al.*, 2005; Yin e Harrison, 2008; Putaud *et al.*, 2010).

Juntamente com a amostragem de partículas e a caracterização química, modelos matemáticos têm se mostrado extremamente úteis para interpretar e compreender a distribuição geográfica, evolução temporal e a origem dos poluentes. Destes, o *Positive Matrix Factorization* (PMF) (Paatero, 1997) é um método avançado para avaliar as contribuições de fontes de partículas e tem sido aplicado com sucesso em muitos lugares ao redor do mundo (Chueinta *et al.*, 2000; Kim *et al.*, 2003).

Tendo em conta que o tráfego veicular é a principal fonte de material particulado urbano e metais atmosféricos (Amato *et al.*, 2010), é de extrema importância que sejam realizados estudos que englobem este contexto. As emissões veiculares, além daquelas oriundas do tubo de escape, também incluem aquelas oriundas da ressuspensão do material depositado nas rodovias, induzidas pelo veículo, e em parte emissões diretas de desgaste do veículo (freios, pneus, discos etc.). Estas emissões não oriundas do escape são muitas vezes da mesma ordem ou até mesmo maiores do que as emissões de escape, especialmente quando os índices pluviométricos são baixos e o *wash-off* da estrada é reduzido (Amato *et al.*, 2009; Kousoulidou *et al.*, 2008; Kristensson *et al.*, 2004; Abu-Allaban *et al.*, 2003).

Assim, a compreensão da composição química e fontes das partículas com menor tamanho é vital. No entanto, poucos estudos foram realizados envolvendo a caracterização química de MP_1 (Cozic *et al.*, 2008; Vecchi *et al.*, 2008; Richard *et al.*, 2011; Bourcier *et al.*, 2012). Dos estudos mencionados, a identificação de fontes somente foi realizada por Vecchi *et al.* (2008) e Richard *et al.* (2011). Estes estudos

são importantes para ajudar a identificar as principais fontes de poluição que afetam o material particulado ambiente e a concentrações no número de partículas.

Em ambientes impactados pelo tráfego veicular, geralmente os níveis de Zn, Ba, Cu e Sb são relativamente altos, quando comparado com regiões industrializadas (Querol *et al.*, 2007). Estes elementos são observados devido à influência da decomposição do pneu nas rodovias (Zn-Ba) e pela abrasão do freio (Cu-Sb). Altas concentrações de Ti, Sr e Zr também são registradas em áreas urbanas como efeito da ressuspensão do material depositado na estrada (Querol *et al.*, 2007). Além destes, quantidades variáveis de Pb, Fe, Cu, Zn, Ni e Cd podem ser observadas devido às emissões de escape de gasolina e diesel dos veículos (Allen *et al.*, 2001).

1.6. Objetivo geral

Estudar a concentração e a distribuição de nanopartículas atmosféricas em áreas de influências de tráfego veicular, determinar as concentrações de metais pesados em MP_1 e caracterizar os grupos funcionais orgânicos em MP_1 aplicando técnicas de espectroscopia.

1.6.1. Objetivos específicos

- Avaliar a concentração em número e a distribuição de tamanho de nanopartículas atmosféricas na área de estudo.

- Estudar os mecanismos de formação, transformação e remoção de nanopartículas na atmosfera na área de estudo.

- Quantificar as variáveis meteorológicas da área de estudo.

- Quantificar os poluentes NOx ($NO + NO_2$), O_3.

- Identificar e quantificar os grupos funcionais em amostras de partículas atmosféricas através das técnicas de espectroscopia do infravermelho, e microscopia eletrônica por varredura e de transmitância.

- Determinar as concentrações de metais pesados em amostras de MP_1.

- Identificar as fontes de metais utilizando o modelo receptor *Positive Matrix Factorization* (PMF).

- Correlacionar as concentrações de tamanho de partículas com dados meteorológicos e com outros poluentes atmosféricos acima citados.

1.7. Área de Estudo

A área de estudo para a coleta de material particulado foi a Região Metropolitana de Porto Alegre - RMPA - situada na região centro–leste do Estado do Rio Grande do Sul (Figura 5). Está delimitada pelos paralelos 28°S e 31°S e os meridianos 50°W e 54°W. A região é formada por 31 municípios, compreende atualmente 9,652.54 km² e, segundo estimativas da Fundação Estadual de Planejamento Metropolitano e Regional do Rio Grande do Sul – METROPLAN – representa 3.76 % da área total do Estado, com uma população de 4 milhões de habitantes, ou seja, 37.21 % da população total do Rio Grande do Sul.

A região constitui o eixo mais urbanizado do Estado e é caracterizada por diferentes tipologias industriais. Entretanto a maior contribuição é originária da frota de veículos, representando cerca de 20% do total de 3.1 milhões de veículos (Teixeira *et al.*, 2008). Os locais de amostragem, Sapucaia do Sul e Canoas, apresentam forte influência veicular, embora Sapucaia do Sul tenha uma influência veicular maior: frota leve e pesada, congestionamentos e velocidades lentas. Este local também tem influência industrial baixa (refinaria de petróleo, siderúrgicas que não utilizam coque) a montante dos ventos dominantes. Já o local de amostragem Canoas está sob forte influência de veículos, congestionamentos diários, base aérea de Canoas, e indústrias (refinaria de petróleo) a montante dos ventos dominantes que têm uma influência média neste local de amostragem. Além destes locais, também serão estudadas as distribuições de nanopartículas nas vias com os maiores fluxos de tráfego na cidade de Porto Alegre.

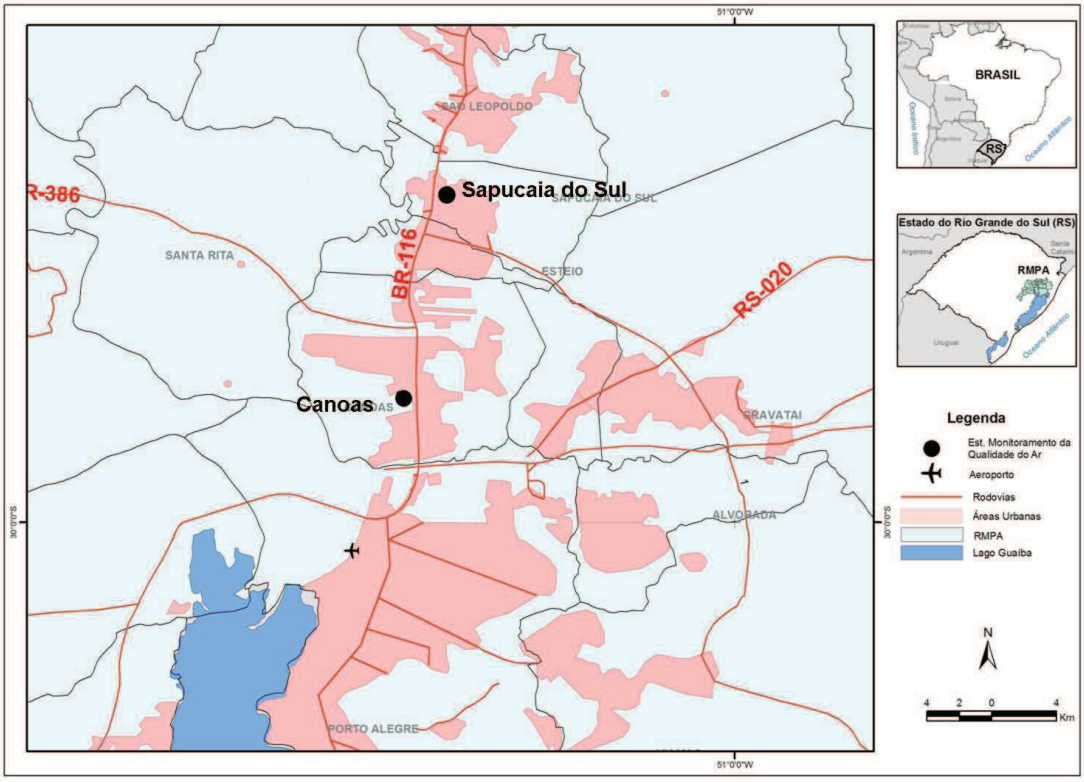

Figura 5. Localização dos pontos de amostragem em Sapucaia do Sul e Canoas na Região Metropolitana de Porto Alegre, RS

Neste estudo, também são consideradas as concentrações de nanopartículas atmosféricas na cidade de Porto Alegre. Foram selecionados 6 locais de amostragem na área urbana, de modo a abranger diferentes características: fluxo de tráfego, composição da frota e arquitetura do local considerado. Os seis locais de amostragem (Figura 6) são descritos a seguir:

- S1 está localizado dentro do Parque Botânico Jardim, cercado por floresta e nenhuma influência veicular, e pode ser considerado como background urbano;

- S2 e S3 correspondem a beira de estradas, localizadas nas avenidas Ipiranga e Bento Gonçalves, com fluxo médio de veículos de 81 e 45 veículos/min, respectivamente, e com 9 e 15% de veículos movidos a diesel, respectivamente .

- S4 e S5 representam cruzamentos, correspondendo às interseções da Av. Farrapos com Av. Sertório e Av. Assis Brasil com Av. Sertório (Figura 6). O fluxo

médio de veículos nestes locais é 75 e 99 veículos/min, com 16% e 14% de veículos movidos a diesel, respectivamente.

- S6 corresponde a um *street canyon* e está localizado na parte central da cidade de Porto Alegre, na Av. Borges de Medeiros (Figura 6). Este local possui um fluxo de veículos médio de 32 veículos/min, com 23% de veículos a diesel, que correspondem principalmente para os ônibus que chegam de diferentes partes da cidade para o centro da cidade. Apesar de S6 mostrar um fluxo de veículos menor do que os outros locais avaliados, há grande circulação de pessoas.

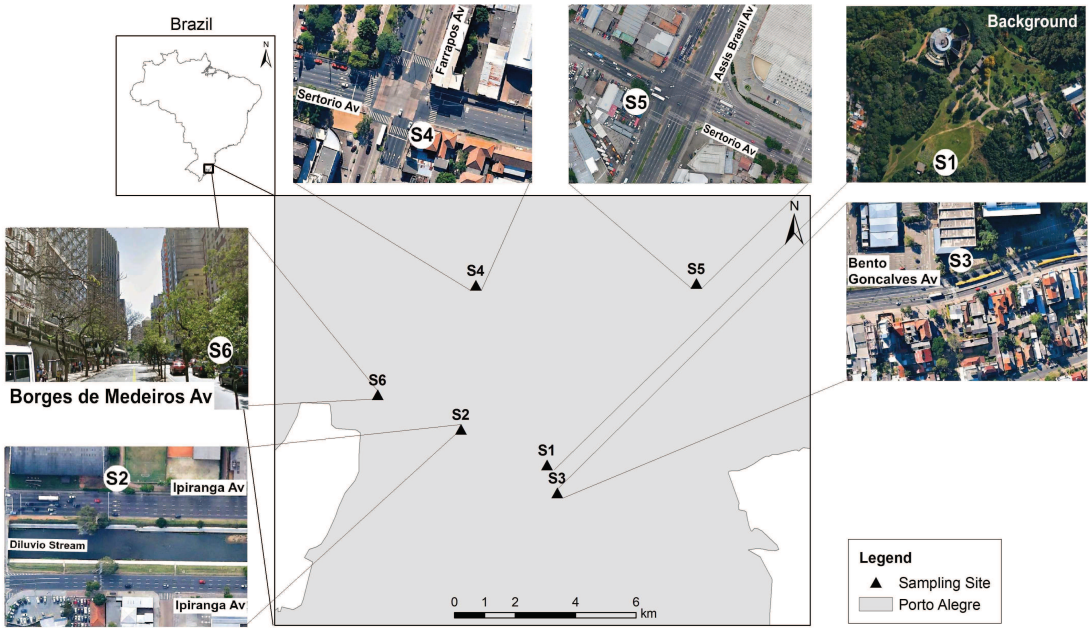

Figura 6. Locais de amostragem de nanopartículas atmosféricas na área urbana de Porto Alegre

1.8. MATERIAIS E MÉTODOS

1.8.1. Amostrador de MP_1

As partículas <1.0 µm foram coletadas utilizando o amostrador automático sequencial de partículas modelo PM162M construído pela Environnement S.A. que coleta amostras de material particulado por deposição em filtros. O amostrador de partículas inclui um jogo de dois recipientes (holders) que funcionam como suporte para os filtros. O equipamento utiliza o método EN 12341 (LECES, n° RC/L 9826) e

trabalha por impacto com vazão volumétrica de 1,0 m^3/h. Possui sensores de temperatura e pressão atmosférica localizados no ponto de amostragem, que regulam a temperatura da linha. Este tubo de amostragem regulado foi desenhado para evitar artefatos no filtro, tais como a condensação ou a perda de compostos semi-voláteis. As amostras de partículas atmosféricas foram coletadas em filtros de politetrafluoretileno (PTFE) de 47 mm de diâmetro durante um período contínuo de 72 horas.

1.8.2. Concentração em número e distribuição de nanopartículas

O equipamento portátil para a medição de nanopartículas foi o *NanoScan SMPS Nanoparticle Sizer* modelo 3910 (TSI Inc. Manufacturer), adquirido por projeto FINEP-FAPERGS. Através deste equipamento serão realizadas medições com uma frequência de 60 s, empregando uma vazão de amostragem de 0.75 L/min e uma vazão no contador de condensação de partículas (CPC) de 0,25 L/min. Este equipamento utiliza álcool isopropílico como líquido de condensação e considera as partículas entre 10 e 420 nm distribuídas em 13 canais.

Figura 7. Imagem do NanoScan modelo 3910 fabricado pela TSI

1.8.3. Espectroscopia de infravermelho

Os espectros de transmitância foram obtidos em um aparelho BOMEM MB-series FTIR Hartmann & Braun Michelson (DRIFTS) equipado com um detector DTGS, pertencente ao Instituto de Física da Universidade Federal do Rio Grande do Sul. Os espectros de transmitância foram medidos com uma resolução de 4 cm^{-1} e 50

varreduras foram tomadas para obter uma relação sinal/ruído apropriada. A faixa espectral medida foi de 400 até 4000 cm^{-1}. Foram obtidos espectros de transmitância para os padrões dos compostos orgânicos avaliados, dos filtros de PTFE e do material particulado MP_1. Os espectros foram calculados usando um filtro branco, sem amostra, como background. Os padrões sólidos foram preparados em pastilhas de KBr sólidas para obter espectros de transmitância por DRIFTS.

1.8.4. Análise de metais pesados em MP_1

As análises de metais pesados foram realizadas nos filtros de PTFE com amostras de MP_1 segundo o procedimento descrito a seguir. Metade de cada filtro foi digerido com uma mistura ácido de HF: HNO_3: $HClO_4$ (2,5: 1,25: 1,25 mL), mantida a 90 ºC em um reator de Teflon durante 6 h, conduzido até à secura. Em seguida, este material foi novamente dissolvido com 1,25 mL de HNO_3 e o extrato é levado a um volume de 25 mL com água. Espectrometria de emissão atômica com plasma acoplado indutivamente (ICP-OES) foi aplicada para a medição dos elementos principais (Al, Ca, K, Mg, Fe, S e Na). A concentração de cerca de 30 metais (como, Ba, Bi, Cd, Ce, Co, Cr, Cs, Cu, Ga, Hf, La, Li, Mn, Mo, Nb, Ni, P, Pb, Rb, Sb , Sc, Se, Sn, Sr, Th, Ti, Tl, U, V, W, Y, Zn e Zr) foi determinada por meio de espectrometria de massa com plasma acoplado indutivamente (ICP-MS). Outro quarto de cada filtro foi lixiviado com água para determinar as concentrações de íons solúveis por cromatografia de íons (sulfato, nitrato e cloreto) e eletrodo íon seletivo (amônio).

1.8.5. Óxidos de nitrogênio (NO, NO_2 e NOx) e ozônio (O_3)

Os parâmetros NOx (NO e NO_2) e O_3 foram medidos pelos equipamentos adquiridos pelo projeto FINEP/FAPERGS/CNPq e pertencentes à Fepam.

Ozônio foi medido com o analisador fotométrico de ozônio LCD/UV modelo O3 42M de absorção de raios UV, trabalhando com o comprimento de onda de 245 nm. A concentração de O_3 é determinada pela diferença entre a absorção de radiação

UV da amostra de ar e da amostra sem O_3 após filtragem no conversor catalítico. Uma média das medidas instantâneas é realizada pelo aparelho.

Óxidos de nitrogênio (NO, NO_2 e NOx) foram medidos utilizando o analisador de quimioluminescência modelo AC32M (método EN 14211 e ISO 7996). O AC32M é um analisador por quimiluminescência que opera sob o princípio que o NO emitirá luz (quimiluminescência) na presença de moléculas de O_3 altamente oxidantes. O NO será oxidado pela presença de O_3 formando moléculas de NO_2 excitado, o qual emitirá radiação luminosa nos comprimentos de onda de 600-1200 nm do espectro. A leitura da radiação é realizada em um fotomultiplicador. Para a medição de NO_2, ele deve ser transformado a NO no forno de molibdênio. A medição é realizada, então, em três etapas: ciclo de referência, ciclo de NO e ciclo de NOx. O cálculo da quantidade de NO_2 é realizado pela diferença entre as concentrações de NO e NOx.

1.8.6. Dados meteorológicos

Os dados meteorológicos como temperatura do ar, radiação solar, umidade relativa, velocidade e direção do vento foram obtidos em estações meteorológicas situadas na área de estudo.

2. ARTIGO: Atmospheric particle number concentration and size distribution in a traffic-impacted area

SCHNEIDER, I. L.; TEIXEIRA, E. C.; SILVA, L. F. O.; WIEGAND, F.. Atmospheric particle number concentration and size distribution in a traffic-impacted area. Atmospheric Pollution Research, 6, 877-885, 2015.

Atmospheric Pollution Research 6 (2015) 877-885

Atmospheric Pollution Research

www.atmospolres.com

Atmospheric particle number concentration and size distribution in a traffic–impacted area

Ismael Luis Schneider [1], Elba Calesso Teixeira [1,2], Luis Felipe Silva Oliveira [3], Flavio Wiegand [2]

[1] *Postgraduate Program in Remote Sensing and Meteorology, Universidade Federal do Rio Grande do Sul, 91501970, Porto Alegre, RS, Brazil*
[2] *Research Department, Fundação Estadual de Proteção Ambiental Henrique Luis Roessler, 90020023, Porto Alegre, RS, Brazil*
[3] *Centro Universitário La Salle, 92000010, Canoas, RS, Brazil*

ABSTRACT

This study measured ambient particle number concentrations (PNC) and the particle number distributions (PND) in the urban area of Porto Alegre, Rio Grande do Sul, Brazil. The samples were analyzed using a NanoScan model 3910 from TSI (diameters between 10 and 420 nm) and were taken from sites with high density of vehicular traffic, including two roadsides, two traffic intersections, one street canyon and one urban background. Association of meteorological variables (temperature, relative humidity, solar radiation, wind direction, and wind speed) on nanoparticle concentrations was examined. The results indicated PNC averages between 4.85×10^4 cm^{-3} and 1.80×10^5 cm^{-3} for locations affected by vehicular traffic, wherein highest concentrations were observed at sites corresponding to traffic intersections. In addition, all sites studied showed a trimodal average PND, with the modes centered at ~14 nm, ~30 nm, and ~105 nm. PND was dominated by nucleation (44.9%) and Aitken (42.0%) modes being representative at the studied sites of the pollution originating from urban traffic, except at the urban background. Meteorological parameters and synoptic meteorological conditions contributed to the variation in the results between the sampled days in the same location.

Keywords: *Nanoparticles, air quality, traffic emissions*

Corresponding Author:
Elba Calesso Teixeira
☎ : *+55-51-3288-9408*
✉ : *gerpro.pesquisa@fepam.rs.gov.br*

Article History:
Received: 12 December 2014
Revised: 11 February 2015
Accepted: 17 March 2015

doi: 10.5094/APR.2015.097

1. Introduction

Urban air pollution is one of the environmental problems having a major concern, and with growing urbanization, it is likely to become more important in the future (Reyes et al., 2000; Xu et al., 2007; Dall'Osto et al., 2012). The air quality in urban centers, which is expressed in terms of pollutants that cause adverse human health effects, contains atmospheric nanoparticles as a major pollutant. However, even if these particles have high potential of being toxic and ability to be deposited in the alveolar region upon inhalation, they are among those pollutants that are not currently regulated by air quality standards for any megacity in any developing or developed country (Kittelson et al., 2006a; Kittelson et al., 2006b; Morawska et al., 2008; Kumar et al., 2011; Young et al., 2012). In an urban environment, motor vehicle emissions usually comprise the most significant source of nanoparticles (Hitchins et al., 2000; Zhu et al., 2002), and the continued growth in the number of gasoline– and diesel–powered vehicles has caused significant concern because of their impact on air quality (Johansson et al., 2007; Keogh et al., 2009; Teixeira et al., 2011).

Nanoparticles are typically measured and expressed in terms of number concentrations of particles per unit volume of air (Morawska et al., 2008), and these particles can originate directly by combustion (primary particles) or gas–to–particle conversion (secondary particles). The details about this topic can be found in the studies of Morawska et al. (2008) and Kumar et al. (2010). These authors also reported that the sizes of particles depend on the multiplicity of sources and processes that lead to their formation, and therefore, on the material from which the particles were formed.

Furthermore, the number concentration and size distribution of these particles in the atmosphere can rapidly change because of the influence of transformation processes such as coagulation and condensation, as well as turbulence, which results in mixing and dilution (Kumar et al., 2011). In addition to these processes, meteorological and environmental factors, such as wind speed, temperature, relative humidity, mixing height, local–scale roadside structures, interactions of multiple streets, and topography could also play an important role in modulating the spatial and temporal variability of particle number size distributions (Hussein et al., 2005; Paatero et al., 2005; Bowker et al., 2007; Ogulei et al., 2007; Jamriska et al., 2008; Sabaliauskas et al., 2012; Young et al., 2012).

In natural or low anthropogenic–influenced environments, particles are also formed in the environment by natural processes; therefore, they are always present at some background levels (Morawska et al., 2008). In such cases, these particles are formed in the atmosphere by the condensation of semi–volatile organic aerosols (O'Dowd et al., 2002), photo–chemically induced nucleation, and/or nucleation by gas–to–particle conversion (Holmes, 2007; Kumar et al., 2009). Therefore, while considering particle concentrations in urban environments, it is important to compare them with background levels for assessing the magnitude of anthropogenic impact.

Given the significant increase in air emissions from mobile sources, associated with an increased number of gasoline vehicles, especially diesel vehicles, as well as the use of lower vehicle technology in urban centers, this study collaborates in the management of air quality supporting the diagnosis of the study area and the Metropolitan Area of Porto Alegre. Therefore, this study aimed to measure ambient particle number concentration (PNC) and the particle number distributions (PND) in the urban area of Porto Alegre, Rio Grande do Sul, Brazil. Different locations in the city, such as urban background, roadsides, traffic intersections, and street canyon were considered in order to evaluate different traffic conditions. Measurements were carried out at the sites during a cold and a warm period.

2. Materials and Methods

2.1. Study area

Porto Alegre, the capital of the State of Rio Grande do Sul (coordinates 30°S and 51°W), Southern Brazil (Figure 1), has an area of 497 km² and a population of 1.41 million inhabitants (IBGE, 2014). The city has 0.80 million vehicles, of which 71.2% are powered by gasoline, 17.3% are powered by diesel, and 11.5% are motorcycles (IBGE, 2014). At present, gasoline–fueled vehicles operate on a mixture of gasoline and 20% ethanol, with a sulfur content of 50 ppm (PETROBRAS, 2014). The diesel, currently used, contains 500 ppm of sulfur with addition of 5% biodiesel (Mattiuzi et al., 2012).

The sampling sites selected in this study were chosen to cover different traffic conditions: traffic flow, fleet composition, and architecture of the considered site. The six sampling locations (Figure 1) are described below:

- S1 is located within the Jardim Botanico Park, which has no vehicular influence and may be considered as an urban background. This park has an area of 39 ha and vegetation comprising native species, especially those endangered.
- S2 and S3 represent roadsides that are located in the Ipiranga and Bento Goncalves avenues, respectively; they have an average vehicle flow of 81 and 45 vehicles min^{-1} (Table 1), respectively, and 9% and 15% of heavy–duty vehicles (HDVs), respectively.
- S4 and S5 represent traffic intersections (TIs), corresponding to the intersections of Av. Farrapos with Av. Sertorio and Av. Assis Brasil with Av. Sertorio, respectively (Figure 1). The average vehicle flow at these locations is 75 to 99 vehicles min^{-1}, with 16% and 14% of HDVs (Table 1), respectively.
- S6 represents a street canyon and is located in the central part of the city of Porto Alegre, Av. Borges de Medeiros (Figure 1). This site has an average vehicle flow of 32 vehicles min^{-1}, with 23% of HDVs (Table 1), which mainly represent buses that arrive from different parts of the city to the downtown area. Despite the fact that S6 showed lower vehicular flow than the other sites evaluated, there was still a large circulation of people.

2.2. Equipment and sampling

Atmospheric nanoparticles were measured using a NanoScan Scanning Mobility Particle Sizer model 3910 (TSI Inc.), every 60 s with a 0.75 L min^{-1} inlet flow and a 0.25 L min^{-1} CPC flow. This equipment uses isopropyl alcohol as condensation liquid, and considers particles between 10 and 420 nm distributed across 13 channels. Meteorological variables such as air temperature (°C), relative humidity (%), wind direction (°), wind speed (m s^{-1}), and solar radiation (kJ m^{-2}) were continuously measured through a weather station.

Sampling was conducted during hot (December 2013 to February 2014) and cold days (July to September 2014, except for S2 and S3 sites, for which data only for the warm period could be collected due to technical problems with the sampling equipment). Measurements were made at a height of 1 m above the ground level along the highways.

Throughout the measurement period, traffic strength was also considered, which was defined as the number of vehicles passing per minute; the vehicles were continuously monitored by a video recorder. After each sampling session, the videotapes were played, and traffic density was manually determined, with a frequency of every 3 min. Diesel–powered heavy–duty vehicles (HDVs), light–duty vehicles (LDVs) that burn gasoline, and motorcycles were counted separately to estimate the traffic density by vehicle type.

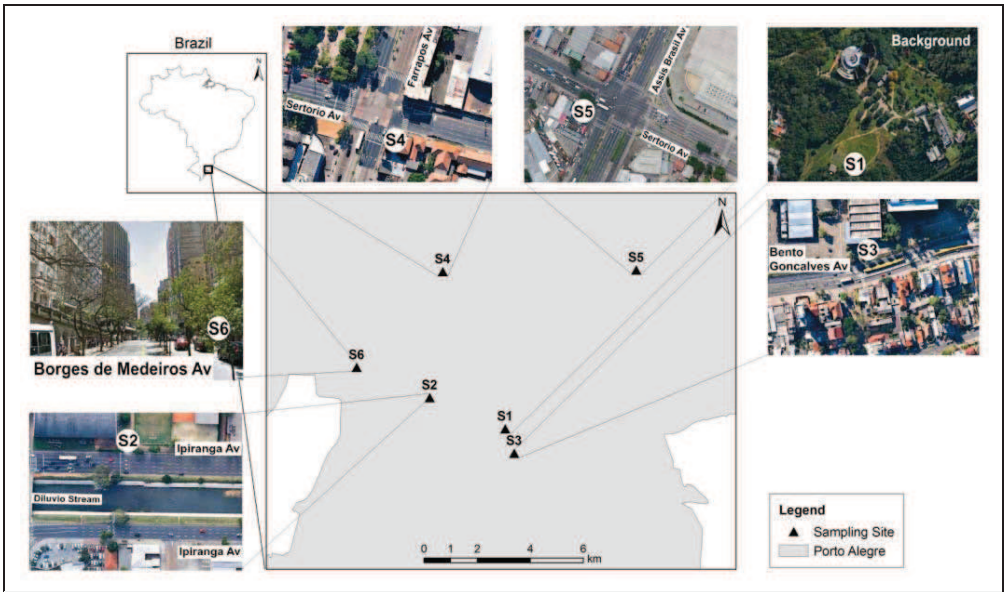

Figure 1. *Study area with the nanoparticle sampling sites in Porto Alegre, Southern Brazil.*

Table 1. *Mean data for traffic strength and for traffic density by type of vehicle. All results are expressed as vehicles min^{-1}*

		Vehicles	LDV	HDV	Motorcycles
S2	Mean	81	70	7	4
	%		86	9	5
S3	Mean	45	33	7	6
	%		72	15	13
S4	Mean	75	57	12	6
	%		76	16	8
S5	Mean	99	75	14	9
	%		77	14	9
S6	Mean	32	23	7	2
	%		71	23	6

2.3. Statistics

For each sampling site, hourly averages for the number concentration and size distribution of atmospheric nanoparticles were calculated. Spearman's correlations were performed between these hourly particle number concentrations (PNC) and meteorological parameters measured to identify factors that predominantly led to the formation of nanoparticles. Statistical analysis was performed using the software SPSS Statistics 22.

To evaluate the modal distribution of the particle sizes, the parameterization of the particle size number distribution (PND) using a multi–lognormal function was applied, as described by Hussein et al. (2005). PND is assumed to consist of several lognormal modes according to the equation:

$$B(D_p)|_{measured} \rightarrow \frac{dN}{d(\log(D_p))} = \sum_{i=1}^{n} \frac{N_i}{\sqrt{2\pi}\log(\sigma_{gi})} \exp\left[-\frac{(\log(D_p) - \log(\overline{D}_{pg,i}))^2}{2\log^2(\sigma_{g,i})}\right] = \sum_{i=1}^{n} N_i A_i(D_p, \overline{D}_{pg,i}\sigma_{g,i}), \quad (1)$$

where B is the measured PND of a certain particle diameter D_p (nm). The three parameters that characterize an individual mode i are as follows: the mode number concentration N_i (cm^{-3}); mode geometric variance $\sigma^2_{g,i}$ (dimensionless); mode geometric mean diameter $D_{pg,i}$ (nm); and the number of individual modes n.

3. Results and Discussion

3.1. Particle Number Concentration (PNC)

Table 2 shows the average PNC for the different studied sites. The PNC average ranged between 8.75×10^3 cm^{-3} (sampling during cold days), observed for S1, and 1.80×10^5 cm^{-3} for S4 and 1.50×10^5 cm^{-3} for S5, for cold and hot days, respectively. These sites had higher concentrations because S4 and S5 had a high traffic flow, from 75 to 99 vehicles min^{-1} (Table 1), besides having ~15% HDVs. This observation was in agreement with other studies showing that diesel–powered vehicles generate a higher amount of nanoparticles (Biswas et al., 2007; Birmili et al., 2009; Can et al., 2011). Furthermore, these sites correspond to TIs, and as reported by Goel and Kumar (2014), these sites have increased PNC caused by complex flow conditions accompanied by frequent changes in driving conditions of vehicles, such as deceleration, idling, acceleration, and cruise (Papson et al., 2012). Particle number emissions released during all these conditions also varied by the constantly changing fuel consumption and engine load (Chen and Yu, 2007; Lei et al., 2010). The higher PNC at S4 and S5 sites was also consistent with earlier studies that showed higher number concentrations at sites impacted by heavy traffic, whereas lower concentrations were distributed more or less homogeneously at background sites (Harrison and Jones, 2005; Bae et al., 2010; Hudda et al., 2010; Young et al., 2012).

Table 2. *Mean particle number concentrations (PNC) and the mean concentrations for the nucleation, Aitken and accumulation modes. All results are expressed as particle cm^{-3}*

		PNC	Nucleation	Aitken	Accumulation
S1	Hot days	3.10x10^4	1.30x10^4	1.54x10^4	2.56x10^3
	Cold days	8.75x10^3	3.79x10^3	3.47x10^3	1.49x10^3
S2	Hot days	4.85x10^4	2.67x10^4	1.65x10^4	5.23x10^3
S3	Hot days	7.76x10^4	3.61x10^4	3.26x10^4	8.89x10^3
S4	Hot days	1.21x10^5	4.64x10^4	5.46x10^4	1.94x10^4
	Cold days	1.80x10^5	7.56x10^4	7.65x10^4	2.76x10^4
S5	Hot days	1.50x10^5	6.86x10^4	6.35x10^4	1.79x10^4
	Cold days	1.35x10^5	6.55x10^4	5.08x10^4	1.85x10^4
S6	Hot days	1.18x10^5	5.16x10^4	5.38x10^4	1.23x10^4
	Cold days	8.38x10^4	3.64x10^4	3.40x10^4	1.33x10^4

The influence of fuel on the formation of nanoparticles was verified by comparing S2 and S4 sites. The site S2 (roadside) is located at the Av. Ipiranga and the site S4 (traffic intersection) at the Av. Farrapos with Av. Sertorio. Although these sites had a similar flow rate, 81 and 75 vehicles min^{-1} (Table 1), respectively, they had different numbers of HDVs, 9% and 16% (Table 1), respectively. As can be seen in Table 2, the average PNC in S4 site is 3.1 times greater than that in S2 site. This is because S4 site had more diesel–powered vehicles, which, as noted above, emitted more nanoparticles. Furthermore, in Brazil, the sulfur content in the fuel is rather high, which is 500 ppm and 50 ppm in diesel and gasoline, respectively (Mattiuzi et al., 2012; PETROBRAS, 2014). As pointed out by Jones et al. (2012), decrease in the sulfur content of diesel from 50 to 10 ppm can result in up to ~30% decrease in PNC.

Table 3 shows the comparison of PNC values obtained herein with those observed in other parts of the world. However, this comparison should be made with caution; characteristics of the different sites evaluated, factors such as size range of particles considered in each study, distance of the measurement location away from the road, topographic settings, and seasonal influences should be considered (Kumar et al., 2014). PNCs in this study (between 4.85×10^4 cm^{-3} and 1.50×10^5 cm^{-3} for sites affected by vehicular traffic) exhibited concentration levels similar to those in developing countries such as China and Taiwan and in some cities in the United States, Barcelona, and London (Table 3). The high PNCs observed in this study, especially when compared with those observed in much of Europe, are primarily caused by the high sulfur content in the Brazilian fuel and by the age of the fleet in use.

3.2. Particle Number Distribution (PND)

It is traditional to describe the particle size distribution by means of the sum of several lognormal distributions (Hussein et al., 2004; Van Dingenen et al., 2005). Each mode can be defined by three parameters: median diameter, geometrical standard deviation and particle concentration. Figure 2 show fitted multimodal particle size distribution indicating these parameters. The results reveal that PND is characterized by three modes: mode–1 (nucleation), mode–2 (Aitken), and mode–3 (accumulation). The geometric mean diameters of mode–1 ranged from 13.8 to 14.8 nm for hot events and between 13.8 and 14.1 nm for cold events. Mode–2 geometric mean diameters ranged between 28.0–34.2 nm and 28.7–30.6 nm for hot and cold events, respectively. In addition

the geometric mean diameters of mode–3 showed small variation of 93.1 to 114.0 nm for both the events.

Table 3. *Mean PNC from this study compared with nanoparticle concentrations reported in other studies*

City (Country)	PNC (cm^{-3})	Size Range (nm)	Source
S1–Porto Alegre (Brazil)	$1.99x10^4$	10–420	This study
S2–Porto Alegre (Brazil)	$4.85x10^4$	10–420	This study
S3–Porto Alegre (Brazil)	$7.76x10^4$	10–420	This study
S4–Porto Alegre (Brazil)	$1.50x10^5$	10–420	This study
S5–Porto Alegre (Brazil)	$1.42x10^5$	10–420	This study
S6–Porto Alegre (Brazil)	$1.01x10^5$	10–420	This study
Barcelona (Spain)	$5.93x10^4$	10+	Paatero et al. (2005)
London (UK)	$7.84x10^4$	10+	Putaud et al. (2010)
Corpus Christi (USA)	$6.60x10^4$	6–220	Wang et al. (2008)
New York (USA)	$6.68x10^4$	8–294	Bae et al. (2010)
Kowoloon (Hong Kong)	$8.97x10^4$	5–3 000	Tsang et al. (2008)
Shanghai (China)	$1.20x10^5$	10–448	Li et al. (2007)
Hsinchu (Tiawan)	$1.35x10^5$	5–200	Chen et al. (2010)
Delhi (India)	$2.90x10^5$	10–1 000	Apte et al. (2011)

Note: Adapted from Kumar et al. (2014)

As shown in Figure 2, it appears that there was no great difference in the mean particle size distribution between the studied sites. Changes in the size distribution may occur with increased distance from the source; however, in this study, these changes can be ignored as all sampling locations were near the vehicular sources. Furthermore, size dsitributions were dominated by nucleation (44.9%) and Aitken (42.0%) modes, being representative, specially for sites S4 and S5, for particles typical for urban traffic (Jones and Harrison, 2006; Kumar et al., 2008; Roth et al., 2008).

Some studies found that nucleation mode particles can be directly emitted from the vehicle exhaust in the particle phase composed of elemental carbon, a fraction of sulfuric acid (H_2SO_4) and organic compounds (unburned oil, etc.) (Burtscher, 2005; Arnold et al., 2006; Rose et al., 2006; Rodriguez and Cuevas, 2007; Fernandez–Camacho et al., 2010), or can be produced during the dilution and cooling of the exhaust emissions in ambient air from cars (Charron and Harrison, 2003; Yao et al., 2005; Casati et al., 2007). This explains, in part, that 44.9% of nucleation mode particles observed were probably originating from direct sources (Wang et al., 2014) for most studied sites. In addition to the direct sources, nucleation mode particles were also formed in the atmosphere through gas–to–particle conversion. In the present study, this type of reaction (secondary particles) occurred in the urban background site (S1), where particle formation occurred through photochemical and chemical reactions. These photochemical reactions might start at about 11:00 h inducing the particle formation, during hot events under high solar radiation. According to Kumar et al. (2013), secondary particle formation through photochemically induced nucleation and condensation of semi–volatile vapors is an important source of nanoparticles, especially in less polluted environments.

In direct emissions, Aitken mode particles, which represent an overlapping fraction of the nucleation and accumulation mode particles, can also be formed (Seinfeld and Pandis, 2006; Kumar et al., 2010), resulting 42% of the particles in this study. Particles thus arise from the growth and coagulation of the nucleation mode particles, as well as are produced by primary occurring in vehicles (Kulmala et al., 2004). In fact, as these two modes are almost overlapping, it is difficult to differentiate accurately nucleation and Aitken modes particles, besides this most sites studied were next to the direct sources.

Accumulation mode particles corresponded to 13.1% of the nanoparticles concentration and, in this study, can refer to the "soot mode", carbonaceous agglomerates (soot and/or ash), for the urban sites, as well as from the coagulation of nucleation mode particles (Kumar et al., 2011).

3.3. Influence of meteorological parameters

Table 4 shows the mean, minimum and maximum values of temperature, relative humidity, wind speed, wind direction and radiation during the sampling days. These variables are explained during the discussion of the correlations. Table 5 presents Spearman's correlation coefficients between PNC and meteorological parameters. Except for S1, S3, and S4 sites, PNC exhibited marginal or no dependency on all meteorological parameters. The low correlation coefficients can be explained as results of the local sources (e.g., emission of primary nanoparticles) that dominated over local wind speed and temperature, thus masking their effect on nanoparticles (Young and Keller, 2004). Furthermore, meteorological phenomena of synoptic scale, such as the input of polar air mass and cold fronts may have contributed to the poor correlations observed.

These phenomena were observed in S1 site, for example, where PNC was lower during the sampling days of low temperature. Since, in the cold days, entrance of a polar air mass over the study region occurred. Such air masses are formed at high latitudes, near the Antarctic Polar Circle, and migrate to lower–latitude regions, like the study area. When they are formed in the polar regions, they acquire the characteristics of that region, low temperature and humidity, high pressure, low cloud cover and low concentrations of particulate matter. Thus, the smaller PNC concentrations observed during this period in site S1 were probably not due to local processes, but rather resulted by atmospheric conditions prevalent in that period.

Table 4. *Mean, minimum and maximum value of temperature, relative humidity, wind speed, wind direction and radiation during the sampling days*

		Temp. (°C)			R.H. (%)			W.S. ($m\ s^{-1}$)			W.D. (°)			Rad. ($kJ\ m^{-2}$)		
		Mean	Min	Max	Mean	Min	Max	Mean	Min	Max	Mean	Min	Max	Mean	Min	Max
S1	Hot days	28.9	18.3	36.1	55	47	71	1.9	0.7	3.1	192	76	341	2 837	378	3 916
	Cold days	13.2	11.0	15.2	59	52	73	2.0	0.7	3.5	221	122	286	2 204	681	2 925
S2	Hot days	27.8	21.1	38.1	50	41	58	1.9	0.9	3.5	161	23	343	2 912	1 464	3 775
S3	Hot days	29.1	25.7	34.3	56	47	67	1.8	0.8	3.3	92	3	282	2 749	1 020	3 966
S4	Hot days	31.7	26.3	36.2	48	35	68	2.4	0.6	3.8	220	9	359	2 751	1 102	3 773
	Cold days	10.9	6.3	18.6	73	50	95	1.8	0.0	4.6	194	96	295	603	0	1 959
S5	Hot days	30.4	26.8	34.9	51	44	58	2.3	1.2	3.5	177	61	316	3 080	1 051	3 916
	Cold days	18.8	15.6	21.7	67	58	77	1.5	1.1	2.2	158	80	259	2 056	912	2 659
S6	Hot days	27.6	20.7	33.0	58	46	75	1.1	0.6	2.6	118	11	346	2 480	829	3 833
	Cold days	16.7	10.7	21.7	67	46	88	1.3	0.4	2.8	95	36	145	1 617	65	2 842

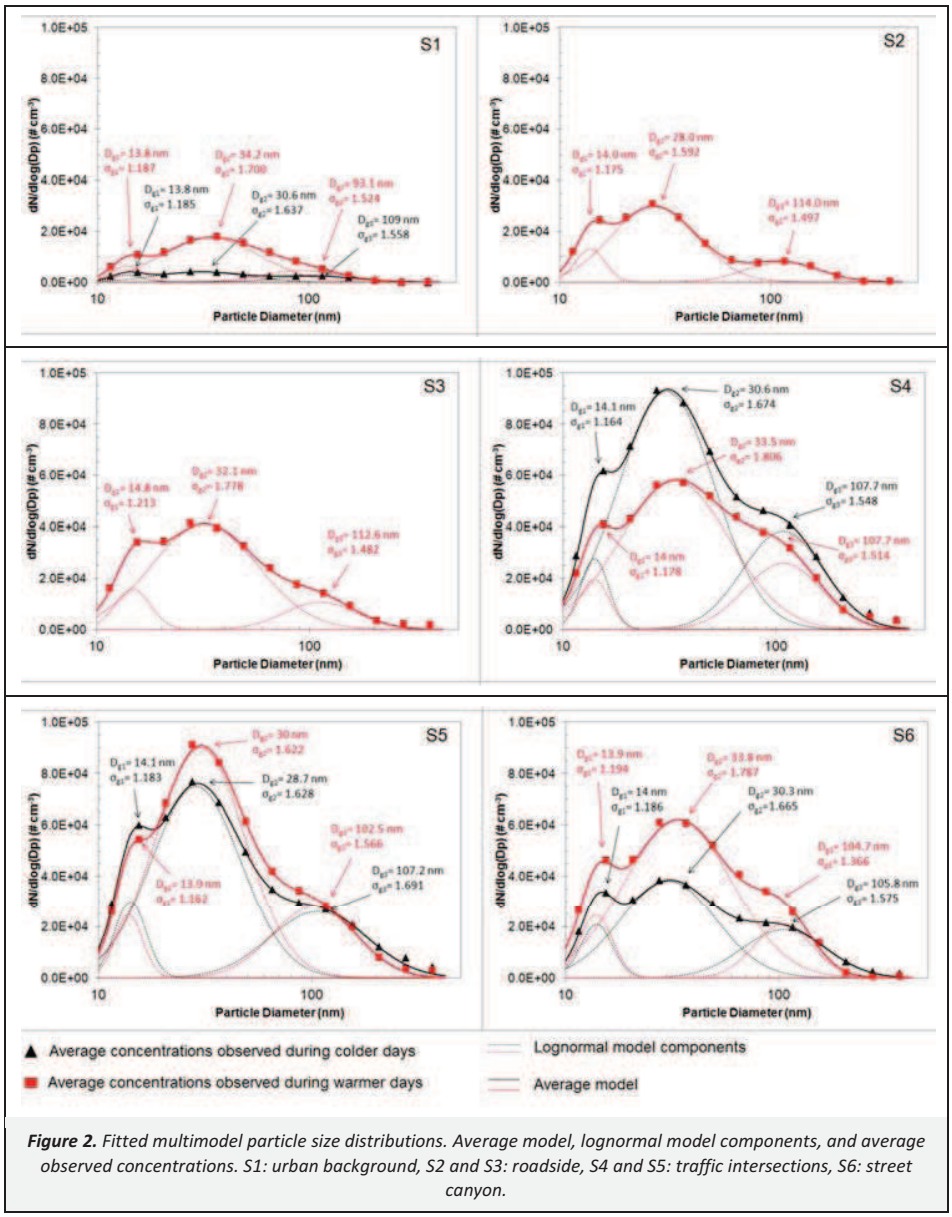

Figure 2. *Fitted multimodel particle size distributions. Average model, lognormal model components, and average observed concentrations. S1: urban background, S2 and S3: roadside, S4 and S5: traffic intersections, S6: street canyon.*

Table 5. *Spearman correlation coefficients for the PNC with the meteorological parameters (Temperature–Temp., Relative Humidity–R.H., Wind Speed–W.S., Wind Direction–W.D. and Radiation–Rad.)*

	Temp.	R.H.	W.S.	W.D.	Rad.
S1	653 [b]	–222	–247	–273	450 [a]
S2	–068	–238	–212	–432	432
S3	–300	532 [a]	–491	–554 [a]	–596 [a]
S4	–743 [b]	828 [b]	–692 [b]	–545 [b]	–766 [b]
S5	071	–138	–262	–206	–129
S6	–246	054	172	–323	–027

[a] *Correlation is significant at the 0.05 level*
[b] *Correlation is significant at the 0.01 level*

The correlation between PNC and wind speed is shown in Table 5. Among the studied sites, S4 was the only one that exhibited a significant correlation with PNC. In this study, the observed wind speeds were low, <2.4 m s^{-1} (Table 4), and under these conditions, traffic–produced turbulence was the dominant process causing the dilution of particles emitted at the street level (Vachon et al., 2002; Di Sabatino et al., 2003; Solazzo et al., 2007), and PNC was independent of wind speed (Kumar et al., 2008). However, under higher wind speed conditions, wind–produced turbulence was the dominant process causing the dilution of particles emitted at the street level (Britter and Hanna, 2003; Kastner–Klein et al., 2004). This can be seen in Figure 3, where the dilution of nanoparticle concentrations by wind occurred during the periods with higher wind speeds. This was in agreement with the atmospheric dispersion theory in which downwind concentrations are inversely related to wind speed (Zhu et al., 2006). Another factor that might be a contributing one to the lack of correlation between PNC and wind speed is the influence of the buildings (architecture) at the sampling sites, which limit wind action, thus minimize its effect on PNC. This effect is even more prominent on the site S6, street canyon, where tall buildings limit the action of wind, resulting even in no influence of wind speed on PNC.

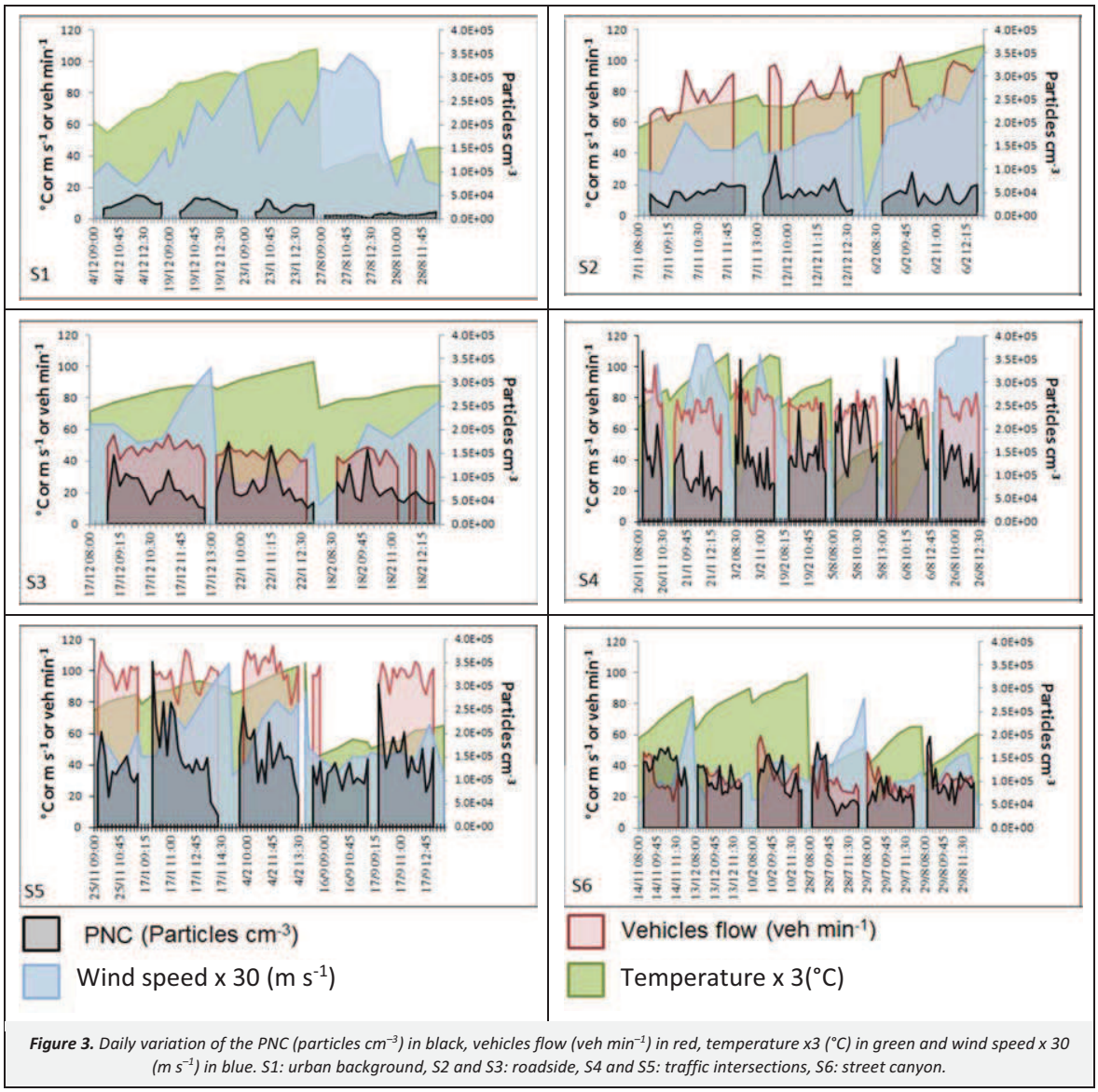

Figure 3. *Daily variation of the PNC (particles cm^{-3}) in black, vehicles flow (veh min^{-1}) in red, temperature x3 (°C) in green and wind speed x 30 (m s^{-1}) in blue. S1: urban background, S2 and S3: roadside, S4 and S5: traffic intersections, S6: street canyon.*

Typically, temperature and relative humidity exhibit inverse correlation, i.e., increased temperature during the day is accompanied by a decreased relative humidity. In general, both parameters play an important role in PNC (Ruuskanen et al., 2001; Charron and Harrison, 2003; Jamriska et al., 2008; Morawska et al., 2008). Table 5 shows a significant correlation between temperature and PNC for S1 and S4 sites. The negative correlation observed at S4 site was in agreement with several studies that reported a lower PNC at higher temperatures (Paatero et al., 2005; Jeong et al., 2006; Sabaliauskas et al., 2012). This may be attributed to the fact that a decrease in ambient air temperature favors the formation of new particles when the exhaust mixes with cool ambient air, when the low and semi volatile compounds are released during the rush hour (Jeong et al., 2006). Similarly, a low temperature, which corresponds to higher levels of relative humidity increase condensation on already formed particles making them grow.

However, for site S1, we observed a positive correlation (0.653) between the temperature and the PNC. This atypical behavior occurred probably due to meteorological conditions of synoptic scale observed during the sampling days with lower temperatures. During these days the sampling site was under the influence of a polar air mass and smaller PNC were observed when compared to the concentrations during the sampling days with higher temperatures, where such meteorological phenomenon was not observed. This can be confirmed considering the data only for the hot sample period, when the influence of temperature on the PNC was negative, resulting from the same factors reported above. The site S2 showed no significant correlation between temperature and PNC (–0.068). This probably occurred because in this case the action of wind direction was predominant in relation to the effect of temperature. This occurred when wind direction was northwest (315–343°), i.e., the sampling site was upstream the highway under investigation. For S5 site, a similar behavior as happened with S1 site was observed, when the meteorological factors of synoptic scale were prevalent in the sampling days of the cold period. In this period, a cold front passed affecting directly the local atmospheric conditions.

The relative humidity positively correlated with PNC (Table 5) for S3 and S4 sites, favoring binary nucleation (water and sulfuric

acid) (Easter and Peters, 1994). At other sites evaluated in this study, no significant correlations were observed between PNC and relative humidity. The negative correlation between PNC and relative humidity for S5 site is due the influence of the architecture and buildings in this region. For site S1, the negative correlation is a result of meteorological factors of synoptic scale, already mentioned as factors influencing during the cold sampling days, as discussed above.

4. Conclusions

This study is a precursor one in the evaluation of atmospheric nanoparticles in Porto Alegre, southern Brazil. Six sampling sites (one urban background, two roadsides, two traffic intersections, and one street canyon) were evaluated, and PNC was observed in the following descending order: traffic intersection > street canyon > roadside > urban background. The PNC levels were similar to some developing countries where the major source of problem is vehicular. The high PNCs observed in this study, especially when compared with those observed in most countries in Europe, were primarily caused by the high sulfur content in the Brazilian fuel and by the age of the fleet in circulation. The results revealed that PND is characterized by three modes: mode–1 (nucleation), mode–2 (Aitken), and mode–3 (accumulation). Size distributions were dominated by nucleation (44.9%) and Aitken (42.0%) modes being representative for local sources near the vehicle exhaust. In this study nucleation and Aitken mode particles were especially originated from primary sources at all study sites, except the urban background. At this site, nucleation mode particles were formed from secondary sources through photochemical and chemical reactions during the warmer days. The relative contributions of cold and hot days for some studied sites were not very clear due to the lack of measurements. The study showed that besides the local meteorological parameters, there was a great influence of meteorological conditions of synoptic scale on PNC and PND. Future studies will include daily and seasonal variations to better understand the mechanisms of nanoparticle formation. Furthermore, some pollutants such as NO_X and CO will also be evaluated as they are indicators of emissions from combustion sources.

Acknowledgments

The authors would like to thank CAPES for funding a PhD scholarship as well to FAPERGS and CNPq for financial support. We are also grateful to the South Air Program of FEPAM for their technical support.

References

Apte, J.S., Kirchstetter, T.W., Reich, A.H., Deshpande, S.J., Kaushik, G., Chel, A., Marshall, J.D., Nazaroff, W.W., 2011. Concentrations of fine, ultrafine, and black carbon particles in auto–rickshaws in New Delhi, India. *Atmospheric Environment* 45, 4470–4480.

Arnold, F., Pirjola, L., Aufmhoff, H., Schuck, T., Lahde, T., Hameri, K., 2006. First gaseous sulfuric acid measurements in automobile exhaust: Implications for volatile nanoparticle formation. *Atmospheric Environment* 40, 7097–7105.

Bae, M.S., Schwab, J.J., Hogrefe, O., Frank, B.P., Lala, G.G., Demerjian, K.L., 2010. Characteristics of size distributions at urban and rural locations in New York. *Atmospheric Chemistry and Physics* 10, 4521–4535.

Birmili, W., Alaviippola, B., Hinneburg, D., Knoth, O., Tuch, T., Borken–Kleefeld, J., Schacht, A., 2009. Dispersion of traffic–related exhaust particles near the Berlin urban motorway – Estimation of fleet emission factors. *Atmospheric Chemistry and Physics* 9, 2355–2374.

Biswas, S., Ntziachristos, L., Moore, K.F., Sioutas, C., 2007. Particle volatility in the vicinity of a freeway with heavy–duty diesel traffic. *Atmospheric Environment* 41, 3479–3493.

Bowker, G.E., Baldauf, R., Isakov, V., Khlystov, A., Petersen, W., 2007. The effects of roadside structures on the transport and dispersion of ultrafine particles from highways. *Atmospheric Environment* 41, 8128–8139.

Britter, R.E., Hanna, S.R., 2003. Flow and dispersion in urban areas. *Annual Review of Fluid Mechanics* 35, 469–496.

Burtscher, H., 2005. Physical characterization of particulate emissions from diesel engines: A review. *Journal of Aerosol Science* 36, 896–932.

Can, A., Rademaker, M., Van Renterghem, T., Mishra, V., Van Poppel, M., Touhafi, A., Theunis, J., De Baets, B., Botteldooren, D., 2011. Correlation analysis of noise and ultrafine particle counts in a street canyon. *Science of the Total Environment* 409, 564–572.

Casati, R., Scheer, V., Vogt, R., Benter, T., 2007. Measurement of nucleation and soot mode particle emission from a diesel passenger car in real world and laboratory in situ dilution. *Atmospheric Environment* 41, 2125–2135.

Charron, A., Harrison, R.M., 2003. Primary particle formation from vehicle emissions during exhaust dilution in the roadside atmosphere. *Atmospheric Environment* 37, 4109–4119.

Chen, K., Yu, L., 2007. Microscopic traffic–emission simulation and case study for evaluation of traffic control strategies. *Journal of Transportation Systems Engineering and Information Technology* 7, 93–99.

Chen, S.C., Tsai, C.J., Chou, C.C.K., Roam, G.D., Cheng, S.S., Wang, Y.N., 2010. Ultrafine particles at three different sampling locations in Taiwan. *Atmospheric Environment* 44, 533–540.

Dall'Osto, M., Beddows, D.C.S., Pey, J., Rodriguez, S., Alastuey, A., Harrison, R.M., Querol, X., 2012. Urban aerosol size distributions over the Mediterranean city of Barcelona, NE Spain. *Atmospheric Chemistry and Physics* 12, 10693–10707.

Di Sabatino, S., Kastner–Klein, P., Berkowicz, R., Britter, R.E., Fedorovich, E., 2003. The modelling of turbulence from traffic in urban dispersion models – Part I: Theoretical considerations. *Environmental Fluid Mechanics* 3, 129–143.

Easter, R.C., Peters, L.K., 1994. Binary homogeneous nucleation – Temperature and relative–humidity fluctuations, nonlinearity, and aspects of new particle–production in the atmosphere. *Journal of Applied Meteorology* 33, 775–784.

Fernandez–Camacho, R., Rodriguez, S., de La Rosa, J., Sanchez de La Campa, A.M., Viana, M., Alastuey, A., Querol, X., 2010. Ultrafine particle formation in the inland sea breeze air flow in Southwest Europe. *Atmospheric Chemistry and Physics* 10, 9615–9630.

Goel, A., Kumar, P., 2014. A review of fundamental drivers governing the emissions, dispersion and exposure to vehicle–emitted nanoparticles at signalised traffic intersections. *Atmospheric Environment* 97, 316–331.

Harrison, R.M., Jones, A.M., 2005. Multisite study of particle number concentrations in urban air. *Environmental Science & Technology* 39, 6063–6070.

Hitchins, J., Morawska, L., Wolff, R., Gilbert, D., 2000. Concentrations of submicrometre particles from vehicle emissions near a major road. *Atmospheric Environment* 34, 51–59.

Holmes, N.S., 2007. A review of particle formation events and growth in the atmosphere in the various environments and discussion of mechanistic implications. *Atmospheric Environment* 41, 2183–2201.

Hudda, N., Cheung, K., Moore, K.F., Sioutas, C., 2010. Inter–community variability in total particle number concentrations in the Eastern Los Angeles air basin. *Atmospheric Chemistry and Physics* 10, 11385–11399.

Hussein, T., Hameri, K.A., Aalto, P.P., Paatero, P., Kulmala, M., 2005. Modal structure and spatial–temporal variations of urban and suburban aerosols in Helsinki – Finland. *Atmospheric Environment* 39, 1655–1668.

Hussein, T., Puustinen, A., Aalto, P.P., Makela, J.M., Hameri, K., Kulmala, M., 2004. Urban aerosol number size distributions. *Atmospheric Chemistry and Physics* 4, 391–411.

IBGE (Instituto Brasileiro de Geografia e Estatistica), 2014. http://cidades.ibge.gov.br/xtras/perfil.php?lang=&codmun=431490&search=rio–grande–do–sul|porto–alegre, accessed in March 2015.

Jamriska, M., Morawska, L., Mergersen, K., 2008. The effect of temperature and humidity on size segregated traffic exhaust particle emissions. *Atmospheric Environment* 42, 2369–2382.

Jeong, C.H., Evans, G.J., Hopke, P.K., Chalupa, D., Utell, M.J., 2006. Influence of atmospheric dispersion and new particle formation events on ambient particle number concentration in Rochester, United States, and Toronto, Canada. *Journal of the Air & Waste Management Association* 56, 431–443.

Johansson, C., Norman, M., Gidhagen, L., 2007. Spatial and temporal variations of PM_{10} and particle number concentrations in urban air. *Environmental Monitoring and Assessment* 127, 477–487.

Jones, A.M., Harrison, R.M., 2006. Estimation of the emission factors of particle number and mass fractions from traffic at a site where mean vehicle speeds vary over short distances. *Atmospheric Environment* 40, 7125–7137.

Jones, A.M., Harrison, R.M., Barratt, B., Fuller, G., 2012. A large reduction in airborne particle number concentrations at the time of the introduction of "sulphur free" diesel and the London Low Emission Zone. *Atmospheric Environment* 50, 129–138.

Kastner–Klein, P., Berkowicz, R., Britter, R., 2004. The influence of street architecture on flow and dispersion in street canyons. *Meteorology and Atmospheric Physics* 87, 121–131.

Keogh, D.U., Ferreira, L., Morawska, L., 2009. Development of a particle number and particle mass vehicle emissions inventory for an urban fleet. *Environmental Modelling & Software* 24, 1323–1331.

Kittelson, D.B., Watts, W.F., Johnson, J.P., 2006a. On–road and laboratory evaluation of combustion aerosols — Part1: Summary of diesel engine results. *Journal of Aerosol Science* 37, 913–930.

Kittelson, D.B., Watts, W.F., Johnson, J.P., Schauer, J.J., Lawson, D.R., 2006b. On–road and laboratory evaluation of combustion aerosols – Part 2: Summary of spark ignition engine results. *Journal of Aerosol Science* 37, 931–949.

Kulmala, M., Vehkamäki, H., Petäjä, T., Dal Maso, M., Lauri, A., Kerminen, V.-M.,Birmili, W., McMurry, P.H., 2004.Formation and growth rates of ultrafine atmospheric particles:a review of observations. *Aerosol Science* 35, 143–176.

Kumar, P., Morawska, L., Birmili, W., Paasonen, P., Hu, M., Kulmala, M., Harrison, R.M., Norford, L., Britter, R., 2014. Ultrafine particles in cities. *Environment International* 66, 1–10.

Kumar, P., Pirjola, L., Ketzel, M., Harrison, R.M., 2013. Nanoparticle emissions from 11 non–vehicle exhaust sources – A review. *Atmospheric Environment* 67, 252–277.

Kumar, P., Ketzel, M., Vardoulakis, S., Pirjola, L., Britter, R., 2011. Dynamics and dispersion modelling of nanoparticles from road traffic in the urban atmospheric environment – A review. *Journal of Aerosol Science* 42, 580–603.

Kumar, P., Robins, A., Vardoulakis, S., Britter, R., 2010. A review of the characteristics of nanoparticles in the urban atmosphere and the prospects for developing regulatory controls. *Atmospheric Environment* 44, 5035–5052.

Kumar, P., Fennell, P., Hayhurst, A., Britter, R., 2009. Street versus rooftop level concentrations of fine particles in a Cambridge Street Canyon. *Boundary–Layer Meteorology* 131, 3–18.

Kumar, P., Fennell, P., Britter, R., 2008. Effect of wind direction and speed on the dispersion of nucleation and accumulation mode particles in an urban street canyon. *Science of the Total Environment* 402, 82–94.

Lei, W., Chen, H., Lu, L., 2010. Microscopic emission and fuel consumption modeling for light–duty vehicles using portable emission measurement system data. *World Academy of Science, Engineering and Technology* 42, 904–911.

Li, X.L., Wang, J.S., Tu, X.D., Liu, W., Huang, Z., 2007. Vertical variations of particle number concentration and size distribution in a street canyon in Shanghai, China. *Science of the Total Environment* 378, 306–316.

Mattiuzi, C.D.P., Palagi, A.C., Teixeira, E.C., Wiegand, F., 2012. Biodiesel Atmospheric Pollution and State of the Art, in Biodiesel: Agronomic and Atmospheric Environmental Impact, edited by Planning and Environmental Management Notebooks no: 6, FEPAM, Porto Alegre, pp. 43–67 (in Portuguese).

Morawska, L., Ristovski, Z., Jayaratne, E.R., Keogh, D.U., Ling, X., 2008. Ambient nano and ultrafine particles from motor vehicle emissions: Characteristics, ambient processing and implications on human exposure. *Atmospheric Environment* 42, 8113–8138.

O'Dowd, C.D., Aalto, P., Hameri, K., Kulmala, M., Hoffmann, T., 2002. Aerosol formation – Atmospheric particles from organic vapours. *Nature* 416, 497–498.

Ogulei, D., Hopke, P.K., Chalupa, D.C., Utell, M.J., 2007. Modeling source contributions to submicron particle number concentrations measured in Rochester, New York. *Aerosol Science and Technology* 41, 179–201.

Paatero, P., Aalto, P., Picciotto, S., Bellander, T., Castano, G., Cattani, G., Cyrys, J., Kulmala, M., Lanki, T., Nyberg, F., Pekkanen, J., Peters, A., Sunyer, J., Forastiere, F., Group, H.S., 2005. Estimating time series of aerosol particle number concentrations in the five HEAPSS cities on the basis of measured air pollution and meteorological variables. *Atmospheric Environment* 39, 2261–2273.

Papson, A., Hartley, S., Kuo, K.L., 2012. Analysis of emissions at congested and uncongested intersections with motor vehicle emission simulation 2010. *Transportation Research Record* 2270, 124–131.

PETROBRAS (Petroleo Brasileiro S.A.), 2014. http://www.petrobras.com.br/pt/produtos-e-servicos/produtos/automotivos/gasolina/, accessed in March 2015.

Putaud, J.P., Van Dingenen, R., Alastuey, A., Bauer, H., Birmili, W., Cyrys, J., Flentje, H., Fuzzi, S., Gehrig, R., Hansson, H.C., Harrison, R.M., Herrmann, H., Hitzenberger, R., Huglin, C., Jones, A.M., Kasper–Giebl, A., Kiss, G., Kousa, A., Kuhlbusch, T.A.J., Loschau, G., Maenhaut, W., Molnar, A., Moreno, T., Pekkanen, J., Perrino, C., Pitz, M., Puxbaum, H., Querol, X., Rodriguez, S., Salma, I., Schwarz, J., Smolik, J., Schneider, J., Spindler, G., ten Brink, H., Tursic, J., Viana, M., Wiedensohler, A., Raes, F., 2010. A European aerosol phenomenology–3: Physical and chemical characteristics of particulate matter from 60 rural, urban, and kerbside sites across Europe. *Atmospheric Environment* 44, 1308–1320.

Reyes, D.R., Rosario, O., Rodriguez, J.F., Jimenez, B.D., 2000. Toxic evaluation of organic extracts from airborne particulate matter in Puerto Rico. *Environmental Health Perspectives* 108, 635–640.

Rodriguez, S., Cuevas, E., 2007. The contributions of "minimum primary emissions" and "new particle formation enhancements" to the particle number concentration in urban air. *Journal of Aerosol Science* 38, 1207–1219.

Rose, D., Wehner, B., Ketzel, M., Engler, C., Voigtlander, J., Tuch, T., Wiedensohler, A., 2006. Atmospheric number size distributions of soot particles and estimation of emission factors. *Atmospheric Chemistry and Physics* 6, 1021–1031.

Roth, E., Kehrli, D., Bonnot, K., Trouve, G., 2008. Size distributions of fine and ultrafine particles in the city of Strasbourg: Correlation between number of particles and concentrations of NO_X and SO_2 gases and some soluble ions concentration determination. *Journal of Environmental Management* 86, 282–290.

Ruuskanen, J., Tuch, T., Ten Brink, H., Peters, A., Khlystov, A., Mirme, A., Kos, G.P.A., Brunekreef, B., Wichmann, H.E., Buzorius, G., Vallius, M., Kreyling, W.G., Pekkanen, J., 2001. Concentrations of ultrafine, fine and $PM_{2.5}$ particles in three European cities. *Atmospheric Environment* 35, 3729–3738.

Sabaliauskas, K., Jeong, C.–H., Yao, X., Jun, Y.–S., Jadidian, P., Evans, G.J., 2012. Five–year roadside measurements of ultrafine particles in a major Canadian city. *Atmospheric Environment* 49, 245–256.

Seinfeld, J.H., Pandis, S.N., 2006. *Atmospheric Chemistry and Physics, from Air Pollution to Climate Change*, John Wiley, New York, 1203 pages.

Solazzo, E., Vardoulakis, S., Cai, X.M., 2007. Evaluation of traffic–producing turbulence schemes within Operational Street Pollution Models using roadside measurements. *Atmospheric Environment* 41, 5357–5370.

Teixeira, E.C., Mattiuzi, C.D.P., Wiegand, F., Feltes, S., Norte, F., 2011. Estimated atmospheric emissions from mobile sources and assessment of air quality in an urban area, edited by Mazzeo N.*A*., Air Quality Monitoring, Assessment and Management, Intech, Rijeka, pp. 149–172.

Tsang, H., Kwok, R., Miguel, A.H., 2008. Pedestrian exposure to ultrafine particles in Hong Kong under heavy traffic conditions. *Aerosol and Air Quality Research* 8, 19–27.

Vachon, G., Louka, P., Rosant, J.M., Mestayer, P.G., Sini, J.F., 2002. Measurements of traffic–induced turbulence within a street canyon during the Nantes'99 experiment. *Water, Air and Soil Pollution: Focus* 2, 127–140.

Van Dingenen, R., Putaud, J.P., Martins–Dos Santos, S., Raes, F., 2005. Physical aerosol properties and their relation to air mass origin at Monte Cimone (Italy) during the first MINATROC campaign. *Atmospheric Chemistry and Physics* 5, 2203–2226.

Wang, D.W., Guo, H., Cheung, K., Gan, F.X., 2014. Observation of nucleation mode particle burst and new particle formation events at an urban site in Hong Kong. *Atmospheric Environment* 99, 196–205.

Wang, Y.G., Zhu, Y.F., Salinas, R., Ramirez, D., Karnae, S., John, K., 2008. Roadside measurements of ultrafine particles at a busy urban intersection. *Journal of the Air & Waste Management Association* 58, 1449–1457.

Xu, X.H., Brook, J.R., Guo, Y.S., 2007. A statistical assessment of saturation and mobile sampling strategies to estimate long–term average concentrations across urban areas. *Journal of the Air & Waste Management Association* 57, 1396–1406.

Yao, X.H., Lau, N.T., Fang, M., Chan, C.K., 2005. Real–time observation of the transformation of ultrafine atmospheric particle modes. *Aerosol Science and Technology* 39, 831–841.

Young, L.H., Wang, Y.T., Hsu, H.C., Lin, C.H., Liou, Y.J., Lai, Y.C., Lin, Y.H., Chang, W.L., Chiang, H.L., Cheng, M.T., 2012. Spatiotemporal variability of submicrometer particle number size distributions in an air quality management district. *Science of the Total Environment* 425, 135–145.

Young, L.H., Keeler, G.J., 2004. Characterization of ultrafine particle number concentration and size distribution during a summer campaign in Southwest Detroit. *Journal of the Air & Waste Management Association* 54, 1079–1090.

Zhu, Y., Kuhn, T., Mayo, P., Hinds, W.C., 2006. Comparison of daytime and nighttime concentration profiles and size distributions of ultrafine particles near a major highway. *Environmental Science & Technology* 40, 2531–2536.

Zhu, Y., Hinds, W.C., Kim, S., Shen, S., Sioutas, C., 2002. Study of ultrafine particles near a major highway with heavy–duty diesel traffic. *Atmospheric Environment* 36, 4323–4335.

3. ARTIGO: FTIR analysis and evaluation of carcinogenic and mutagenic risks of nitro-polycyclic aromatic hydrocarbons in $PM_{1.0}$

SCHNEIDER, I. L.; TEIXEIRA, E. C.; AGUDELO-CASTAÑEDA, D. M.; SILVA E SILVA, G.; BALZARETTI, N.; BRAGA, M. F.; OLIVEIRA, L. F. S.. FTIR analysis and evaluation of carcinogenic and mutagenic risks of nitro-polycyclic aromatic hydrocarbons in $PM_{1.0}$. Science of the Total Environment, 541, 1151-1160, 2016.

Science of the Total Environment 541 (2016) 1151–1160

Contents lists available at ScienceDirect

Science of the Total Environment

journal homepage: www.elsevier.com/locate/scitotenv

FTIR analysis and evaluation of carcinogenic and mutagenic risks of nitro-polycyclic aromatic hydrocarbons in $PM_{1.0}$

Ismael Luís Schneider [a], Elba Calesso Teixeira [a,b,*], Dayana Milena Agudelo-Castañeda [a], Gabriel Silva e Silva [c], Naira Balzaretti [d], Marcel Ferreira Braga [a], Luís Felipe Silva Oliveira [c]

[a] Programa de Pós-graduação em Sensoriamento Remoto, Universidade Federal do Rio Grande do Sul (UFRGS), Porto Alegre, RS, Brazil
[b] Fundação Estadual de Proteção Ambiental Henrique Luís Roessler, Porto Alegre, RS, Brazil
[c] Laboratory of Environmental Researches and Nanotechnology Development, Centro Universitário La Salle, Mestrado em Avaliação de Impactos Ambientais em Mineração, Canoas, RS, Brazil
[d] Instituto de Física, Universidade Federal do Rio Grande do Sul (UFRGS), Porto Alegre, RS, Brazil

HIGHLIGHTS

- Emissivity and transmittance spectra of nitro-PAHs in $PM_{1.0}$ samples using FTIR
- Solid standards results allowed effectively identifying nitro-PAHs in $PM_{1.0}$.
- Main spectral features of nitro-PAHs occurred between 1300 and 1600 cm^{-1}.
- Samples showed broader bands with lower intensity than the NPAH standards.
- $PM_{1.0}$ samples presented higher carcinogenic than mutagenic risk.

GRAPHICAL ABSTRACT

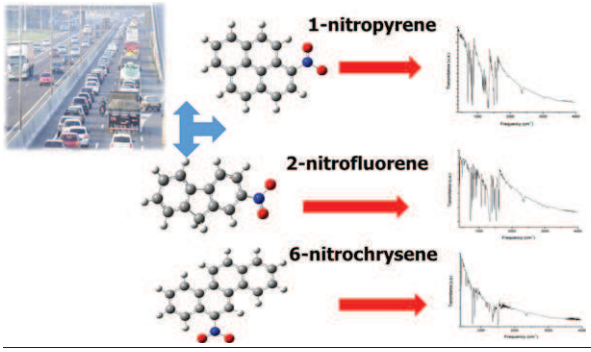

ARTICLE INFO

Article history:
Received 14 August 2015
Received in revised form 21 September 2015
Accepted 27 September 2015
Available online 11 November 2015

Editor: D. Barcelo

Keywords:
NPAH
FTIR
Emissivity
Transmittance
Toxicity
$PM_{1.0}$

ABSTRACT

Nitro-polycyclic aromatic hydrocarbons (NPAHs) represent a group of organic compounds of significant interest due to their presence in airborne particulates of urban centers, wide distribution in the environment, and mutagenic and carcinogenic properties. These compounds, associated with atmospheric particles of size <1 μm, have been reported as a major risk to human health. This study aims at identifying the spectral features of NPAHs (1-nitropyrene, 2-nitrofluorene, and 6-nitrochrysene) in emissivity and transmittance spectra of samples of particulate matter <1 μm ($PM_{1.0}$) using infrared spectrometry. Carcinogenic and mutagenic risks of the studied NPAHs associated with $PM_{1.0}$ samples were also determined for two sampling sites: Canoas and Sapucaia do Sul. The results showed that NPAH standard spectra can effectively identify NPAHs in $PM_{1.0}$ samples. The transmittance and emissivity sample spectra showed broader bands and lower relative intensity than the standard NPAH spectra. The carcinogenic risk and the total mutagenic risk were calculated using the toxic equivalent factors and mutagenic potency factors, respectively. Canoas showed the highest total carcinogenic risk, while Sapucaia do Sul had the highest mutagenic risk. The seasonal analysis suggested that in the study area the ambient air is more toxic during the cold periods. These findings might of significant importance for the decision and policy making authorities.

1. Introduction

Particulate matter, especially in urban areas, is a mixture of primary particulate emissions from industries, transportation, power generation, natural sources, and secondary material formed by gas-to-particle conversion mechanisms (Seinfeld and Pandis, 2006). Atmospheric

* Corresponding author at: Fundação Estadual de Proteção Ambiental Henrique Luís Roessler, Porto Alegre, RS, Brazil.
E-mail address: gerpro.pesquisa@fepam.rs.gov.br (E.C. Teixeira).

http://dx.doi.org/10.1016/j.scitotenv.2015.09.142
0048-9697/

particles are complex mixtures of various chemical compounds, which serve as a catalyst for many chemical reactions (Feilberg and Nielsen, 2000; Turpin et al., 2000). These compounds include hazardous elements, black carbon, polycyclic aromatic hydrocarbons (PAHs), and nitro-polycyclic aromatic hydrocarbons (NPAHs), the latter being considered to be carcinogenic and/or mutagenic (Tang et al., 2005; Silva et al., 2009; Ribeiro et al., 2010; Oliveira et al., 2012a, 2012b; Cerqueira et al., 2011, 2012; Quispe et al., 2012; Arenas-Lago et al., 2013). Moreover, NPAHs (nitro-PAHs) can be 100,000 times more mutagenic and 10 times more carcinogenic as compared with the unsubstituted parent PAHs (Onchoke et al., 2006), even if they are present at much lower concentrations than their parent compounds (Ritter et al., 2002; IARC, 2013). Consequently, there is great interest in determining their structure and reactivity.

NPAHs can be released in the atmosphere directly from incomplete combustion emissions or produced by chemical reactions between PAHs and nitrogen oxides (Bamford et al., 2003). Reactions between PAHs at the gas phase are initiated by hydroxyl radicals (OH) during the day and by nitrate radical (NO_3) in the night (Arey, 1998). PAHs associated with the particulate phase react with N_2O_5 or HNO_3 and produce NPAHs (Nielsen, 1984; Kamens et al., 1990). Thus, the different isomers of NPAHs formed in the atmosphere by direct emissions can be distinguished from those formed from chemical reactions, on the basis of different formation mechanisms. These compounds are widely distributed in the environment and are mainly associated with airborne particles (Arey, 1998; Atkinson and Ashcmann, 1994; Teixeira et al., 2011), especially fine particles (Yang et al., 2005; Pham et al., 2013). Fine particles, particularly those <1 μm ($PM_{1.0}$), are of special concern because they can remain suspended in the air for weeks and penetrate into the deeper part of the respiratory system (Kumata et al., 2006; Slezakova et al., 2007), thus posing a greater risk to human health. Airborne particles have been receiving increasing attention over the years because of their environment, climate and health effects, and heterogeneous atmospheric processes associated with the complex environmental behaviors of atmospheric particles (Zhao and Chen, 2010).

The Fourier transform infrared spectroscopy (FTIR) technique has been used to analyze $PM_{1.0}$ samples. This technique is based on the interaction of electromagnetic radiation in the thermal infrared region (Hammes, 2005). Also known as vibrational spectroscopy, it measures different types of vibrations between the atoms according to their atomic bonds. Due to the complexity of environmental samples and the need for identification of different isomers, various chromatographic techniques have been widely used to identify NPAHs (Jinhui and Lee, 2001; Crimmins and Baker, 2006; Teixeira et al., 2011). However, the FTIR technique, although rarely used compared with chromatographic techniques, has many advantages, such as being is more economic, quicker, and lossless. Also, infrared spectroscopy can detect small amounts of compounds without requiring their extraction or derivatization; and the instrumentation can be taken directly to the sampling site, which eliminates environmental losses or transformations during freezing, transportation, and storage (Yu et al., 1998; Reff et al., 2005; Coury and Dillner, 2008). A specific functional chemical group in a molecule shows its spectral characteristics in certain region of the spectrum (Griffiths and Haseth, 2007). Other bands indicate significant movement of only a few atoms, although their frequency varies from one molecule to another, containing the particular functional group. In this way, different molecules containing similar functional groups can be distinguished. These are thus often known as fingerprint bands (Griffiths and Haseth, 2007).

There are very few studies, for instance, those of Carrasco-Flores et al. (2004, 2007) and Onchoke and Parks (2011), on the identification of functional groups of NPAHs using the FTIR technique. However, our laboratory used emissivity spectra besides transmittance spectra, which is a rather new approach for the identification of functional groups of NPAHs in $PM_{1.0}$. In addition, no study, to the best of our knowledge, has evaluated NPAHs in particulate matter, especially for $PM_{1.0}$. However, the FTIR technique allows the distinction of the bands associated with the functional groups of interest in the spectra generated by using data from the literature.

The aim of this study was to analyze spectral features of 1-nitropyrene, 2-nitrofluorene, and 6-nitrochrysene solid standards in transmittance and emissivity FTIR spectra in order to identify NPAHs in $PM_{1.0}$ samples collected from the study area. We also conducted an assessment of carcinogenic and mutagenic risks of the studied NPAHs in the $PM_{1.0}$ samples.

2. Study area

The study area is the metropolitan area of Porto Alegre (MAPA), located in the central-eastern region of the state of Rio Grande do Sul, Brazil (Fig. 1). This area has its limits within 29°54′ to 29°20′ S and 51°17′ to 50°15′ W. According to the Brazilian Institute of Geography and Statistics (IBGE, 2010), this region comprises an area of 9653 km^2, representing 3.76% of the total area of the state, and has a population of 4.12 millions of inhabitants, i.e., 37.7% of the total population of Rio Grande do Sul. This metropolitan area is the most urbanized one in Rio Grande do Sul, and characterized by different types of industries, including some stationary sources of pollution. In addition to the different types of industries found in MAPA, it is estimated that the most significant contributions are made by mobile sources due to the large number of vehicles in circulation in the region that accounts 37% of the total of 5.37 million cars representing the Sate fleet (DETRAN/RS, 2013). In 2009, the distribution of the fleet by fuel type in MAPA was 69% gasoline, 16% gasoline (motorcycles), 11% diesel, and 4% alcohol (Teixeira et al., 2011). In January 2013, the region had about 1.96 million vehicles (DETRAN/RS). Sampling sites for $PM_{1.0}$ were Canoas and Sapucaia do Sul (Fig. 1). These sites were chosen due to various reasons. Canoas is under a strong vehicular influence, daily traffic congestions, location of Canoas Air Force Base, and industries (an oil refinery); its geographical location is upstream of the prevailing winds that have a medium influence on this sampling site. Sapucaia do Sul site has a greater vehicular influence: light and heavy fleet, traffic congestions, and slow speeds. This site also has low industrial influence (oil refinery, steel mills that do not use coke, and Canoas Air Force Base) upstream of prevailing winds.

3. Material and methods

3.1. Sampling and NPAH standards

$PM_{1.0}$ sampling was performed in an automatic sequential particle sampler model PM162M from Environment S.A. $PM_{1.0}$ samples were collected using Zefluor™ membrane PTFE (polytetrafluoroethylene) filters of 47 mm diameter, specifically designed for organic sampling (Peltonen and Kuljukka, 1995). Sampling was carried out at a constant flow rate of 1 m^3/h for 72 and 12 h for the determination of emissivity (FTIR) and transmittance spectra, respectively. These sampling times were found to be most appropriate for a good resolution of bands corresponding to organic species (Agudelo-Castañeda et al., 2015). Several studies have shown that PTFE filters are more suitable for FTIR tests and have lower absorption bands (overlapping peaks) in infrared analysis than nucleopore or quartz filters (Ghauch et al., 2006).

In this study, the following NPAH standards were used: 6-nitrochrysene, 2-nitrofluorene, and 1-nitropyrene. These NPAH standards were purchased from Aldrich Chemical Company with 99% purity.

3.2. Instruments

Emissivity spectra of $PM_{1.0}$ samples and NPAH standards were obtained with a hand-portable thermal infrared spectrometer model 102F manufactured by Designs & Prototypes. The analyses were performed at the Centro Estadual de Pesquisa em Sensoriamento Remoto e Meteorologia (CEPSRM) (State Research Center for Remote Sensing

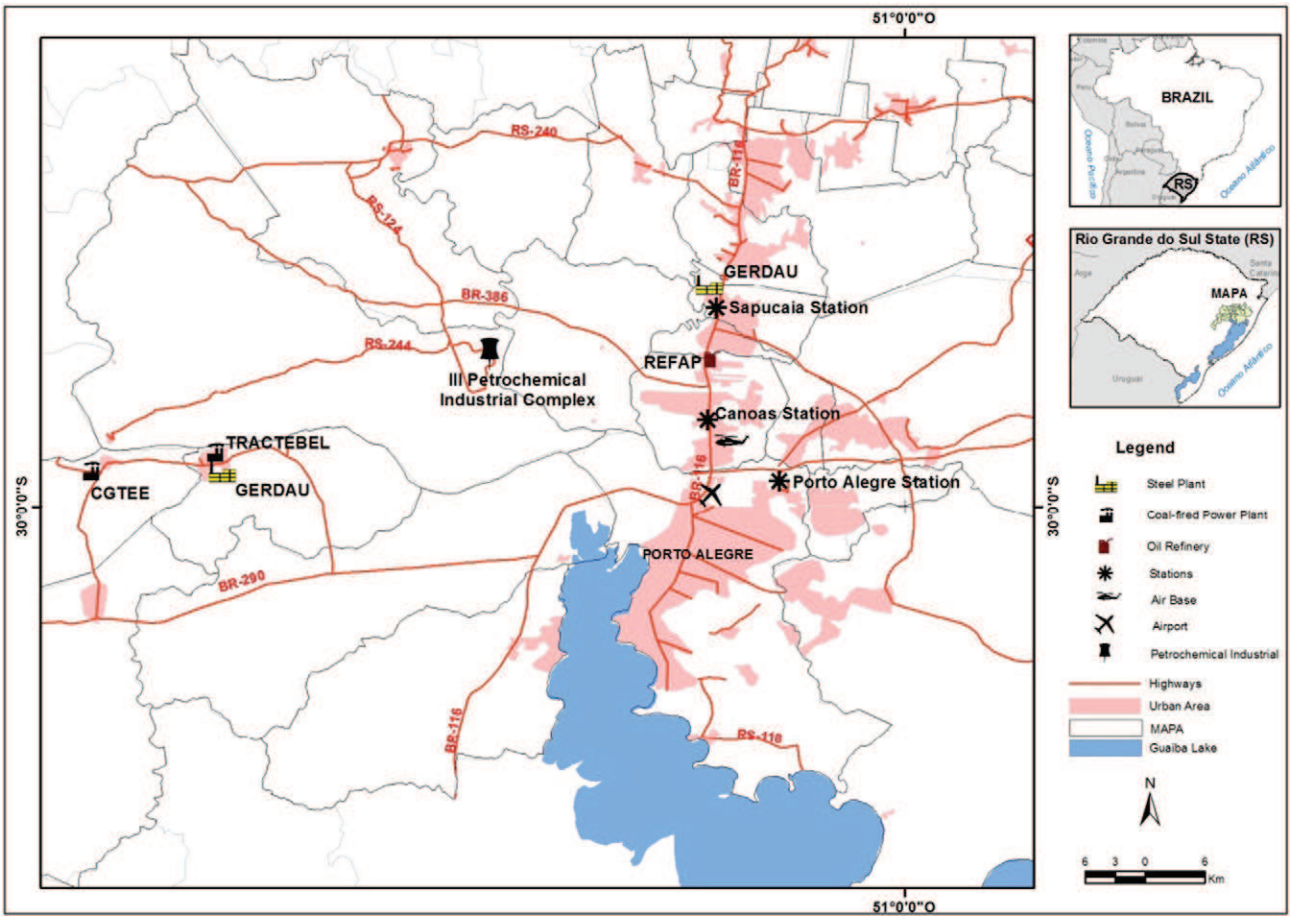

Fig. 1. Location of the sampling sites (Canoas and Sapucaia do Sul).

and Meteorology) of the Federal University of Rio Grande do Sul (UFRGS). The data were obtained from an average of 100 scans, i.e., 100 co-added interferograms. The measurements were performed at a distance of less than 50 cm to minimize atmospheric attenuation (Korb et al., 1996) using a fore optic of diameter 2.54 cm to ensure that the field of view was smaller than the sample with a diameter of 47 mm. In addition, all emissivity measurements were performed under conditions of clear sky without clouds and low to moderate relative humidity (<60%). Calibration and operation procedures of the FTIR spectrometer were the same as described by Agudelo-Castañeda et al. (2015). After optimizing the measurements using certified solid standards, measurements for $PM_{1.0}$ samples were taken. The spectra were analyzed in the range of 1660–700 cm^{-1}, with a spectral resolution of 4 cm^{-1} and a spectral accuracy of ± 1 cm^{-1}.

Transmittance spectra were obtained by a BOMEM MB-series FTIR-Hartmann & Braun Michelson spectrometer equipped with DTGS detector at the Institute of Physics of the Federal University of Rio Grande do Sul. Fifty scans of transmittance spectra with a resolution of 4 cm^{-1} were performed in the range of 400–4000 cm^{-1} to obtain an appropriate signal-to-noise ratio. Transmittance spectra were collected from each sample of $PM_{1.0}$ and are presented in arbitrary units (a.u.) using a background spectrum of blank filter.

3.3. Preparation and analysis of the NPAH solid standards and $PM_{1.0}$ samples

3.3.1. Transmittance spectra

The NPAH solid standards (6-nitrochrysene, 2-nitrofluorene, and 1-nitropyrene) were prepared in solid KBr pellets to obtain transmittance spectra. $PM_{1.0}$ samples were analyzed directly without any preparation. The molecular vibrations of transmittance spectra were identified on the basis of earlier studies (Semmler et al., 1991; Carrasco-Flores et al., 2005; Onchoke et al., 2006; Onchoke and Parks, 2011).

3.3.2. Emissivity spectra

NPAH solid standards were used as received and were placed in 50 mm diameter dishes, and then the spectra were acquired. The samples were analyzed directly without any preparation. The molecular vibrations corresponding to the peaks in the spectra were identified based on the earlier studies (Semmler et al., 1991; Carrasco-Flores et al., 2005; Onchoke et al., 2006; Onchoke and Parks, 2011).

3.4. Toxicity calculation

Carcinogenic risk was estimated using toxic equivalent factors (TEFs). The "toxic equivalent" scheme weighs the toxicity of the less toxic compounds as fractions of the toxicity of the most toxic PAH, benzo[a]pyrene (BaP). BaP is believed to be the most toxic PAH and has been well characterized toxicologically. However, less information is available about other organic compounds, and their toxicity is expressed in terms of equivalent toxicity of BaP (Jung et al., 2010). TEF data comparing the inhalation unit risk factor of a compound relative to the inhalation unit risk factor of BaP were obtained by OEHHA (OEHHA, 2005) and other works (Di Filippo et al., 2010). Eq. (1) was used to calculate the carcinogenic risk:

$$\text{Carcinogenic risk} = \left[\sum_i [\text{NPAH}]_i \text{TEF}_{\text{NPAH}_i}\right] \times \text{UR}_{\text{B[a]P}}, \quad (1)$$

where $[NPAH]_i$ is the individual atmospheric concentrations of NPAHs (expressed in ng/m^3) and TEF_{NPAHi} is the individual TEFs of each NPAH. $UR_{B[a]P}$ is the inhalation cancer unit risk factor of BaP ($=1.1 \times 10^{-6}$ (ng/m^3)$^{-1}$) calculated from cancer potency factors (CPFs) using the following relationship:

$$UR_i = \frac{CPF_i \times 20\,m^3}{70\,kg \times CV}, \quad (2)$$

where CPF_i is the inhalation cancer potency factor of the compound i ($=3.9$ (mg(kg day)$^{-1}$)$^{-1}$ for BaP), 20 m^3 is the reference human inspiration rate per day, 70 kg is the reference human body weight, and CV is the conversion factor from mg to ng ($=1 \times 10^6$) (OEHHA, 2005).

Mutagenic risk was calculated using Eq. (1), replacing the TEF data by the mutagenic potency factors (MEFs) established by Durant et al. (1996).

4. Results and discussion

4.1. Solid standard transmittance and emissivity spectra

Transmittance and emissivity spectra of the solid standards 1-nitropyrene, 2-nitrofluorene, and 6-nitrochrysene (99% purity) were analyzed and the functional groups of each of these NPAHs were identified. The same wavelengths were considered for the molecular vibrations found in the transmittance spectra as well as in the emissivity spectra. The identification of the vibrations of the molecules was based on previous studies, which investigated them with theoretical methods and matrix isolation methods (Carrasco-Flores et al., 2004, 2007; Onchoke and Parks, 2011).

Fig. 2 shows the transmittance spectra for 1-nitropyrene, 2-nitrofluorene, and 6-nitrochrysene for the region 4000–450 cm^{-1}. Infrared spectra of NPAH displayed transmittance features of high intensity in three regions of the mid-infrared range. Symmetric and asymmetric stretching vibrations of the nitro group appeared between 1330 and 1350 cm^{-1} and between 1520 and 1590 cm^{-1}, respectively. Low-intensity absorptions, near 1300 cm^{-1}, are caused by C–N stretching vibrations and C–H out-of-plane bending. Broad and weak absorptions between 3100 and 3000 cm^{-1}, due to C–H stretching vibrations, are present in the spectra of all compounds.

Fig. 3 represents the emissivity spectra of all studied NPAH standards. For emissivity, the 1660–3330 cm^{-1} range was not analyzed due to a low signal-to-noise ratio of the equipment in this range, and also in this range, the transmittance is low due to the presence of absorption bands of methane, CO_2, and water vapor (Korb et al., 1996; Agudelo-Castañeda et al., 2015). Table 1 shows the vibrational assignment of the representative peaks observed in the experimental transmittance and emissivity spectra of 1-nitropyrene, 2-nitrofluorene, and 6-nitrochrysene. The absorption bands corresponding to CO_2 and atmospheric water vapor in the range of 700 cm^{-1} and 1646 cm^{-1} have been excluded from Table 1 (Jellison and Miller, 2004; Agudelo-Castañeda et al., 2015). Thus, the region of greatest utility in Fourier transform infrared spectra of nitro-PAHs is from 1590 to 500 cm^{-1}. The band due to C–H stretch around 3100 cm^{-1} is usually broad and of very low intensity in comparison with other bands in the spectrum. A small number of bands are found near 500 cm^{-1}, but these are also of low intensity and therefore have less analytical importance. The low-intensity absorption caused by C–H stretch is just discernible near 3080 cm^{-1}.

4.1.1. 1-Nitropyrene

1-Nitropyrene is formed from direct emissions and can be used as a tracer of diesel engine emission in the atmosphere, as reported by Hien et al. (2007). This compound can form spontaneously through atmospheric reaction of nitrogen oxide with pyrene in the presence of a trace amount of nitric acid and photochemical oxidation of 1-aminopyrene under ultraviolet irradiation (Chan, 1996).

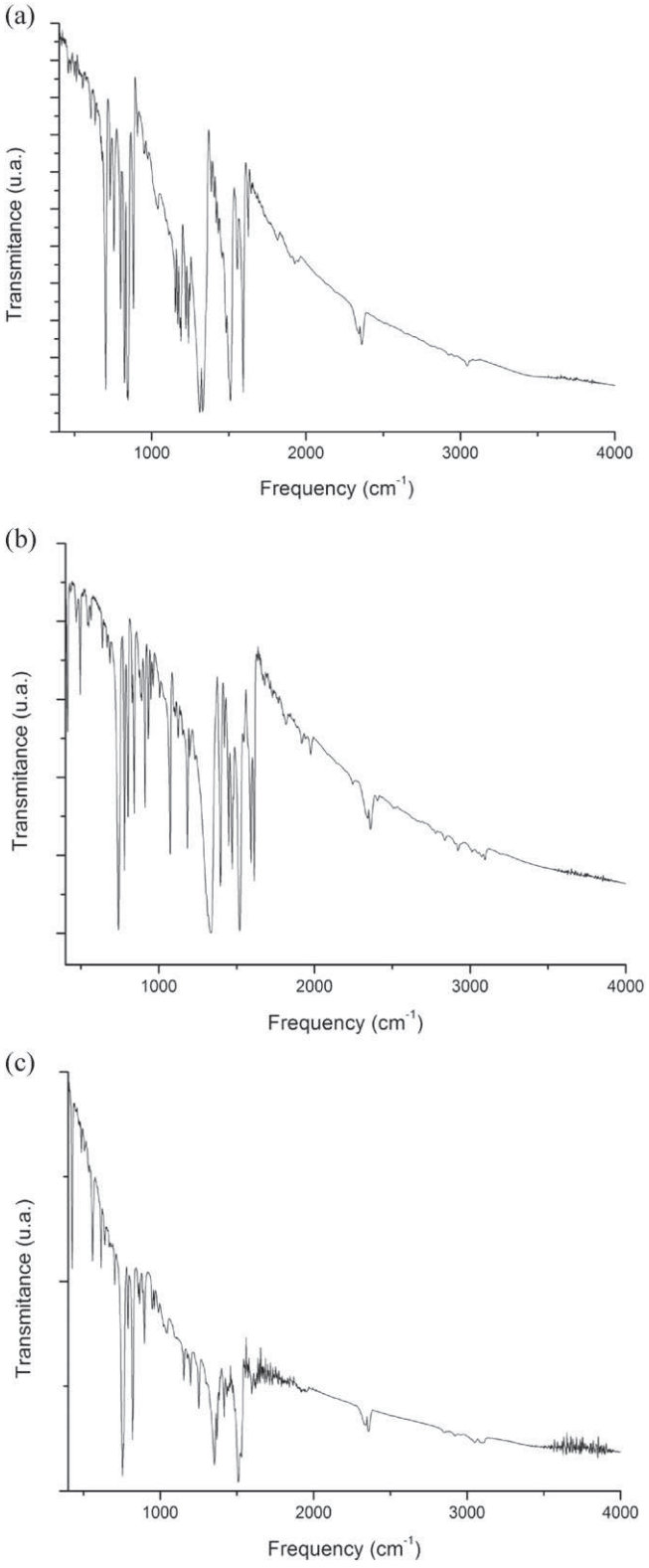

Fig. 2. Transmittance spectra of 1-nitroyrene (a), 2-nitrofluorene (b) and 6-nitrochrysene (c) solid standards recorded on KBr pellets.

Figs. 2(a) and 3(a) show the transmittance and emissivity spectra of 1-nitropyrene, and Table 1 presents the vibrational assignment of the representative peaks observed. As can be seen, the strongest features are due to the symmetric and antisymmetric stretching of the NO_2 group that appeared at 1330 and 1510 cm^{-1}, respectively. Another

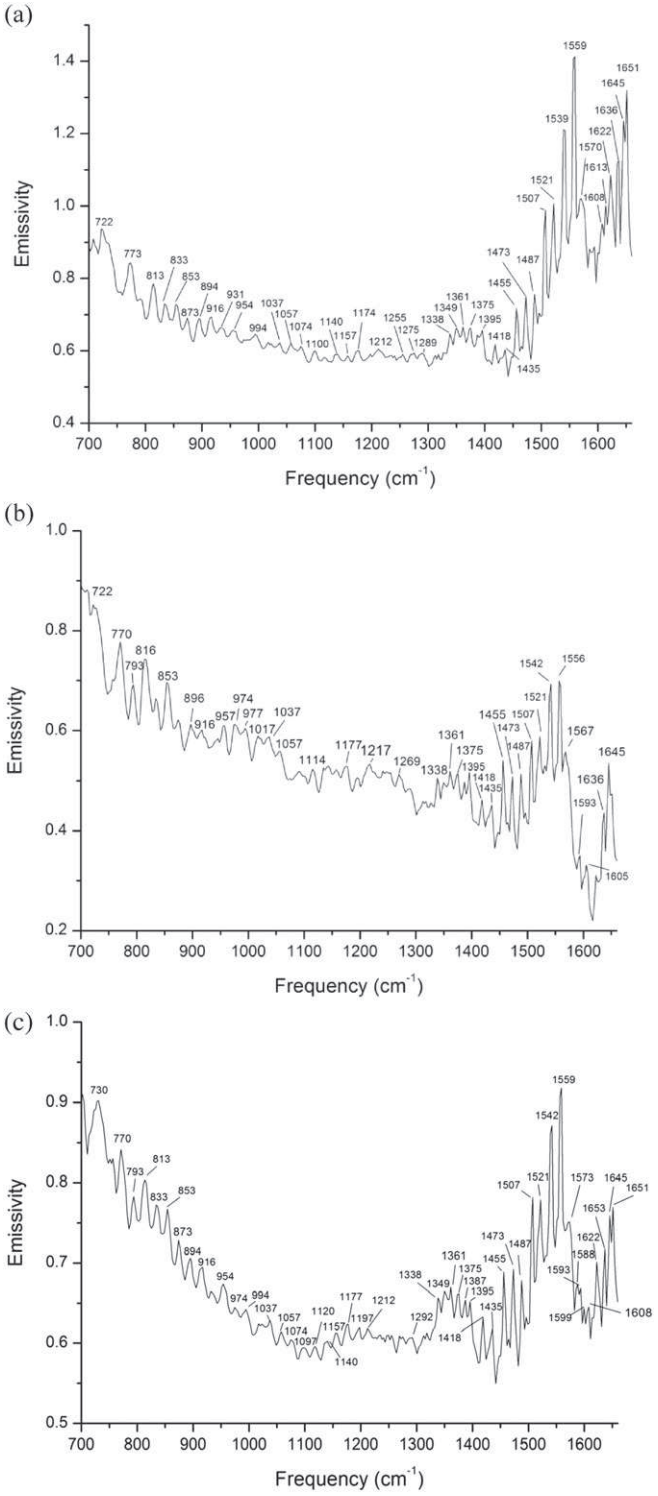

Fig. 3. Emissivity spectra of 1-nitropyrene (a), 2-nitrofluorene (b) and 6-nitrochrysene (c) solid standards recorded in 47-mm dishes.

strong band appears at 1309 cm^{-1} and is related to the C–N stretching of the nitro group. We also observed fundamental stretching modes related to C═C of the conjugated systems (between 1593 cm^{-1} and 1650 cm^{-1}) and ring stretching and C–H in-plane deformation (1238 cm^{-1}), i.e., characteristic vibrational modes of the chromophore (Carrasco-Flores et al., 2004). Bands of lower intensity are observed related to ring stretching modes, mainly in-plane C–C stretches within the aromatic ring, whereas C–H bending corresponds to in-plane C–C–H angle deformation around the aromatic ring. The in-phase wagging is introduced to indicate a collective vibration where all the out-of-plane C–H wags are in the same direction (Carrasco-Flores et al., 2004).

4.1.2. 2-Nitrofluorene

Nitrofluorenes are present in diesel exhaust and can be formed by photochemical reactions and as a result of nitration of fluorene too (Beije and Möller, 1988). 2-Nitrofluorene is a compound with low symmetry and therefore has vibration bands that are active in the infrared region. Transmittance and emissivity spectra of this compound are shown in Figs. 2(b) and 3(b). The designation of the identified features in the experimental transmittance spectra is presented in Table 1. The most intense infrared bands were assigned to the NO_2 symmetric

Table 1
Designation of features identified in the experimental transmittance (400–4000 cm^{-1}) and emissivity spectra (700–1660 cm^{-1}) of the solid standards of 1-nitropyrene, 2-nitrofluorene, and 6-nitrochrysene. Unit: cm^{-1}.

1-Nitropyrene		2-Nitrofluorene		6-Nitrochrysene		Vibrational assignment
Trans.	Emis.	Trans.	Emis.	Trans.	Emis.	
		495		559		Ring deformation
605						Ring twisting
				615		Ring deformation
634						Ring breathing
				703		Ring deformation
730	722				730	CH wag
		740				CH out-of-plane def. + CH_2 twisting
756				754		CH wag
				761		CH wag
	773	779	770		770	CH out-of-plane def. + CH_2 twisting
				790	793	CH wag
798		804				Ring deformation
823	813		816	819	813	Ring deformation + CH wag
	833					CH wag + CH out-of-plane def.
846	853	842				CH wag + CH out-of-plane def.
			853	856	853	Ring deformation
				865		CH wag
881		883				Ring deformation + CH wag
		889		896	894	CH out-of-plane def. + CH_2 wag
908	916	912	916			CH out-of-plane def. + CH_2 wag
		933				CH out-of-plane def. + CH_2 wag
		950		948	954	CH out-of-plane def. + CH wag
		964	957	962		CH wag
		1074				CH wag
	1100		1114			CCH in-plane def.
1153	1157			1153	1157	CCH in-plane def.
1168	1174		1177		1177	CCH in-plane def.
1189		1184				CCH in-plane def. + CH_2 wag
				1197	1197	CCH in-plane def.
1220	1212		1217			CCH in-plane def.
1238						CCH in-plane def. + Ring str.
				1251		CCH in-plane def.
1309						CN str. + CCH in-plane def.
1330	1338	1334	1338	1352	1349	NO_2 symm. str + CN str.
				1369	1375	CC str. + CH in-plane def.
		1396	1395		1395	CC str. + CH in-plane def.
	1418			1417		CC str. + CH in-plane def.
	1455	1448	1455		1455	CC str. + CH in-plane def.
	1473	1471	1473		1473	CC str. + CH in-plane def.
	1487		1487		1487	CC str. + CH in-plane def.
1510	1507	1519	1507	1510	1507	NO_2 antisymm. str.
	1539		1542	1531	1542	CC stretching
1554	1559		1556		1559	CC stretching
1593		1591	1593	1596		NO_2 antisymm. str. + CC str.
1625	1622				1622	CC stretching
	1636		1636			CC stretching
	1651		1645		1651	CC stretching
3045						CH stretching

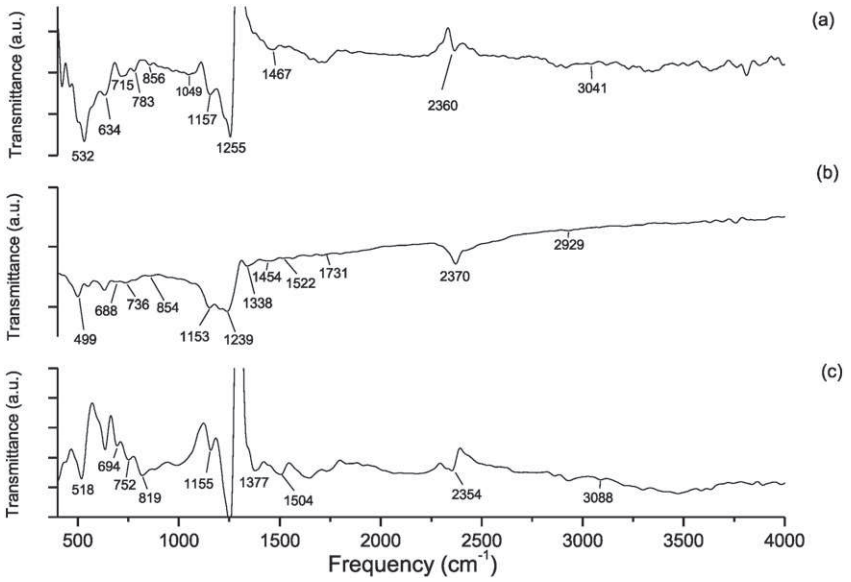

Fig. 4. Transmittance spectra of PM_1 sample in (a) Sapucaia do Sul, May 11, 2013, (b) Canoas, May 27, 2013 and (c) Canoas, May 4, 2013.

stretching mode at 1334 cm^{-1} and to the antisymmetric mode at 1519 and 1591 cm^{-1}. The CN stretching band was observed at 1334 cm^{-1}. Bands appearing in the region 1400–1650 cm^{-1} were assigned to CC stretching modes; the most intense bands below 1000 cm^{-1} were attributed to out-of-plane CH modes. Planar CH bending modes, i.e., C–H in-plane deformation, are clearly observed between 1000 and 1300 cm^{-1}.

4.1.3. 6-Nitrochrysene

6-Nitrochrysene is emitted directly by diesel vehicles (Albinet et al., 2007). Figs. 2(c) and 3(c) show the infrared transmittance and emissivity spectra of 6-nitrochrysene. A band at 1352 cm^{-1} assigned to the symmetric stretching and a band at 1510 cm^{-1} corresponding to the asymmetric stretching of the NO_2 group can also be seen; both bands displayed a strong relative intensity. The asymmetry and broadness of

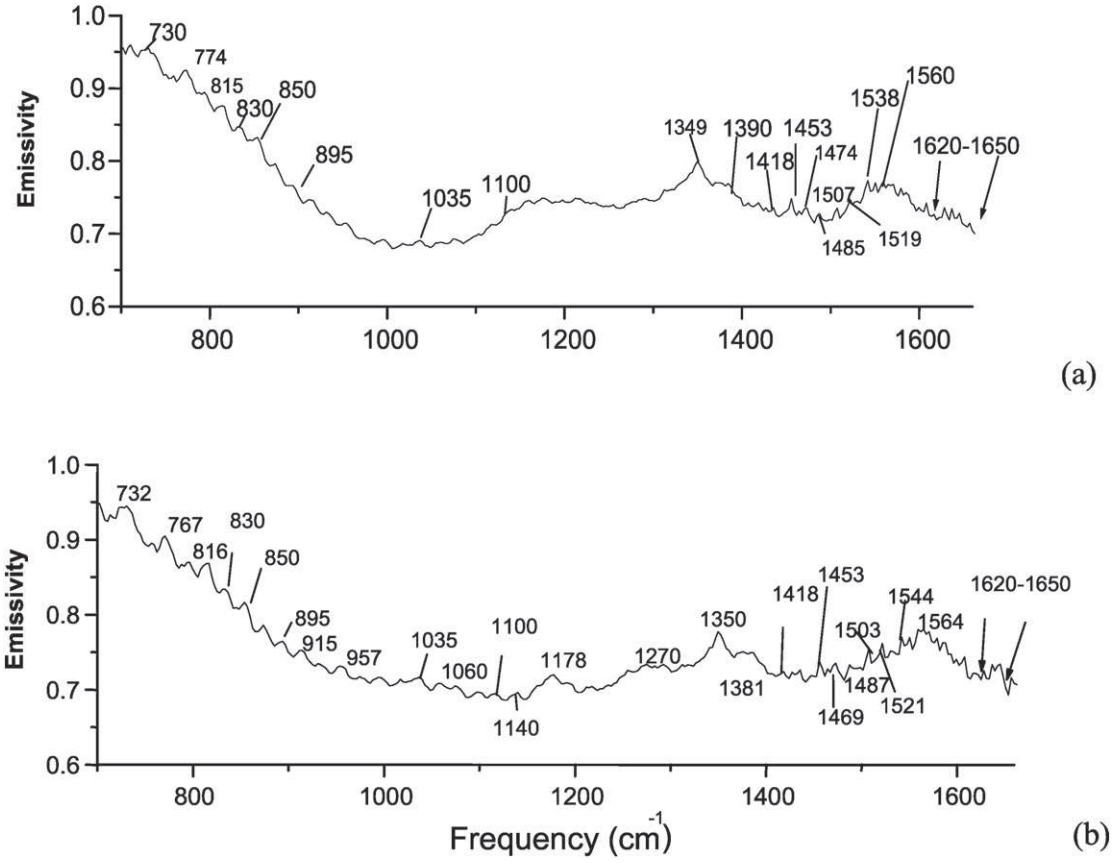

Fig. 5. Emissivity spectra of PM_1 sample in Canoas (a), May 2–5, 2012, and in Sapucaia do Sul (b), Jan 22–25, 2012.

Table 2
Average NPAH concentrations in PM_1 for winter and summer in Canoas and Sapucaia do Sul sites reported by Garcia et al. (2014). Concentrations expressed in ng/m^3.

NHPAs	Canoas		Sapucaia do Sul	
	Winter	Summer	Winter	Summer
1-Nitronaphthalene	0.1864	0.0063	0.1141	0.0094
1-Nitropyrene	0.0170	0.0098	0.0345	0.0201
2-Nitrofluorene	0.0138	0.0078	0.0197	0.0212
3-Nitrofluoranthene	0.0288	0.0170	0.0512	0.0426
6-Nitrochrysene	0.0429	0.0105	0.0342	0.0128

the first band suggests the existence of another mode probably involving the nitro group: the CN stretching vibration (Carrasco-Flores et al., 2005). The aromatic CC stretching modes are observed between 1370 and 1650 cm^{-1}, whereas the bands observed between 1530 and 1600 cm^{-1} are also attributable to inter-ring CC stretching modes (Carrasco-Flores et al., 2005). The fact that some bands are not observed in the spectrum of 6-Nchr could be associated with an anchorage effect induced by an interaction between the oxygen atoms of the nitro group and the adjacent H atoms.

Out-of-plane CH modes are observed between 1000 and 700 cm^{-1}. Ring deformations are present in the region of the lower frequency. At least three medium bands at 896, 790, and 703 cm^{-1} are observable only in the spectrum of 6-Nchr; this is probably due to a molecular symmetry descent imposed by the NO_2 group.

4.2. Atmospheric particulate matter samples ($PM_{1.0}$)

In this study, NPAHs were characterized especially by bands of the NO_2 functional group, their fingerprint bands. Figs. 4 and 5 show the transmittance and emissivity spectra of the samples of $PM_{1.0}$, respectively, for the Canoas and Sapucaia do Sul sites. It is noteworthy that both the transmittance and emissivity spectra of the samples (Figs. 4 and 5) are showing broader bands and lower relative intensity upon comparison with the spectra of NPAH standards (Figs. 2 and 3). This is due to the fact that the intensity and width of the bands depend on composition and density of these compounds (Kubicki, 2001). Furthermore, broadening of the bands (in comparison with the solid standards) in the $PM_{1.0}$ sample spectra can be attributed as a result of the interaction between organic compounds and the filter surface (Dabestani and Ivanov, 1999; Agudelo-Castañeda et al., 2015), and attributed to the fact that the particulate matter was collected in a heterogeneous medium (e.g., adsorbed onto a filter). In addition, the forms, intensities, and number of features depend on the relative masses and bonding forces (Hamilton, 2010).

Moreover, the low concentrations of NPAHs in the study area should be considered as a factor that caused broader bands in the sample spectra, as reported by Garcia et al. (2014). They reported average concentrations of hydrocarbons, for Sapucaia do Sul, in the following order: 1-nitropyrene (0.0276 ng/m^3) > 6-nitrochrysene (0.0240 ng/m^3) > 2-nitrofluorene (0.0205 ng/m^3). For Canoas, the observed order was 6-nitrochrysene (0.0284 ng/m^3) > 1-nitropyrene (0.0138 ng/m^3) > 2-nitrofluorene (0.0111 ng/m^3). Therefore, as can be seen by comparing the transmittance and emissivity spectra of the samples (Figs. 4 and 5) with the spectra of the solid standards (Figs. 2 and 3), the standards showed clearer and stronger bands than those of $PM_{1.0}$ samples. However, for many vibrational modes, the frequency is characteristic of the specific functional group in which the motion is centered and is minimally affected by the nature of other atoms in the molecule (Griffiths and Haseth, 2007). Therefore, in general, transmittance and emissivity show significant spectral response, and provide useful outcomes upon comparison. So, it is possible to identify the vibrational interactions of the main functional groups present in the standards of 1-nitropyrene, 2-nitrofluorene, and 6-nitrochrysene.

Fig. 4(a) and (c) show the transmittance spectra of $PM_{1.0}$ samples at Sapucaia do Sul on May 11, 2013 (Fig. 4(a)) and at Canoas on May 27, 2013 (Fig. 4(b)) and on May 4, 2013 (Fig. 4(c)). Canoas transmittance spectrum sampled on May 27, 2013 (Fig. 4(b)) showed less strong peaks than other spectra (Fig. 4(a) and (c)). This can be explained by particulate matter concentration; and as well the NPAH compounds present in this sample were lower in quantity than those in the other samples.

The spectra in Fig. 4(a)–(c) show different peaks in 600–900 cm^{-1} spectral range, corresponding to the vibrations of the aromatic rings, which can also be seen in the spectra of NPAH standards. Some peaks are also centered in the 1000–1500 cm^{-1} spectral range, corresponding to the C=C stretching of aromatics, in addition to the C–H in-plane angular deformation. Nevertheless, in the transmittance spectra, the peaks in the 1250–1300 cm^{-1} range are strongly affected by the presence of the carbon–fluorine (C–F) bond. In this region, a high intensity peak was observed due to the influence of the filter (PTFE), and therefore it is difficult to unambiguously identify bands of the compounds at this frequency. Low-intensity peaks corresponding to C–H vibrations of the aromatic groups are observed in the region between 3000 and 3100 cm^{-1}. The bands in this spectral range are observable only for the samples presented in Fig. 4(a) and (c), and completely absent in the sample of Canoas site in Fig. 4(b). Consequently, the bands observed in the $PM_{1.0}$ samples show low intensity in this spectral region and, as reported earlier, this can be attributed to low organic compound level (few nanograms per cubic meter), especially of NPAHs (Garcia et al., 2014).

The transmittance spectrum of $PM_{1.0}$ (Sapucaia do Sul on May 11, 2013) (Fig. 4(a)) in the 600–900 cm^{-1} spectral range showed a peak at 634 cm^{-1} that was identified in the spectrum of 1-nitropyrene (Table 1). However, at this frequency (634 cm^{-1}) molecular vibrations from sulfite ions (SO_3^{2-}) present in the particulate matter can also be observed (Tsai and Kuo, 2006). The peaks observed at 715, 783, and

Table 3
NPAH toxic equivalent factors (TEFs) and mutagenic potency factors (MEFs) relative to BaP.

Compounds	TEFs[a]	MEFs[b]
1-Nitronaphthalene	–	–
1-Nitropyrene	0.1	0.025
2-Nitrofluorene	0.01	–
3-Nitrofluoranthene	–	0.0026
6-Nitrochrysene	10	–

[a] Data from OEHHA (2005).
[b] Data from Durant et al. (1996).

Table 4
Total carcinogenic risk calculated from three NPAHs considering the TEFs.

NHPAs	Canoas		Sapucaia do Sul	
	Winter	Summer	Winter	Summer
1-Nitronaphthalene	–	–	–	–
1-Nitropyrene	1.90E−09	1.09E−09	3.84E−09	2.23E−09
2-Nitrofluorene	1.54E−10	8.70E−11	2.20E−10	2.37E−10
3-Nitrofluoranthene	–	–	–	–
6-Nitrochrysene	4.78E−07	1.17E−07	3.81E−07	1.43E−07
Total	4.80E−07	1.18E−07	3.85E−07	1.46E−07

Table 5
Total mutagenic risk calculated from three NPAHs considering the MEFs.

NHPAs	Canoas		Sapucaia do Sul	
	Winter	Summer	Winter	Summer
1-Nitronaphthalene	–	–	–	–
1-Nitropyrene	4.75E−10	2.73E−10	9.61E−10	5.59E−10
2-Nitrofluorene	–	–	–	–
3-Nitrofluoranthene	8.36E−11	4.92E−11	1.48E−10	1.23E−10
6-Nitrochrysene	–	–	–	–
Total	5.58E−10	3.23E−10	1.11E−09	6.82E−10

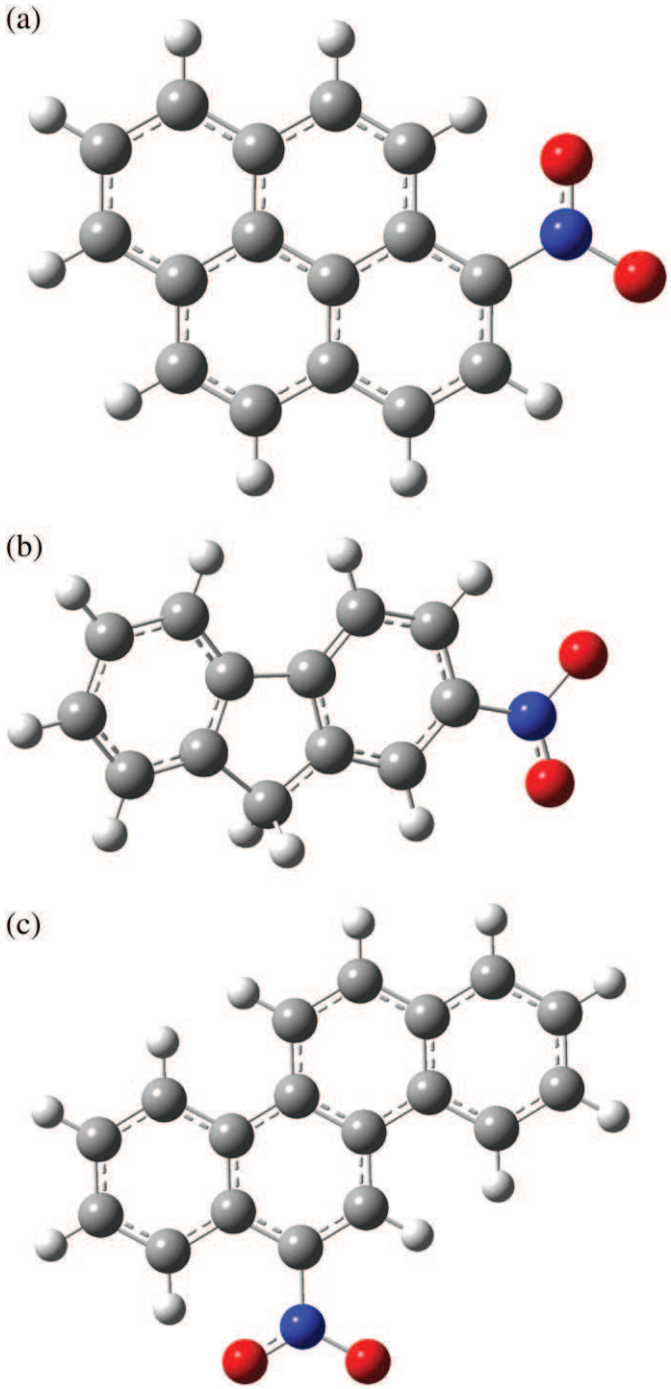

Fig. 6. Molecules (a) 1-nitropyrene, (b) 2-nitrofluorene, and (c) 6-nitrochrysene.

856 cm^{-1} correspond to 5, 3, and 2 C–H neighboring units (connected) in the aromatic rings, respectively (Semmler et al., 1991; Agudelo-Castañeda et al., 2015). In 1000–1500 cm^{-1} spectral range, the transmittance spectrum shows peaks at 1049, 1157, 1255, and 1467 cm^{-1}. Some of these bands are identified in the 1-nitropyrene, 2-nitrofluorene, and 6-nitrochrysene spectra (Table 1) due to C–H out-of-plane angular deformations or C–H wagging. At 1049 cm^{-1} and 783 cm^{-1} frequencies, overlapping may occur due to SiO_4^{-4} ion, which also contributes to frequencies in this region, typical of silicate ions (Tsai and Kuo, 2006). A peak is also identified at 3041 cm^{-1} due to aromatic C–H stretch observed in the spectra of 1-nitropyrene.

The transmittance spectrum of $PM_{1.0}$ in Fig. 4(b) (Canoas on May 27, 2013) shows peaks at 688 cm^{-1}, 736 cm^{-1}, and 854 cm^{-1} due to C–H out-of-plane angular deformations of 5, 4, and 2 CH neighboring units, respectively. Nonetheless, at 688 cm^{-1}, molecular vibrations arising from sulfite ions (SO_3^{2-}) may occur (Tsai and Kuo, 2006). Bands are also identified at 1153 and 1239 cm^{-1} due to C–H in-plane angular deformations, and at 1454 cm^{-1} due to C–C stretch and C–H in-plane angular deformations, respectively. The bands observed at 1338 and 1522 cm^{-1} are due to the NO_2 group, related to the symmetric stretching for 1-nitropyrene and 2-nitrofluorene and to the antisymmetric stretching for 2-nitrofluorene, respectively. As explained above, no bands in 3000–3100 cm^{-1} spectral range could be seen. Vibrations from carbonyl and aliphatic groups can be inferred by the presence of bands at 1731 and 2929 cm^{-1}, respectively (Agudelo-Castañeda et al., 2015).

The transmittance spectrum of $PM_{1.0}$ in Fig. 4(c) (Canoas on May 4, 2013) shows peaks at 694, 752, and 819 cm^{-1}. As shown in Table 1, these peaks are related to the ring deformation and CH wagging of the 6-nitrochrysene. Also, at 694 cm^{-1}, molecular vibrations from sulfite ions (SO_3^{2-}) may occur (Tsai and Kuo, 2006). The peak presented at 1504 cm^{-1} is due to NO_2 antisymmetric stretching. We could not observe the symmetric stretch of the NO_2 group due to the presence of the C–F bond in the 1250–1300 cm^{-1} region. A peak in the 3000–3100 cm^{-1} spectral range, at 3088 cm^{-1}, corresponding to C–H stretching, can also be observed.

Fig. 5(a) and (b) show the emissivity spectra of $PM_{1.0}$ samples in Canoas and Sapucaia do Sul, respectively. In the emissivity spectra (Fig. 5), peaks may be observed in the range of 730–1000 cm^{-1} resulting from ring deformation, C–H wagging, and C–H out-of-plane angular deformation. Peaks in the range of 1390–1560 cm^{-1} resulting from C–C stretch vibrations and related to C–H in-plane angular deformation were observed between 1100 and 1490 cm^{-1}. The emissivity spectra of $PM_{1.0}$ samples (Fig. 5) displayed different peaks appearing in the 1620–1650 cm^{-1} spectral range. An array of compounds absorb radiation in this region, including –OH present in water, alcohols, and carboxylic acids, and the carbonyl stretch (C═O) such as amides that are more conjugated than aldehydes, ketones, and acids (Reff et al., 2005). It is worth to mention that the vibrational mode ν_2 of liquid water appears at 1640 cm^{-1}. Thus, these bands overlap and hinder the identification of organic compounds. Moreover, the emissivity spectra exhibit a peak at ~1100 cm^{-1}, which corresponds to the carbon–fluorine bond (C–F); consequently, bands at this frequency may overlap and, therefore, cannot be identified unambiguously (Ghauch et al., 2006; Agudelo-Castañeda et al., 2015).

For the identification of NPAHs, it is important to observe the spectral features related to the nitro group. The bands at 1338 and 1349 cm^{-1} are assigned to the symmetric stretching and the band at 1507 cm^{-1} corresponds to the antisymmetric stretching of the NO_2 group. Thus, although it is not possible to quantitatively determine the NPAH contents of this sample through the emissivity spectra, it is possible to infer the presence of the three NPAHs evaluated in this study: both samples showed symmetrical stretching of the nitro group at 1338 cm^{-1} for 1-nitropyrene and 2-nitrofluorene and at 1349 cm^{-1} for 6-nitrochrysene, and due to the antisymmetric stretching bands at 1507 cm^{-1} for the three compounds.

4.3. Toxicity

For risk calculation we used the NPAHs concentrations in $PM_{1.0}$ reported by Garcia et al. (2014). They determined concentrations of five NPAHs by gas chromatography with an electron capture detector. Table 2 shows the average NPAH concentrations in $PM_{1.0}$ for winter and summer in Canoas and Sapucaia do Sul sites (Garcia et al., 2014).

Table 3 presents TEFs and MEFs relative to BaP. TEFs were not available for 1-nitronaphthalene and 3-nitrofluoranthene, and there were no MEFs for 1-nitronaphthalene, 2-nitrofluorene, and 6-nitrochrysene. Therefore, the total carcinogenic and mutagenic risks were calculated considering only the NPAHs, for those equivalent factors were available,

by using Eq. (1). Tables 4 and 5 show the total carcinogenic risk and the total mutagenic risk calculated considering the TEFs and MEFs, respectively.

According to IARC classification, 6-nitrochrysene and 1-nitropyrene are classified as belonging to Group 2A (probably carcinogenic to humans), 2-nitrofluorene to Group 2B (possibly carcinogenic to humans), and 3-nitrofluoranthene and 1-nitronaphthalene to Group 3 (not classifiable as carcinogenic to humans). As reported by Onchoke (2008) and Onchoke et al. (2009), one of the main reasons for these differences in the carcinogenic classification is the position of the nitro group in the molecule. For example, in the case of mono nitrated fluoranthene isomers, there are significant differences in their mutagenic properties (2-, 3-, and 8-isomers are more toxic than 1- and 7-isomers) (Onchoke and Parks, 2011). As indicated in these studies, these mutagenic effects of NPAHs were related to the nitro group orientation relative to the aromatic moiety. Based on the observed mutagenic potencies and X-ray diffraction structures of NPAHs (e.g., 6-nitrobenzo[a]pyrene and 7-nitrobenz[a,h]anthracene [Fu et al., 1998; Warner et al., 2003]), it has been proposed that nitro-PAHs with planar CCNO dihedral angles relative to the aromatic moiety tend to exhibit greater mutagenic potencies compared with nonplanar NPAHs. Thus, correlations between vibrational spectra and biological activities can have predictive powers for toxicity of nitro-PAHs. In this study, we have shown some examples of molecules, e.g., 1-nitropyrene, 2-nitrofluorene, and 6-nitrochrysene (Fig. 6).

The risks associated with NPAH have already been reported (Albinet et al., 2008; Di Filippo et al., 2010). The carcinogenic and mutagenic risks are higher during the cold periods, as expected, as the winter presented higher compound concentrations (Di Filippo et al., 2010; Garcia et al., 2014). The results indicated that the carcinogenic risk is higher than the mutagenic risk. The carcinogenic risk associated with the studied NPAHs can reach close to 99% of the total risk due to the presence of 6-nitrochrysene, especially due to their TEF = 10, higher than that indicated by other studied NPAHs.

The 85% levels of the mutagenic risks are associated with 1-nitropyrene. Probably, because 1-nitropyrene MEF is about 10 times higher than that associated with 3-nitrofluoranthene (included in the calculation of the mutagenic risk). Another consideration that must be taken into account is that the calculation of carcinogenic and mutagenic risks involved different NPAHs, as the equivalent factors were unavailable for all the compounds.

In this study, the carcinogenic risk from NPAHs in airborne particles varied between 1.18×10^{-7} and 4.80×10^{-7} (Table 4) and showed similar levels to those observed in the studies of Albinet et al. (2008) and Huang et al. (2014). The mutagenic risk varied between 3.23×10^{-10} and 1.11×10^{-9} (Table 5). We are not aware about any other study that evaluated the mutagenic risk, and therefore we are not able to make comparisons with other locations around the world.

The greatest carcinogenic risk levels were found in Canoas, while in contrast, the highest mutagenic risk levels were observed in Sapucaia do Sul. As can be seen in Table 2, Sapucaia do Sul showed higher concentrations of 1-nitropyrene than Canoas. This compound originates from incomplete combustion, especially from diesel engine exhaust, and is formed by electrophilic nitration (Arey, 1998; Garcia et al., 2014). Thus, as the mutagenic risk is mainly associated with the concentration of 1-nitropyrene, as shown in Table 2, higher levels of this compound in winter can be verified in Sapucaia do Sul. On the other hand, Canoas showed higher carcinogenic risk due to higher levels of 6-nitrochrysene observed at this location, especially in winter. This compound is directly emitted by diesel engines (Feilberg et al., 2001; Albinet et al., 2007; Garcia et al., 2014), and in this site, there is a great influence of heavy vehicles.

These results indicate that the total lifetime cancer and mutagenic risks induced by NPAHs in the study area should not be neglected and may represent some concern, especially by direct emissions generated by the incomplete combustion processes and/or by means of chemical reactions between PAHs (Albinet et al., 2008; Fan et al., 1995; Walgraeve et al., 2010; Wang et al., 2010). These compounds are favored by stagnant meteorological conditions during the cold season. This impact could be even more negative for the most sensitive population: elderly people and children.

5. Conclusions

The measurements of both emissivity and transmittance spectra using infrared spectroscopy allowed us to identify organic functional groups in atmospheric particulate matter of size <1.0 μm ($PM_{1.0}$). In addition, transmittance and emissivity spectra of the solid standards (1-nitropyrene, 2-nitrofluorene, and 6-nitrochrysene) contributed in the identification of NPAHs in $PM_{1.0}$.

Although organic compounds in atmospheric particulate matter are poorly studied, this study ratifies that NPAHs may be differentiated by their infrared spectral fingerprints using the two methods described in this work: transmittance and emissivity spectra.

The results of toxicity risk relative to NPAHs in $PM_{1.0}$ indicated that the carcinogenic risk is higher than the mutagenic risk. The carcinogenic and mutagenic risks were higher during the cold periods, explained by higher NPAHs concentrations in this period.

The carcinogenic and mutagenic risks for the studied NPAHs were found to be about 99% and 85% for 6-nitrochrysene and 1-nitropyrene, respectively.

The results also point to the possibility of negative impacts on the health of people exposed in the study area, urban region with a greater vehicular influence: light and heavy fleet.

The role of NPAHs in atmospheric particle toxicity needs further investigations; in particular, the relation between vibrational spectra and biological activities that can have predictive powers for toxicity of nitro-PAHs. In addition, the position of the nitro groups in the molecule can have significant differences in their carcinogenic and mutagenic properties.

Acknowledgments

We would like to thank CAPES and CNPq for their financial support.

References

Agudelo-Castañeda, D.M., Teixeira, E.C., Schneider, I.L., Rolim, S.B.A., Balzaretti, N., Silva e Silva, G., 2015. Comparison of emissivity, transmittance, and reflectance infrared spectra of polycyclic aromatic hydrocarbons with those of atmospheric particulates (PM_1). Aerosol Air Qual. Res. 15 (4), 1627–1639.

Albinet, A., Leoz-Garziandia, E., Budzinski, H., Villenave, E., 2007. Polycyclic aromatic hydrocarbons (PAHs), nitrated PAHs and oxygenated PAHs in ambient air of the Marseilles area (south of France): concentrations and sources. Sci. Total Environ. 384 (1–3), 280–292.

Albinet, A., Leoz-Garzilandia, E., Budzinski, H., Villenave, E., Jaffrezo, J.L., 2008. Nitrated and oxygenated derivatives of polycyclic aromatic hydrocarbons in the ambient air of two French alpine valleys — part 1: concentrations sources and gas/particle partitioning. Atmos. Environ. 42 (1), 43–54.

Arenas-Lago, D., Veja, F.A., Silva, L.F.O., Andrade, M.L., 2013. Soil interaction and fractionation of added cadmium in some Galician soils. Microchem. J. 110, 681–690.

Arey, J., 1998. Atmospheric reactions of PAHs including formation of Nitroarenes. In: Neilson, A.H. (Ed.), PAHs and related compounds. The Handbook of environmentalchemistry, pp. 347–385.

Atkinson, R., Ashcmann, S., 1994. Products of the gas-phase reactions of aromatic hydrocarbons: effect of NO_2 concentration. In. J. Chem. Kinet. 26 (9), 929–932.

Bamford, H.A., Bezabeh, D.Z., Schantz, M.M., Wise, S.A., Baker, J.E., 2003. Determination and comparison of nitrated-polycyclic aromatic hydrocarbons measured in air and diesel particulate reference materials. Chemosphere 50 (5), 575–587.

Beije, B., Möller, L., 1988. 2-Nitrofluorene and related compounds: prevalence and biological effects. Mutat. Res. 196 (2), 177–209.

Carrasco-Flores, E.A., Clavijo, R.E., Campos-Vallette, M.M., Aroca, R.F., 2004. Vibrational spectra and surface-enhanced vibrational spectra of 1-nitropyrene. Appl. Spectrosc. 58 (5), 555–561.

Carrasco-Flores, E.A., Campos-Vallete, M.M., REC, C., Leyton, P., Díaz, G.F., Koch, R., 2005. SERS spectrum and DFT calculations of 6-nitrochrysene on silver islands. Vib. Spectrosc. 37 (2), 153–160.

Carrasco-Flores, E.A., Campos-Vallette, M.M., Clavijo, R.E., 2007. Surface-enhanced vibrational spectra of 2-nitrofluorene. Spectrochim. Acta A 66 (2), 474–479.

Cerqueira, B., Vega, F.A., Serra, C., Silva, L.F.O., Andrade, M.L., 2011. Time of flight secondary ion mass spectrometry and high-resolution transmission electron microscopy/energy dispersive spectroscopy: a preliminary study of the distribution of Cu^{2+} and Cu^{2+}/Pb^{2+} on a Bt horizon surfaces. J. Hazard. Mater. 195, 422–431.

Cerqueira, B., Vega, F.A., Silva, L.F.O., Andrade, L., 2012. Effects of vegetation on chemical and mineralogical characteristics of soils developed on a decantation bank from a copper mine. Sci. Total Environ. 421–422, 220–229.

Chan, P.C., 1996. Technical Report on Toxicity Studies of 1-Nitropyrene. National Toxicology Program Toxicity, Report Series Number 34. United States Department of Health and Human Services.

Coury, C., Dillner, A.M., 2008. A method to quantify organic functional groups and inorganic compounds in ambient aerosols using attenuated total reflectance FTIR spectroscopy and multivariate chemometric techniques. Atmos. Environ. 42 (23), 5923–5932.

Crimmins, B.S., Baker, J.E., 2006. Improved GC/MS methods for measuring hourly PAH and nitro-PAH concentrations in urban particulate matter. Atmos. Environ. 40 (35), 6764–6779.

Dabestani, R., Ivanov, N.I., 1999. A compilation of physical, spectroscopic and photophysical properties of polycyclic aromatic hydrocarbons. Photochem. Photobiol. 70 (1), 10–34.

DETRAN — Departamento Estadual de Trânsito (RS), 2013. Available in: http://www.detran.rs.gov.br/index.php?action=estatistica&codItem=99.

Di Filippo, P., Riccardi, C., Pomata, D., Buiarelli, F., 2010. Concentrations of PAHs and nitro- and methyl-derivatives associated with a size segregated urban aerosol. Atmos. Environ. 44 (23), 2742–2749.

Durant, J.L., Busby Jr., W.F., Lafleur, A.L., Penman, B.W., Crespi, C.L., 1996. Human cell mutagenicity of oxygenated, nitrated and unsubstituted polycyclic aromatic hydrocarbons associated with urban aerosols. Mutat. Res. 371 (3–4), 123–157.

Fan, Z., Chen, D., Birla, P., Kamens, R.M., 1995. Modeling of nitro-polycyclic aromatic hydrocarbon formation and decay in the atmosphere. Atmos. Environ. 29 (10), 1171–1181.

Feilberg, A., Nielsen, T., 2000. Effect of aerosol chemical composition on the photodegradation of nitro-polycyclic aromatic hydrocarbons. Environ. Sci. Technol. 34 (5), 789–797.

Feilberg, A.B., Poulsen, M.W., Nielsen, T., Skov, H., 2001. Occurrence and sources of particulate nitro-polycyclic aromatic hydrocarbons in ambient air in Denmark. Atmos. Environ. 35 (2), 353–366.

Fu, P.P., von Tungeln, L.S., Chiu, L.H., Zhan, D.J., Deck, J., Bucci, T., Wang, J.C., 1998. Structure, tumorigenicity, microsomal metabolism and DNA binding of 7-nitrodibenz[a,h]anthracene. Chem. Res. Toxicol. 11 (8), 937–945.

Garcia, K.O., Teixeira, E.C., Agudelo-Castañeda, D.M., Braga, M., Alabarse, P.G., Wiegand, F., Kautzamann, R.M., Silva, L.F.O., 2014. Assessment of nitro-polycyclic aromatic hydrocarbons in PM_1 near an area of heavy-duty traffic. Sci. Total Environ. 479–480, 57–65.

Ghauch, A., Deveau, P.A., Jacob, V., Baussand, P., 2006. Use of FTIR spectroscopy coupled with ATR for the determination of atmospheric compounds. Talanta 68 (4), 1294–1302.

Griffiths, P.R., Haseth, J.A., 2007. Fourier Transform Infrared Spectrometry. 2th ed. John Wiley & Sons, Inc., New Jersey.

Hamilton, V.E., 2010. Thermal infrared (vibrational) spectroscopy of Mg–Fe olivines: a review and applications to determining the composition of planetary surfaces. Chem. Erde-Geochem. 70 (1), 7–33.

Hammes, G.G., 2005. Spectroscopy for the Biological Sciences. 1st ed. John Wiley & Sons, Inc., New York.

Hien, T.T., Thanh, L.T., Kameda, T., Takenaka, N., Bandow, H., 2007. Nitro-polycyclic aromatic hydrocarbons and polycyclic aromatic hydrocarbons in particulate matter in an urban area of a tropical region: Ho Chi Minh City, Vietnam. Atmos. Environ. 41 (36), 7715–7725.

Huang, B., Liu, M., Bi, X., Chaemfa, C., Ren, Z., Wang, X., et al., 2014. Phase distribution, sources and risk assessment of PAHs, NPAHs and OPAHs in a rural site of Pearl River Delta region, China. Atmos. Pollut. Res. 5 (2), 210–218.

IARC – International Agency for Research on Cancer, 2013. In: Straif, K., Cohen, A., Samet, J. (Eds.), Air Pollution and Cancer. IARC Scientific Publications vol. 161.

IBGE — Instituto Brasileiro de Geografia e Estatística, 2010. Available in: http://www.ibge.gov.br/home/estatistica/populacao/censo2010/default.shtm.

Jellison, G.P., Miller, D.P., 2004. Plume structure and dynamics from thermocouple and spectrometer measurements. Proc. SPIE 5425, 232–243.

Jinhui, X., Lee, F.S.C., 2001. Analysis of nitrated polynuclear aromatic hydrocarbons. Chemosphere 42 (3), 245–250.

Jung, K.H., Yan, B., Chillrud, S.N., Perera, F.P., Whyatt, R., Camann, D., et al., 2010. Assessment of benzo(a)pyrene-equivalent carcinogenicity and mutagenicity of residential indoor versus outdoor polycyclic aromatic hydrocarbons exposing young children in New York City. Int. J. Environ. Res. Public Health 7 (5), 1889–1900.

Kamens, R.M., Guo, J., Guo, Z., Mcdow, S.R., 1990. Polynuclear aromatic hydrocarbon degradation by heterogeneous reactions with N_2O_5 on atmospheric particles. Atmos. Environ. 24 (5), 1161–1173.

Korb, A.R., Dybwad, P., Wadsworth, W., Salisbury, J.W., 1996. Portable Fourier transform infrared spectroradiometer for field measurements of radiance and emissivity. Appl. Opt. 35 (10), 1679–1692.

Kubicki, J.D., 2001. Interpretation of vibrational spectra using molecular orbital theory calculations. Rev. Mineral. Geochem. 42 (1), 459–483.

Kumata, H., Uchida, M., Sakuma, E., Uchida, T., Fujiwara, K., Tsuzuki, M., et al., 2006. Compound class specific ^{14}C analysis of polycyclic aromatic hydrocarbons associated with PM_{10} and $PM_{1.1}$ aerosols from residential areas of suburban Tokyo. Environ. Sci. Technol. 40 (11), 3474–3480.

Nielsen, T., 1984. Reactivity of polycyclic aromatic hydrocarbons toward nitrating species. Environ. Sci. Technol. 18 (3), 157–163.

OEHHA — Office of Environmental Health Hazard Assessment, 2005. Air Toxics Hot Spots Program Risk Assessment Guidelines. Part II: Technical Support Document for Describing Available Cancer Potency Factors. Office of Environmental Health Hazard Assessment (Available in: http://www.oehha.ca.gov/air/hot_spots/pdf/May2005Hotspots.pdf).

Oliveira, M.L.S., Ward, C.R., Izquierdo, M., Sampaio, C.H., de Brum, I.A.S., Kautzmann, R.M., et al., 2012a. Chemical composition and minerals in pyrite ash of an abandoned sulphuric acid production plant. Sci. Total Environ. 430, 34–47.

Oliveira, M.L.S., Ward, C.R., French, D., Hower, J.C., Querol, X., Silva, L.F.O., 2012b. Mineralogy and leaching characteristics of beneficiated coal products from Santa Catarina, Brazil. Int. J. Coal Geol. 94, 314–325.

Onchoke, K.K., 2008. Density functional theoretical study of mono-nitrated fluoranthenes. Polycycl. Aromat. Compd. 28 (3), 193–212.

Onchoke, K.K., Parks, M., 2011. Experimental and theoretical study of vibrational spectra of 3-nitrofluoranthene. J. Mol. Struct. 999 (1–3), 22–28.

Onchoke, K.K., Hadad, C.M., Dutta, P.K., 2006. Structure and vibrational spectra of mononitrated benzo[a]pyrenes. J. Phys. Chem. A 110 (1), 76–84.

Onchoke, K.K., Parks, M., Nolan, A.H., 2009. A DFT study of the vibrational spectra of 1-, and 2-nitrotriphenylene. Spectrochim. Acta A 74 (2), 579–587.

Peltonen, K., Kuljukka, T., 1995. Air sampling and analysis of polycyclic aromatic hydrocarbons. J. Chromatogr. A 710 (1), 93–108.

Pham, C.T., Kameda, T., Toriba, A., Hayakawa, K., 2013. Polycyclic aromatic hydrocarbons and nitropolycyclic aromatic hydrocarbons in particulates emitted by motorcycles. Environ. Pollut. 183, 175–183.

Quispe, D., Pérez-López, R., Silva, L.F.O., Nieto, J.M., 2012. Changes in mobility of hazardous elements during coal combustion in Santa Catarina Power Plant (Brazil). Fuel 94, 495–503.

Reff, A., Turpin, B.J., Porcja, R.J., Giovennetti, R., Cui, W., Weisel, C.P., et al., 2005. Functional group characterization of indoor, outdoor, and personal $PM_{2.5}$: results from RIOPA. Indoor Air 15 (1), 53–61.

Ribeiro, J., Flores, D., Ward, C.R., Silva, L.F.O., 2010. Identification of nanominerals and nanoparticles in burning coal waste piles from Portugal. Sci. Total Environ. 408 (23), 6032–6041.

Ritter, C.L., Culp, S.J., Freeman, J.P., Marques, M.M., Beland, F.A., Malejka-Giganti, D., 2002. DNA adducts from nitroreduction of 2,7-dinitrofluorene, a mammary gland carcinogen, catalyzed by rat liver or mammary gland cytosol. Chem. Res. Toxicol. 15 (4), 536–544.

Seinfeld, J.H., Pandis, S.N., 2006. Atmospheric Chemistry and Physics: From Air Pollution to Climate Change. 2nd ed. John Wiley, New York.

Semmler, J., Yang, P.W., Crawford, G.E., 1991. Gas chromatography/Fourier transform infrared studies of gas-phase polynuclear aromatic hydrocarbons. Vib. Spectrosc. 2 (4), 189–203.

Silva, L.F.O., Moreno, T., Querol, X., 2009. An introductory TEM study of Fe-nanominerals within coal fly ash. Sci. Total Environ. 407 (17), 4972–4974.

Slezakova, K., Pereira, M.C., Reis, M.A., Alvim-Ferraz, M.C., 2007. Influence of traffic emissions on the composition of atmospheric particles of different sizes — part 1: concentrations and elemental characterization. J. Atmos. Chem. 58 (1), 55–68.

Tang, N., Hattori, T., Taga, R., Igarashi, K., Yang, X.Y., Tamura, K., et al., 2005. Polycyclic aromatic hydrocarbons and nitro polycyclic aromatic hydrocarbons in urban air particulates and their relationship to emission sources in the Pan–Japan sea countries. Atmos. Environ. 39 (32), 5817–5826.

Teixeira, E.C., Garcia, K.O., Meincke, L., Leal, K.A., 2011. Study of nitro-polycyclic aromatic hydrocarbons in fine and coarse atmospheric particles. Atmos. Res. 101 (3), 631–639.

Tsai, Y., Kuo, S., 2006. Development of diffuse reflectance infrared fourier transform spectroscopy for the rapid characterization of aerosols. Atmos. Environ. 40 (10), 1781–1793.

Turpin, B.J., Saxena, P., Andrews, E., 2000. Measuring and simulating particulate organics in the atmosphere: problems and prospects. Atmos. Environ. 34 (18), 2983–3013.

Walgraeve, C., Demeestere, K., Dewulf, J., Zimmermann, R., Langenhove, H.V., 2010. Oxygenated polycyclic aromatic hydrocarbons in atmospheric particulate matter: molecular characterization and occurrence. Atmos. Environ. 44 (15), 1831–1846.

Wang, F., Costabile, F., Li, H., Fang, D., Alligrini, I., 2010. Measurements of ultrafine particle size distribution near Rome. Atmos. Res. 98 (1), 69–77.

Warner, S.D., Lebuis, A.M., Farant, J.P., Butler, I.S., 2003. Crystal structure of 6-nitrobenzo(a)pyrene. J. Chem. Crystallogr. 33 (3), 213–217.

Yang, H.H., Chien, S.M., Chao, M.R., Lin, C.C., 2005. Particle size distribution of polycyclic aromatic hydrocarbons in motorcycle exhaust emissions. J. Hazard. Mater. 125 (1–3), 154–159.

Yu, J., Flagan, R.C., Seinfeld, J.H., 1998. Identification of products containing –COOH, –OH, and –C=O in atmospheric oxidation of hydrocarbons. Environ. Sci. Technol. 32 (16), 2357–2370.

Zhao, Y., Chen, Z., 2010. Application of Fourier transform infrared spectroscopy in the study of atmospheric heterogeneous processes. Appl. Spectrosc. Rev. 45 (1), 63–91.

4. ARTIGO: Chemical characterization and source apportionment of PM_1 in a metropolitan area of Brazil

SCHNEIDER, I. L.; TEIXEIRA, E. C.; SILVA, L. F. O.; AGUDELO-CASTAÑEDA, D. M.; LANDIM, A.A.; QUEROL, X.. Chemical characterization and source apportionment of PM1 in a metropolitan area of Brazil. Atmospheric Environment, *under review*.

Chemical characterization and source apportionment of PM_1 in a metropolitan area of Brazil

Ismael Luís Schneider[a], Elba Calesso Teixeira[a,b,1] Luis Felipe Oliveira Silva[c], Dayana Milena Agudelo-Castañeda[d], Albert Ayres Landim[e], Xavier Querol[f]

[a] Postgraduate Program in Remote Sensing and Meteorology, Universidade Federal do Rio Grande do Sul. Av. Bento Gonçalves, 9500, Porto Alegre, RS, Brazil, 91501-970.

[b] Research Department, Fundação Estadual de Proteção Ambiental Henrique Luís Roessler, Av. Borges de Medeiros, 261, Porto Alegre, RS, Brazil, 90020-021.

[c] Laboratory of Environmental Researches and Nanotechnology Development, Centro Universitário La Salle, Mestrado em Avaliação de Impactos Ambientais, Av. Victor Barreto, 2288, Canoas, RS, Brazil, 92010–000.

[d] Research group in Environmental Management and Sustainability. Faculty of Environmental Sciences. Universidad De La Costa. Calle 58 #55-66, Barranquilla, Colombia, 080002.

[e] Universidade Federal do Pampa. Av. Pedro Anunciação, 111, Caçapava do Sul, RS, Brazil, 96570-000.

[f] Institute of Environmental Assessment and Water Research (IDAEA), CSIC, Barcelona, Spain

Abstract

We evaluated the ambient concentrations of particulate matter <1 μm (PM_1) and metals, as well as we identified and quantified the source contributions using the Positive Matrix Factorization (PMF) receptor modeling in the Metropolitan Area of Porto Alegre, Rio Grande do Sul, Brazil. PM_1 samples were collected on PTFE filters from December 2012 to December 2014. Major and trace elements and soluble ion concentrations were determined. Results evidenced significantly higher levels in winter than in summer; also that most of PM_1 and the analyzed PM species and elements originated from anthropogenic sources, especially road traffic, combustion processes and industrial activities, grouped in 7 major contributing sources or mixed sources contributions. A back trajectory analysis showed that the long range transport of pollutants is not relevant concerning contribution to PM_1 and metal concentrations, and that most probably regional-local sources account for most of these ambient air loads.

Keywords: PM_1, Trace elements, Source apportionment, PMF, Back trajectory.

[1] Corresponding author: Tel: +55 51 32889408

E-mail address: gerpro.pesquisa@fepam.rs.gov.br (E. Calesso Teixeira)

1. Introduction

Atmospheric particulate matter (PM) originates from a variety of emission sources, including the natural and anthropogenic ones. Moreover, PM may be emitted directly into the atmosphere (primary PM) or formed in the atmosphere from gaseous precursors (secondary PM) (Pey et al., 2009). Among emission sources, heavy industries are considered to be a major anthropogenic trace metal sources (Zheng et al., 2010; Zhou et al., 2014), although traffic emissions could also be considered an important source of PM and metals in urban atmospheres (Lough et al., 2005; Birmili et al., 2006; Johansson et al., 2009). Particles emitted from combustion process can be formed through transfer of inherent mineral matter into PM with minor phase changes (mostly coarse particles, in the range of 1 to 10 μm (PM_{1-10}), with the exception of the diesel soot, with a mode around 0.04-0.06 μm, and through nucleation and condensation of gaseous precursors, and agglomeration of nanoparticles (in this case yielding ultrafine and fine particles) (Ninomiya et al., 2004 ; Yoo et al., 2005; Saarnio et al., 2014). However, modern city waste incineration plants have extremely low nanoparticle emissions (Buonanno et al., 2009; Ragazzi et al., 2013).

Atmospheric PM is one of the most important atmospheric pollutants and undergoes a high variability concerning levels and composition (Nazir et al., 2011). Different components of PM may have diverse health impacts, and although increased PM-mass concentration is associated to increased mortality and morbidity, it is still unclear which specific components should be abated to diminish the health effects from ambient aerosols (WHO, 2013).

The chemical composition of PM is particularly important for environmental assessment of specific source contributions to ambient air PM (Almeida et al., 2006). There is a wide range of known sources contributing to the increase of metal levels, such as Na, Ca, K, Al, Fe, As, Se, Ti and heavy metals, in the finer PM fractions (Sanderson et al., 2014). Concentrations of metals with lower boiling point (As, Cd, Zn) were found to decrease with particle size, whereas those with higher boiling points (Co, Cr, Fe, Sb, Sc, Sm, Th, Eu, Yb) increase with particle size. The more volatile elements emitted in gaseous form at high temperatures nucleate or condense during cooling (Helble, 2000; Sanderson et al., 2014), whereas less volatile elements remained in the solid phase (Buonanno et al., 2011).

Particles with different aerodynamic diameters have different impacts on human health because fine particles may penetrate more deeply into the respiratory system. The fine

particles contain higher concentrations of toxic metals, such as Pb, Cd, and Ni (Kauppinen and Pakkanen, 1990; Lin et al., 2005; Yoo et al., 2005; Tao et al., 2012; Cheng et al., 2014). Studies identifying trace elements tracing the contribution of specific emission sources to particulate matter (based on receptor source profiles) based on air quality data are relatively scarce, due to the fact that (1) it is difficult to establish a direct link between markers and specific emission sources for some elements; and (ii) tracers are generally not unique and source profiles may change with time (Querol et al., 2007 as an example). Some of these studies focus on road traffic emissions, while others present tracers of industrial sources, mostly from combustion processes, smelters and other high temperature processes. Nevertheless, few data are available on specific tracer elements for specific industrial processes.

Receptor modeling is one of the most commonly used tools to identify and quantify the contribution of individual emission sources to ambient levels of atmospheric particulate matter. It offers a way to achieve this by measuring the concentration of pollutants at a sampling site (Hopke, 1991). One type of receptor model is the multivariate model, which was recently improved significantly due to a new approach called positive matrix factorization (PMF) developed by Paatero and others (Paatero and Tapper, 1994; Paatero, 1997) using a least squares approach. PMF is an advanced source apportionment method to assess particle source contributions successfully, applied in many different places around the world (Aldabe et al., 2011).

As a consequence of the growing interest of the scientific community in submicron particulate matter and of the lack on PM_1 data (Caggiano et al., 2010), especially in Latin America, we started a temporal extended study on this fraction to obtain statistically significant data from the Metropolitan Area of Porto Alegre, Rio Grande do Sul, Brazil. The work included the following aspects: (1) a chemical characterization of PM_1 samples, (2) source apportionment analysis for source contributions, and (3) a cross-correlation analysis of major and trace elements and calculation of the enrichment factors to support source attributions. Therefore, the results of this research represent an important contribution to the knowledge of submicron particles measured at ground level and evaluate these particles impact on environment and human health in the study area. The data obtained may be useful

for programs to reduce air pollution and could motivate future studies on metal distribution, source contribution and enrichment factor on the clean atmospheric background.

2. Material and methods

2.1. Study area

The Metropolitan Area of Porto Alegre (MAPA), located in southern Brazil, is the most urbanized area of the state of Rio Grande do Sul. This region is characterized by different types of industries, including some stationary sources such as the Alberto Pasqualini Refinery (REFAP), steel mills which do not use coke, III Petrochemical Industrial Complex, coal-fired power plants, and a cement grinding mill (Figure 1). Besides, it is estimated that there is a significant contribution of mobile sources due to the large number of vehicles in circulation in the region (Teixeira et al., 2008, 2010; Agudelo-Castañeda et al., 2014). Currently, gasoline-fueled vehicles use a mixture of gasoline and 20% of ethanol and the diesel used contains 500 ppm of sulfur and 5% of biodiesel is added (Mattiuzi et al., 2012; PETROBRAS, 2012). Even if the diesel fleet in the region is less than 7%, the environmental impact caused by this source in the air is elevated and that they are responsible for most particulate matter and NO_X emissions (Teixeira et al., 2012).

The sampling sites locations (Sapucaia do Sul and Canoas), located to the north of Porto Alegre, are shown in Figure 1. Sapucaia do Sul sampling site has a greater industrial (oil refinery and steel mills) and vehicular influence than Canoas, it is located near a highway where there is heavy vehicle traffic of light and heavy fleet with daily traffic congestion. Whereas, Canoas site is located beside the same highway, although in the opposite side, downstream of the prevailing winds. Canoas is also under a strong road traffic influence, with daily traffic congestion, and the Canoas air base and industries (oil refinery).

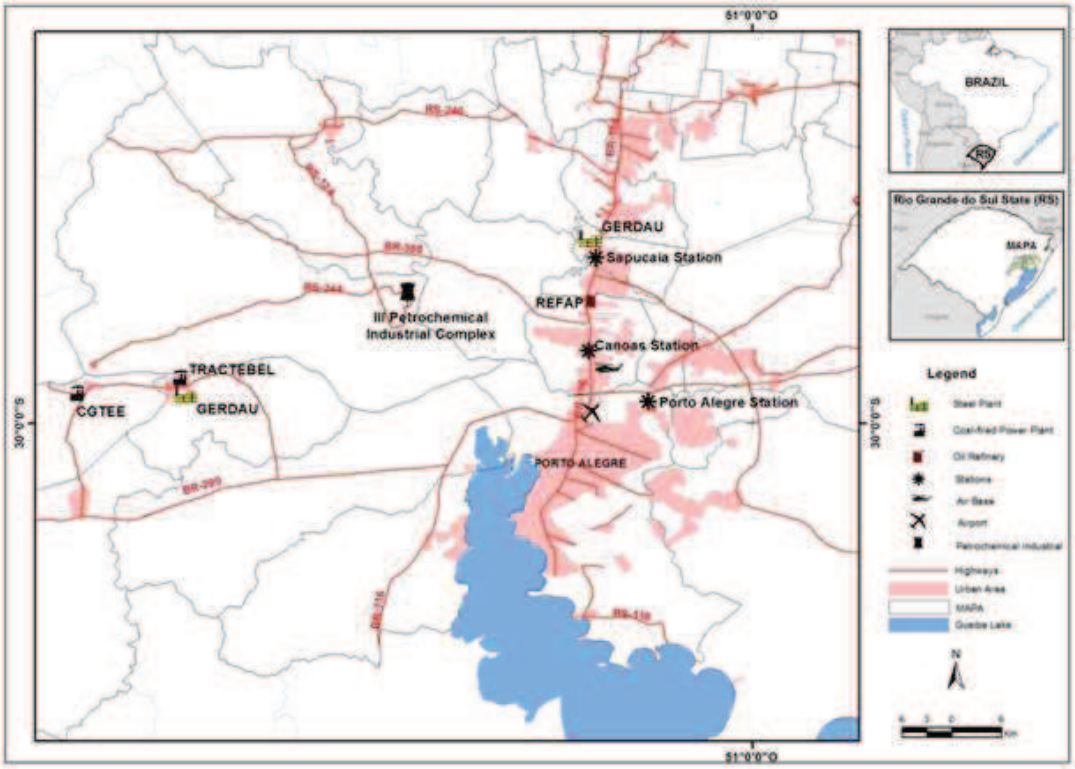

Figure 1. Location of the sampling sites (Canoas and Sapucaia do Sul).

2.2. Sampling and analysis

Sampling of atmospheric PM_1 followed the criteria established by the USEPA (1994), using a sequential automatic particle sampler model PM162M of the Environnement S.A.. PM_1 sampler used the EN 12341 method (LECES, nº RC/L 9826) and included a set of two holders that act as support for the filters. Samples were collected on PTFE filters of 47 mm diameter for a continuous period of 72 h with a flow rate of 1.0 m^3/h. Were selected 38 samples of PM_1 for Sapucaia do Sul and 40 samples for Canoas from December 2012 to December 2014, in order to consider different seasonal conditions.

PM mass concentrations were determined by standard gravimetric procedures. Thereafter, ½ of each filter was acid digested ($HF:HNO_3:HClO_4$) for the determination of major (Al, Ca, Fe, K, Na, Mg, S, Ti, P) and trace elements (Li, Ti, V, Cr, Mn, Co, Ni, Cu, Zn, As, Se, Rb, Sr, Cd, Sn, Sb, Ba, rare earths, Pb, Bi, Th, U) by Inductively Coupled Plasma Atomic Emission and Mass Spectrometry (ICP-AES and ICP-MS). Another ¼ of each filter was water leached to determine soluble ion concentrations by ion chromatography (SO_4^{2-},

NO_3^- and Cl^-) and ion selective electrode (NH_4^+). More analytical details may be found in Querol et al. (2001).

A microscopy analysis of PM_1 samples was performed to check the chemical composition by applying Field Emission Scanning Electron Microscopy (FE-SEM). A manual analysis was performed with this scanning electron microscopy in order to evaluate the morphology and composition of individual particles. The particles were analyzed individually with energy-dispersive spectrometer mounted on a SEM (JEOL-7100 F) with an accelerating voltage of 20 keV.

2.3. Data analysis

2.3.1. Enrichment Factors

Enrichment Factors (EF) were calculated to identify the contribution of anthropogenic sources on the levels of a specific element in PM1.0 airborne particles. This information is very useful to identify the anthropogenic origin of the different elements, not only at the urban scale but also at a regional extent. In previous studies performed in atmospheric PM, several elements have been suggested as reference element of the natural crust (for example Al, Ti, and Fe) (Moreno et al., 2013). In this study, Ti was chosen as the reference element. To obtain such factors it is necessary to compare the concentration of the element in a sample to its concentration in the Upper Continental Crust (UCC), calculated with Equation 1:

$$EF_{Ti}(X_i) = (X_i/Ti)_{PM}/(X_i/Ti)_{Crust} \quad (1)$$

where, $(X_i/Ti)_{Crust}$ is the average ratio of the element of interests (X) and crustal representative element (Ti) (Mason, 1966), and $(X_i/Ti)_{PM}$ is the same ratio in particulate matter.

The degree of enrichment of trace metals with respect to the Earth's crust can be ranked in various levels: an EF close to 1 will suggest a natural origin for a certain element, whereas higher values will indicate an anthropogenic source to be more likely. However, despite a low EF be an indicative of its ''crustal'' origin, this cannot exclude the involvement of anthropogenic processes, like resuspension of rock-forming mineral dust by agriculture, construction works or traffic for example. Several authors indicate that a significant non-crustal source is assumed to be predominant when EF > 10, natural sources when EF < 1, and mixed sources when 1 < EF < 10 (Wu et al., 2009; Witt et al., 2010; Niu et al., 2015).

2.3.2. Source apportionment

A Positive Matrix Factorization (PMF) model was applied to the chemical dataset (78 samples) obtained through the chemical analysis, in order to investigate the temporal variability of the main PM_1 sources. PMF is a multivariate factor analysis tool that decomposes the data matrix into two matrices: factor contributions and factor profiles (Paatero and Tapper, 1994; Paatero, 1997) with a residual matrix (Vestenius et al., 2011). The fundamental principle of source/receptor relationships in receptor models is that mass conservation can be assumed and a mass balance analysis can be used to identify and apportion sources of airborne particulate matter in the atmosphere (Hopke, 2003):

$$x_{ij} = \sum_{k=1}^{p} g_{ik} f_{ik} + \sigma_{ij} \qquad i = 1, 2, \ldots, m \qquad j = 1, 2, \ldots, n \qquad (2)$$

where x_{ij} is the j^{th} species concentration measured in the i^{th} sample, g_{ik} is the contribution of the k^{th} source to the i^{th} sample, f_{jk} is the concentration of the j^{th} species in the k^{th} source and σ_{ij} is the residual associated with the j^{th} species concentration measured in the i^{th} sample. The task of PMF is to minimize the sum of the squares of the residuals weighted with the estimated uncertainties. The uncertainties were estimated according to the following equations:

$$\sigma_i = \sigma_i^a + 0.05 * x_i \qquad \text{if } x_i > DL_i \qquad (3)$$

$$\sigma_i = \frac{3}{2} * DL_i \qquad \text{if } x_i < DL_i$$

where x_i is the concentration of the i species, $\sigma^a{}_i$ is the analytical error calculated for the i species and DL_i are the detection limits calculated for each species calculated following the three-sigma criterion. Chemical species were selected based on the signal to noise ratio, the percentage of values above the detection limit and on the database size requirements. Based on these criterions, only 25 species were selected as strong species.

In this study we used the US-EPA PMF model version 5.0. This receptor model is described in more detail in other published studies (Amato et al., 2010; Minguillón et al., 2012; Teixeira et al., 2013; Agudelo-Castañeda and Teixeira, 2014).

2.3.3. Back trajectory analysis

In order to interpret the variation of PM_1 levels over time and the possible contribution of long range transport, the origin of air masses reaching the study area was investigated by

means of meteorological back trajectories. The Hysplit model (Draxler and Rolph, 2003; Stein et al., 2015) was used to calculate daily back-trajectories ending at 12:00 UTC for 5 days at 100 m and 1000 m above ground level. These heights were selected because they are within the boundary layer where the greater part of the interactions affecting the aerosols occurs and because represent mid to high layers of the boundary layer, respectively. Height different air mass scenarios were considered for this study according to the cardinal and collateral points of the initial position of each trajectory. To determine the pollutant sources, all the air mass back trajectories were clustered into eight types that were manually identified by visual analysis. The proportions of air masses associated with each track and the corresponding concentrations of PM_1 and chemical elements associated to each receptor model factor were calculated.

3. Results and discussion

3.1. PM_1 levels and elemental concentrations

Table 1 shows the PM_1 average concentration levels obtained in the two sampling sites. The average concentrations were 12.8 ±8.1 and 15.2 ±10.3 μg/m^3 for Canoas and Sapucaia do Sul sites, respectively. Higher $PM_{1.0}$ average concentration level in Sapucaia do Sul than in Canoas was observed. As stated above, this site has a stronger vehicular influence by dense traffic of passenger cars, but also of light and heavy-duty vehicles, frequent traffic congestion, and slow vehicle speed. This site receives also the industrial influence (oil refinery and steel mills that do not use coke) upstream from the prevailing winds, as reported in other studies (Teixeira et al., 2012, 2013; Agudelo-Castañeda and Teixeira, 2014). Compared with other works, PM1.0 average concentrations presented similar values to the other cities, except for Wuhan (China) (Cheng et al., 2014), where the concentrations were close to 10 times higher than those observed in the present study. These higher PM1.0 average concentrations, principally in China, are because this is a strongly polluted area impacted by intense particles sources emission such as traffic and coal-fired power combustion.

Table 1. Comparison of mean PM_1 levels and composition of this study with those from different areas reported around the world.

	Canoas [a]	Sapucaia [a]	Broechem/ Belgium [b]		Brisbane / Australia [c]	Tehran/Iran [d]	Brno/ Czech Republic [e]		/Australia [f]	Salento/Italy [g]	Frankfurt am Main/ Germany [h]	Tito Scalo/Italy [i]	Milan/Italy [j]		Helsinki/Finland [k]	Wuhan/China [l]		Barcelona/Spain [m]
µg/m³	Mean	Mean	Event day	Non event day			Summer	Winter					Winter	Summer		Wu Da	Tiang Hong	
PM_1	12.7	15.2	36.7	14.8	11.0	7.0-32.0	11.6	13.0	2.3-10.6	15.0		8.00	41.0	16.4	11.0	117	123	19.0
Al	0.13	0.15			0.002	0.03-0.07				0.07		0.11	0.02	0.01	0.02			
Ca	0.12	0.14			0.03					0.03		1.00	0.02	0.02	0.02	0.14	0.30	
Fe	0.09	0.13			0.02	0.13-0.17			0.001-1.27	0.06		0.10	0.09	0.04	0.06			
K	0.21	0.33	0.32	0.17	0.01					0.14		0.10	0.26	0.08	0.02	1.39	1.34	
Mg	0.01	0.02								0.005		0.00			0.01	0.05	0.05	
Na	0.11	0.15			ND					0.03		0.10			0.03	1.30	0.33	
SO_4^{2-}	1.10	1.41	5.80	1.70			1.01	1.27		2.30					1.29			2.90
NO_3^-	1.36	1.16	11.3	3.10			0.08	2.46		0.23					0.06	21.6	21.3	1.70
Cl^-	0.79	0.58			0.02					0.03			0.29	0.04	0.01	20.7	21.6	
NH_4^+	0.72	0.57	4.20	1.20			0.40	1.14		0.75					0.58	1.72	1.76	1.10
ng/m³																		
Ti	4	5			2	12-15			ND-3.7		5	6	7	4	1	10	12	2
V	0.6	0.8	7	3	0.6	ND-3			0.6-1	3	1		5	4	8			6
Cr	2	3	1	ND	3	2 - 3			ND-4	4	4	38	2	1				1
Mn	5	8	6	4	4	20-23			0.6-32	1	3	3	9	4	2			4
Ni	0.7	0.7	5	3	0.9	4-5			0.8-4	3	2	6	4	2	4			3
Cu	19	10	8	7	3	14-20			ND-25	2	11	4	4	3	2			12
Zn	33	59	63	30	6	84-161			3-146			6	66	32	7			48
As	0.5	1	4	2		4					0.6		2	1	0.4			0.6
Rb	0.8	1													0.1			0.2
Sr	0.3	0.4	1	ND	10	1									0.1			0.9
Cd	0.3	0.4			5.5	0.3				0.1		4			0.1			0.3
Sn	3	4				12-20												2
Sb	4	7									0.5				0.4			0.9
Ba	1	4				10-15				4					1			9
Pb	9	11	31	17	10	55-71				4	5	12	35	15	2			17
Region	urban	urban + industrial	urban		urban	urban	urban		industrial	urban	urban	industrial	urban		urban	urban		urban

a - This Study; b - Buczyńska et al. (2014); c - Crilley et al. (2014); d - Hassanvand et al. (2015); e - Mikuska et al. (2011); f - Mohiuddin et al. (2014); g - Perrone et al. (2013); h - Wiseman and Zereini (2014); i – Caggiano et al. (2010); j – Vecchi et al. (2004); k - Pakkanen et al. (2003); l – Cheng et al. (2014); m - Perez et al. (2008) ND - non detected

Average elemental concentrations in PM_1 measured at Canoas and Sapucaia do Sul compared with other researches are reported in Table 1. Major components of PM_1 were SO_4^{2-} and NO_3^-, followed by $NH4^+$ and Cl^-, and some crustal elements. Moreover, crustal elements and majors ions did not show much variation when compared with other studies, with the exception of Ca, for which high levels were obtained in our study, together with Tito Scalo (Italy) and Tiang Hong (China). Tito Scalo (Italy) was the site of highest level of Ca (1.0 $\mu g/m^3$) due, probably, to higher fine mineral dust particles emissions (Caggiano et al., 2010).

SO_4^{2-} and NO_3^- concentrations in Canoas and Sapucaia do Sul sites were found to be lower than Broechem-Antwerp (Belgium), Tito Scalo (Italy), Barcelona (Spain) and especially Wuhan (China) (~22.0 $\mu g/m^3$) (see references in Table 1). This last site shows significant differences in relation to other sites, influenced by high pollution sources as coal combustions (SO_2) and vehicles (NO_3^-). Some studies related the NO_3^-/SO_4^{2-} ratio to different anthropogenic sources (Cheng et al., 2014). The NO_3^-/SO_4^{2-} ratios of Canoas and Sapucaia do Sul were 1.2 and 0.8, respectively. For Canoas, the ratio suggested higher vehicular influence (>1.0) and stationary sources (<1.0) as dominant sources in Sapucaia do Sul for NO_3^- and SO_4^{2-}. Though, the influence of vehicle exhaust in Sapucaia do Sul site should not be neglected due to the rapid increase in the number of motor vehicles, confirmed by other studies (Teixeira et al., 2008; Agudelo-Castañeda and Teixeira, 2014).

Trace elements concentrations were compared with other researches done in cities around the world. PM_1 show enriched levels of Cu, Zn, Mn and Pb for Canoas and Sapucaia do Sul, although different in comparison with other cities. Concentrations of Zn differs from mostly all the cities, although levels were higher than Brisbane (Australia), Tito Scalo (Italy), Helsinki (Finland) and similar to Barcelona (Spain) and Broechem (Belgium) (see references for these sites in Table 1). Cu mean concentration for Canoas (19 ng/m^3) was different to mostly all countries, with higher values than the others studies except for Iran (Tehran) and Australia (New South Wales and Whyalla). For Sapucaia do Sul, Cu mean concentration (10 ng/m^3) was similar to Frankfurt (Germany) and Barcelona (Spain), and higher than the other studies, except for the studies done in Iran (Tehran) and Australia (New South Wales and Whyalla), countries with higher values than the results obtained in this research. Pb levels also were low compared to other countries, except for Iran (see references in Table 1). Ti and Sn showed similar or higher levels, except for Iran. Sb presented higher concentrations than all the compared countries, as can be observed in Table 1.

Table 2. Spearman's correlation (ρ) matrix for major and trace components in PM_1. Correlations in red correspond to summer and in black to winter.

	Al	Ca	Fe	K	Mg	Na	SO_4^{2-}	NO_3^-	Cl^-	NH_4^+	Ti	V	Cr	Mn	Ni	Cu	Zn	As	Rb	Sr	Cd	Sn	Sb	Ba	Pb	PM_1
Al	1.00	-0.15	0.33	0.23	0.72**	0.42*	.38*	-0.20	0.08	-0.06	0.33	0.12	0.21	0.25	0.13	0.30	0.17	0.45**	0.21	0.56**	0.22	0.47**	0.21	0.49**	0.21	0.18
Ca	0.38*	1.00	-0.02	0.17	0.01	0.43*	0.36*	-0.03	-0.11	-0.14	-0.51**	0.72**	.376*	-0.21	0.33	-0.34	0.00	0.29	-0.01	0.05	0.13	-0.22	-0.32	0.35*	-0.17	0.07
Fe	-0.01	-0.01	1.00	0.37*	0.23	0.19	0.24	-0.35*	-0.25	-0.01	0.20	0.15	0.46**	0.65**	0.31	0.34	0.46**	0.34	0.37*	0.33	0.09	0.28	0.50**	0.44**	0.31	0.22
K	-0.05	-0.16	0.64**	1.00	0.27	0.44**	0.66**	-0.02	-0.14	0.31	0.19	0.19	0.19	0.26	0.45**	0.42*	0.42*	0.61**	0.92**	0.53**	0.64**	0.11	0.56**	0.50**	0.56**	0.54**
Mg	0.83**	0.53**	0.07	-0.09	1.00	0.45**	0.42*	-0.21	0.14	-0.11	0.39*	0.19	0.25	0.11	0.16	0.04	0.12	0.48**	0.21	0.70**	0.19	0.28	-0.03	0.58**	0.03	0.11
Na	0.42*	0.38*	0.41*	0.53**	0.45**	1.00	0.72**	0.03	-0.08	-0.02	-0.20	0.38*	0.41*	0.06	0.46**	0.24	0.24	0.42*	0.39*	0.44*	0.47**	0.15	0.10	0.43*	0.34	0.14
SO_4^{2-}	0.07	-0.12	0.61**	0.35*	-0.11	0.18	1.00	0.15	-0.10	0.46**	-0.09	0.54**	0.49**	0.26	0.63**	0.22	0.45**	0.59**	0.64**	0.50**	0.63**	0.25	0.28	0.51**	0.32	0.53**
NO_3^-	0.01	-0.10	0.29	0.12	-0.02	0.01	0.13	1.00	0.02	0.25	-0.19	0.13	-0.09	-0.24	0.20	-0.07	-0.24	-0.03	0.06	-0.22	0.30	-0.02	0.00	-0.18	0.03	-0.09
Cl^-	0.24	-0.40*	0.13	0.20	0.14	0.07	0.28	0.24	1.00	-0.09	0.04	0.07	0.04	-0.01	-0.08	0.04	-0.04	0.15	-0.10	0.12	0.16	-0.07	0.05	-0.08	0.09	-0.26
NH_4^+	-0.12	-0.26	0.15	-0.01	-0.16	-0.20	0.25	0.81**	0.44**	1.00	0.05	0.04	0.00	0.09	0.47**	0.11	0.30	0.13	0.40*	0.12	0.30	0.09	0.45**	-0.03	0.16	0.44**
Ti	0.19	-0.29	0.63**	0.29	0.16	0.22	0.58**	0.20	0.31	0.21	1.00	-0.36*	-0.17	0.12	-0.09	0.20	0.06	0.11	0.22	0.48**	-0.11	0.18	0.22	0.19	0.11	0.18
V	0.50**	0.65**	0.02	0.00	0.62**	0.22	-0.07	-0.13	-0.17	-0.25	-0.16	1.00	0.67**	0.04	0.50**	-0.18	0.20	0.51**	0.12	0.23	0.29	0.02	-0.11	0.40*	-0.06	0.34*
Cr	0.23	0.70**	0.33*	0.26	0.32	0.54**	0.12	-0.04	-0.31	-0.24	-0.02	0.47**	1.00	0.22	0.41*	-0.02	0.46**	0.34*	0.18	0.23	0.17	0.13	0.04	0.31	0.15	0.32
Mn	0.04	-0.01	0.93**	0.68**	0.10	0.47**	0.56**	0.25	0.17	0.11	0.55**	0.06	0.34*	1.00	0.27	0.54**	0.66**	0.18	0.35*	0.29	0.29	0.43*	0.46**	0.20	0.34*	0.11
Ni	0.31	0.64**	0.37*	0.22	0.40*	0.55**	0.09	-0.03	-0.27	-0.23	0.13	0.48**	0.89**	0.38*	1.00	0.25	0.44**	0.32	0.46**	0.27	0.46**	0.18	0.22	0.23	0.31	0.40*
Cu	0.24	0.25	0.32	0.38*	0.27	0.35*	0.12	0.08	0.02	0.02	0.24	0.25	0.34*	0.35*	0.37*	1.00	0.55**	0.11	0.45**	0.36*	0.46**	0.34	0.65**	0.00	0.74**	0.15
Zn	0.00	0.23	0.78**	0.73**	0.08	0.49**	0.41*	0.16	-0.11	-0.05	0.26	0.26	0.52**	0.85**	0.44**	0.35*	1.00	0.33	0.47**	0.38*	0.52**	0.31	0.41*	0.28	0.65**	0.29
As	0.07	0.06	0.62**	0.89**	0.01	0.51**	0.34*	0.15	0.13	-0.01	0.23	0.29	0.42*	0.66**	0.40*	0.46**	0.77**	1.00	0.59**	0.58**	0.64**	-0.01	0.34	0.70**	0.41*	0.37*
Rb	-0.06	-0.20	0.65**	0.98**	-0.13	0.50**	0.39*	0.15	0.18	0.02	0.31	0.00	0.22	0.70**	0.20	0.40*	0.72**	0.89**	1.00	0.45**	0.72**	0.15	0.63**	0.42*	0.57**	0.48**
Sr	0.42*	0.39*	0.56**	0.28	0.51**	0.47**	0.41*	0.13	0.11	0.09	0.52**	0.32	0.35*	0.49**	0.38*	0.45**	0.45**	0.38*	0.24	1.00	0.40*	0.32	0.28	0.60**	0.35*	0.32
Cd	0.14	-0.02	0.52**	0.74**	0.05	0.52**	0.49**	0.03	0.11	-0.03	0.30	0.21	0.31	0.57**	0.24	0.58**	0.66**	0.78**	0.77**	0.36*	1.00	0.17	0.44**	0.36*	0.63**	0.20
Sn	0.02	-0.15	0.46**	0.53**	0.10	0.43**	0.10	0.08	0.17	-0.08	0.39*	0.01	0.06	0.51**	0.17	0.38*	0.35*	0.49**	0.59**	0.14	0.48**	1.00	0.05	0.30	0.27	-0.02
Sb	0.21	-0.01	0.38*	0.59**	0.13	0.39*	0.18	0.20	0.18	0.07	0.16	0.11	0.17	0.43**	0.19	0.81**	0.42**	0.59**	0.63**	0.25	0.61**	0.47**	1.00	0.12	0.52**	0.28
Ba	0.35*	0.14	0.68**	0.41*	0.39*	0.40*	0.54**	0.10	0.18	0.06	0.67**	0.28	0.32	0.67**	0.33*	0.49**	0.62**	0.44**	0.42**	0.63**	0.51**	0.37*	0.40*	1.00	0.17	0.24
Pb	0.08	0.02	0.52**	0.73**	0.05	0.46**	0.29	0.14	0.06	0.04	0.28	0.12	0.29	0.58**	0.27	0.78**	0.66**	0.74**	0.77**	0.34*	0.82**	0.55**	0.83**	0.57**	1.00	0.20
PM_1	0.14	0.02	0.07	0.31	0.01	0.33	0.03	-0.19	-0.01	-0.16	0.07	-0.01	-0.01	0.07	-0.01	0.39*	0.15	0.26	0.33*	0.11	0.36*	0.21	0.40*	0.25	0.45**	1.00

For this study, Cu, Sn, Sb and Zn, may be emitted from road traffic and mainly, from break wear (Furuta et al., 2005; Gugamsetty et al., 2012; Hassanvand et al., 2015). Cu and Zn are commonly observed in submicron particles (Sanderson et al., 2014), as observed in our study. For both sites, between the trace elements, Zn was found the most abundant element (33 ng/m^3 for Canoas and 59 ng/m^3 for Sapucaia do Sul). Sapucaia do Sul presented higher concentrations because the presence of steel mills, smelters and more vehicular traffic, that characterize the study area. However, Zn concentration (59 ng/m^3) in Sapucaia do Sul was smaller than in Tehran/Iran (Hassanvand et al., 2015). Moreover, variable amounts of Pb, Fe, Cu, Zn, Ni and Cd, in the sampling sites, can be observed due to contribution of both sources, from industrial processes and from traffic (Vecchi et al. 2004; Hassanvand et al., 2015). Correlations between elements were observed in Table 2 and these findings are discussed in detailed later.

As explained above, these studied elements are preferably associated with submicron particles, mainly in the fraction PM_1. This not only results in large areas that are available for reaction with fluids within the human body, but also allows them to be transported over distances of hundreds of kilometers. Although the studies shown in Table 1 were carried out at different periods and have used different experimental procedures (sampling techniques and methodologies - analytic techniques), this study shows agreements with them, especially with regard to type of source and common metal.

3.2. Enrichment Factors (EFs)

Figure 2 show the mean EFs for Canoas and Sapucaia do Sul PM_1 samples. EFs less than 1 were only observed for Mg and Sr for both sites, showing that their compositions were very close to that of the upper continental crust and indicating a natural origin. Other elements, such as Al, Ca, Fe, K, Na, V, Mn, Ni, Rb and Ba presented EFs between 1 and 10, indicating the contribution of both natural and anthropogenic sources.

EF >10 were observed for K and Rb (Sapucaia do Sul site) and Cr (both sites) indicating some anthropogenic contribution. However, the highest EF, i.e., EF >100 and in some case EF >>100 for both sites, were observed for Cu, Zn, As, Cd, Sn, Sb and Pb, indicating very high anthropogenic contributions. These elements are usually derived by road traffic and industrial emissions, as will be discussed below in the source apportionment analysis. Other major anthropogenic sources in the study area are the combustion of

petroleum products, non-ferrous metal production and coal combustion. The enrichment of these elements in the particles affects the air quality of the study region and they result from high anthropogenic emissions and by low renovation of the air masses at the regional scale which results in an elevated proportion of low dispersive conditions.

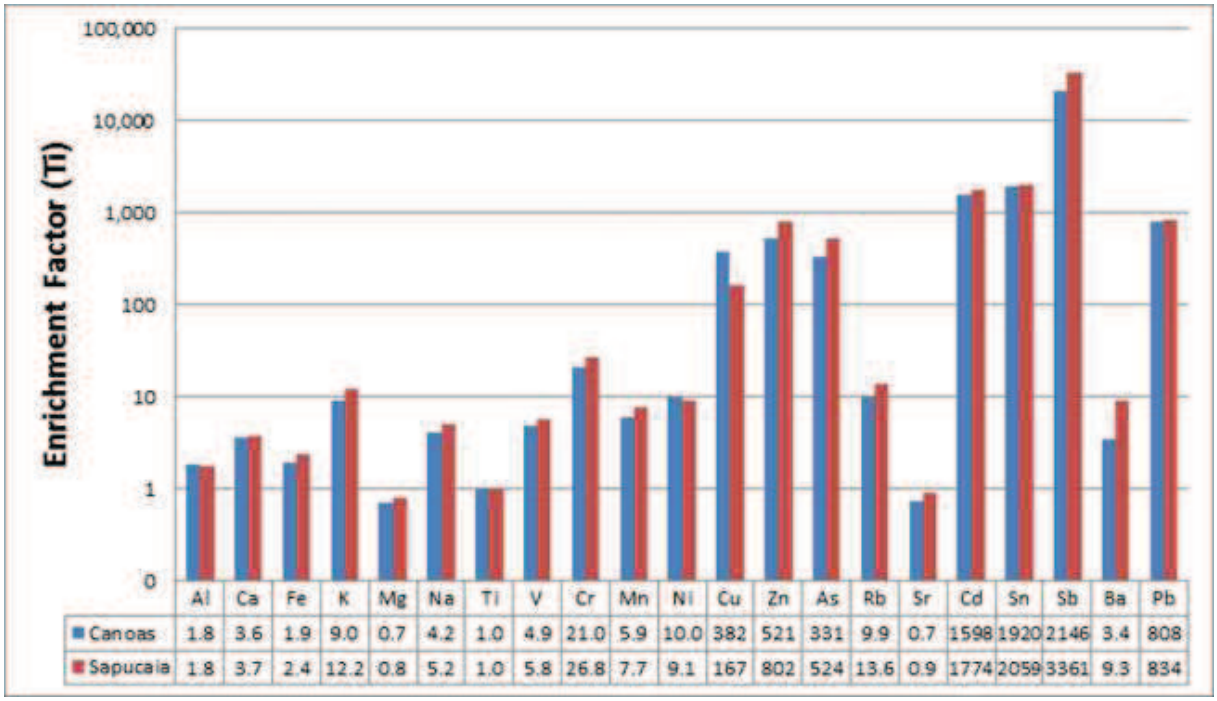

	Al	Ca	Fe	K	Mg	Na	Ti	V	Cr	Mn	Ni	Cu	Zn	As	Rb	Sr	Cd	Sn	Sb	Ba	Pb
Canoas	1.8	3.6	1.9	9.0	0.7	4.2	1.0	4.9	21.0	5.9	10.0	382	521	331	9.9	0.7	1598	1920	2146	3.4	808
Sapucaia	1.8	3.7	2.4	12.2	0.8	5.2	1.0	5.8	26.8	7.7	9.1	167	802	524	13.6	0.9	1774	2059	3361	9.3	834

Figure 2. Mean EF for PM_1 samples in Canoas and Sapucaia do Sul.

3.3. Microscopy analysis

Figure 3 shows photomicrographs of SEM images of PM_1 particles, with irregular shapes and crustal origin were typically particles associated to Al, Si, Na, Ca, K, Mg, Mn, and Fe. In addition, fine particles with iron and manganese oxides and with elements considered potential toxic as Cr, Zn, Pb, and Ni were also observed. Some mineral grains identified with the largest sizes (especially irregular forms) may have originated from dust resuspension. Alteration of rocks such as alkali feldspar and resuspension due to wind of minerals rich in K, can evidence the presence of K in the atmospheric particles. Ca, Mg, and Na can be explained by rocks and it may be easily found in the atmosphere due to resuspension (Migliavacca et al., 2009).

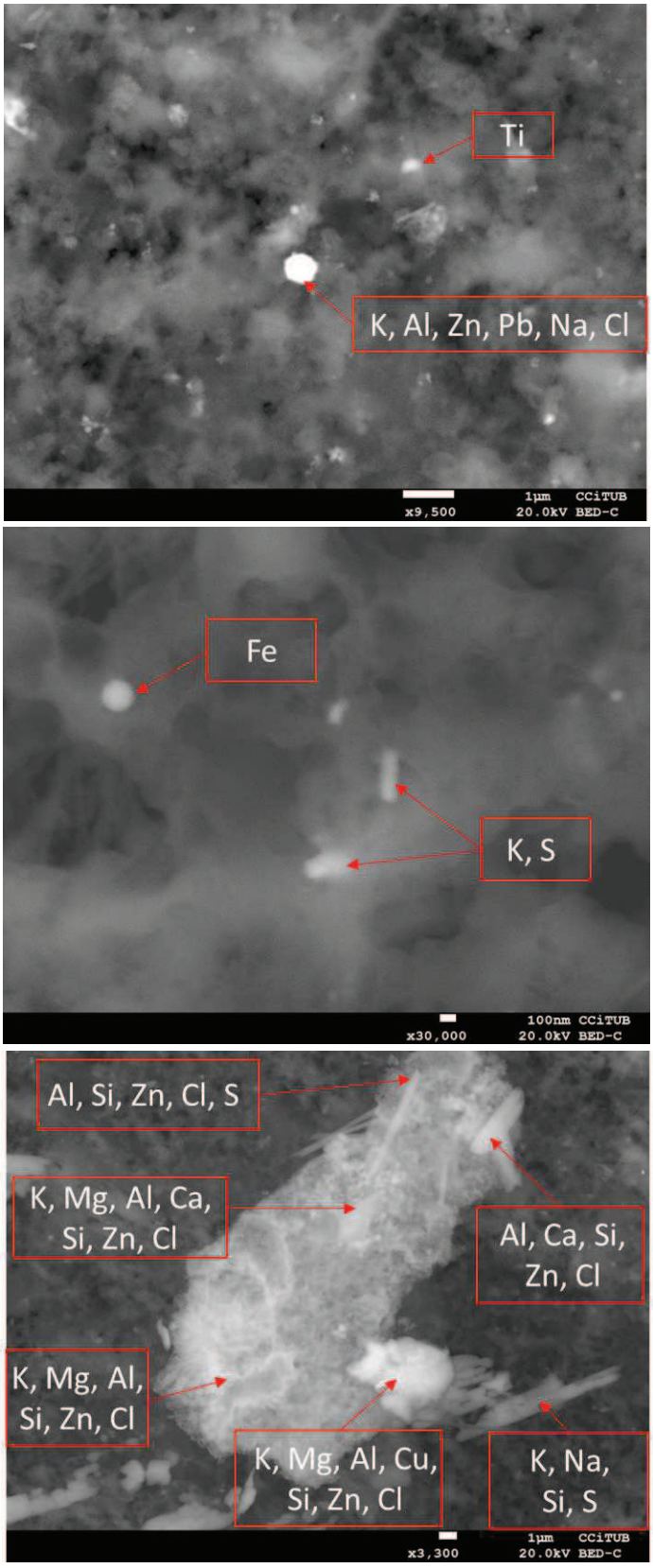

Figure 3. Scanning electron microscopy images of PM_1 samples: a and b – Canoas, c – Sapucaia do Sul.

The frequent occurrence of S in fine particles also was evidenced and can be associated with excess sulfate concentrated on these particles (Sippula et al., 2009). It is known that Mn is an important element for the production of steel and, together with iron, it is melted to generate a metallic alloy crucial for the automobile and construction industries. In the study region we find several steel plants and the Gravataí Automotive Complex which most certainly use this metallic alloy. Besides, these steel plants are a strong contributor of Cr and Ni due to the manufacture of stainless steel. The presence the Zn in PM_1 was also identified in another study in this region (Migliavacca et al., 2009) and this element is widely used for galvanizing steel or iron to protect them from corrosion.

3.4. Source apportionment

The PMF was performed on the assembled dataset of PM_1 samples from both Canoas and Sapucaia do Sul. Samples of the two sampling sites were analyzed together after a previous analysis that indicated a similar source contribution in both sites. Figure 4 shows the source profiles, whose columns and square represent the mass contribution of species to the factor ($\mu g/m^3$) and the percentage of species in the factor, respectively. Seven factors were identified and are discussed below.

Factor 1 was characterized by high contributions of NO_3^- (89%) and NH_4^+ (60%), and was assigned as secondary nitrate (Figure 4). These correspond to secondary pollutants and are results from the transformation of their precursors NO_x and NH_3, respectively, and probably are related to emissions from road traffic, high temperature industrial processes, power generation and biomass burning (Drechsler et al., 2006; Cheng et al., 2014). As indicated in Figure 5, Factor 1 represents 35% of the average contribution in the PM_1 samples in an annual basis, with lower contributions being observed during the summer, what can be attributed to the ammonium nitrate (NH_4NO_3) thermal instability (Querol et al., 2001; Mariani and Mello, 2007; Cusack et al., 2013a,b). During the summer the mean concentration observed was 0.13 $\mu g/m^3$, while during the winter the mean concentration was 3.14 $\mu g/m^3$. This can be seen in Figure 5, where the contribution to the mass increases to 50% in winter and decrease to only 4% in summer. Significant positive correlation (Table 2) of NH_4^+ with secondary NO_3^- was observed in the winter ($\rho = 0.81$). However, these compounds do not present correlation during the summer, what can be explained by their volatilization in the atmosphere in warmer conditions (Parker et al., 2008).

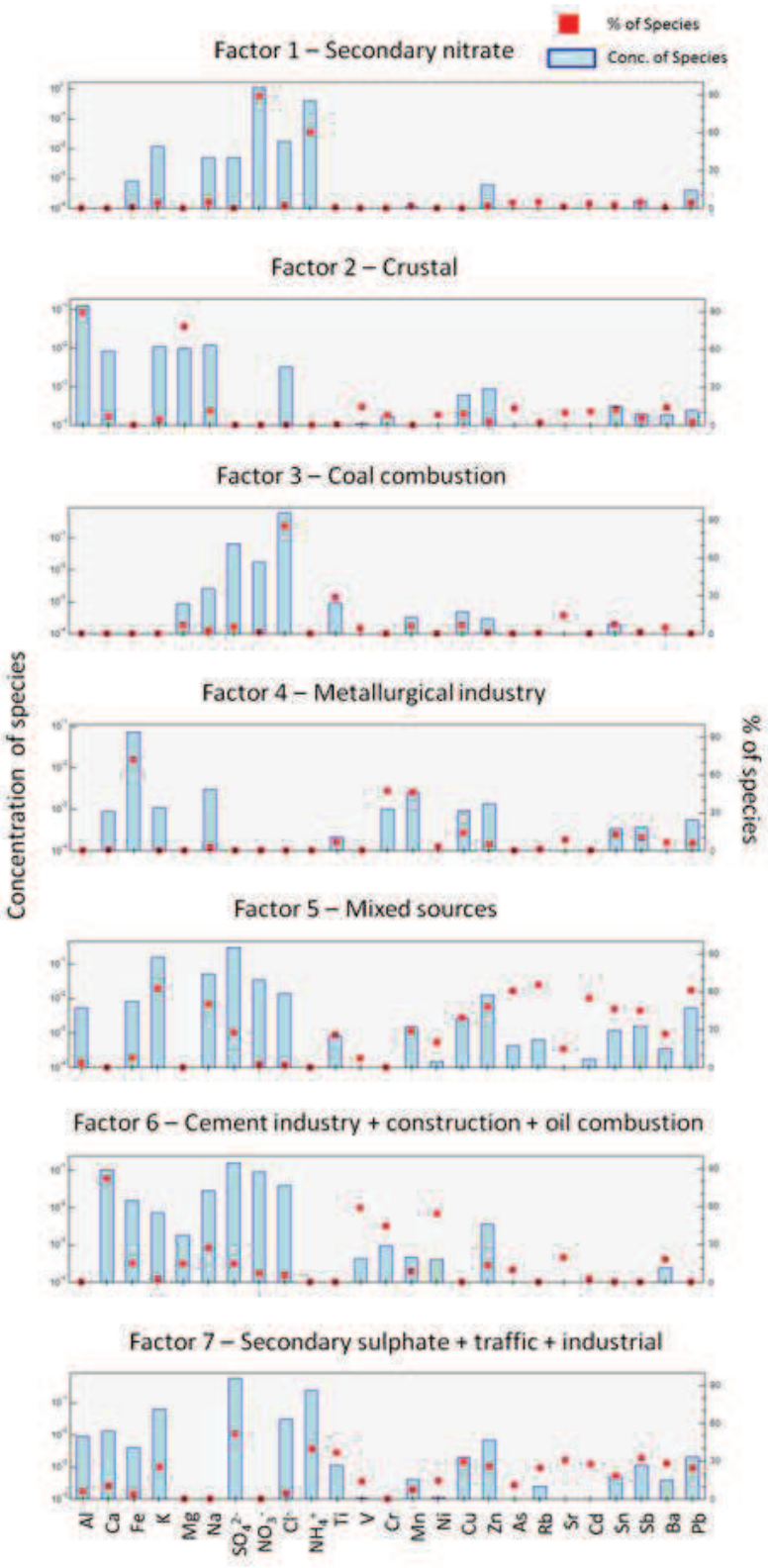

Figure 4. Source profiles identified for PM_1 samples. The mass of each species apportioned to the factor (blue bar, left axis) and the percent of each species apportioned to each factor (red square, right axis) is shown.

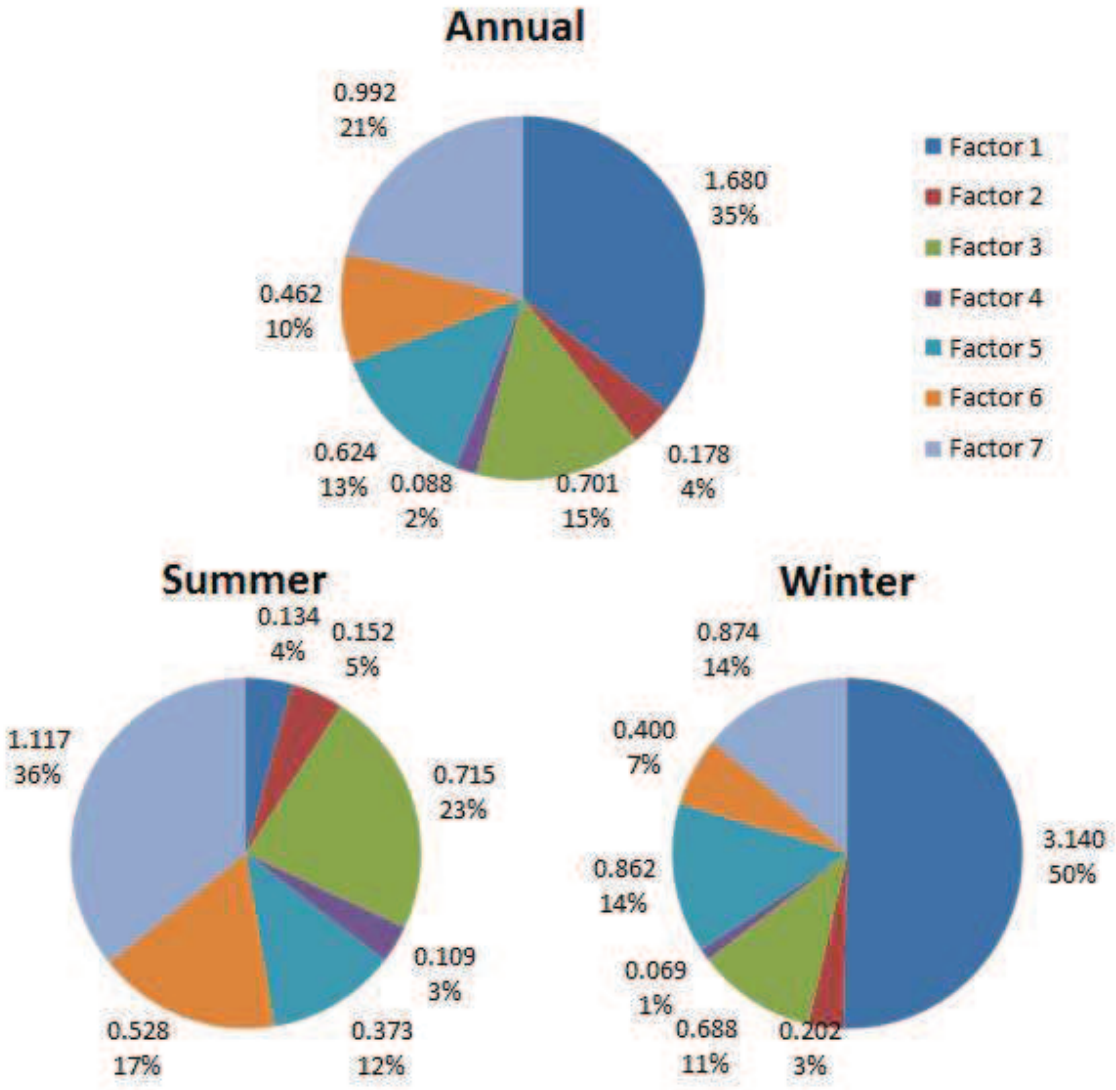

Figure 5. Average contribution of each source (µg/m^3) to PM_1 obtained by PMF.

Factor 2 represents 4% of the average contribution in the PM_1 samples (Figure 5). This factor presents higher contributions of Al and Mg, 90% and 78%, respectively (Figure 4). These elements in general are defined as being from crustal origin (Vecchi et al., 2004; Park and Kim, 2005; Perez et al., 2008; Caggiano et al., 2010; Sánchez de la Campa et al., 2010; Crilley et al., 2014). The low concentrations of metals associated with crustal mineral, average of 0.18 µg/m^3 (Figure 5), can be explained because they generally are accumulated in coarser particles (Pakkanen et al., 2003; Perez et al., 2008; Buczynska et al., 2014; Crilley et al., 2014). Factor 2 does not show a clear seasonal variation. Its average contribution of concentration was 0.15 µg/m^3 (5%) and 0.20 µg/m^3 (3%) for summer and winter, respectively

(Figure 4). In addition, significant positive correlations (Table 2) were observed between Al and Mg for summer and winter (ρ = 0.72 and 0.83, respectively), not revealing seasonal variation.

Factor 3 was characterized by high Cl^- contribution (85%) (Figure 4), whose origin can be attributed to a coal fired power station, located near the sampling site. Contribution of Cl^- from coal fired power station source has been identified by others studies (He et al., 2001; Duan et al., 2004; Wang et al., 2005; Cheng et al., 2014). In addition, Cl^- in the atmosphere could also be associated to some fugitive emissions from waste or garbage burning close to the sampling sites and from industrial activities in the area, such as a paper manufacturing. Factor 3 contributed with 0.70 $\mu g/m^3$ (15%) of the average contributions in an annual basis, with seasonal variation: 0.69 $\mu g/m^3$ (11%) during the winter and 0.72 $\mu g/m^3$ (23%) during the summer. The low Na levels associated to this factor, about 2% of the total Na concentration, suggest that there is no marine contribution to the Cl^- levels observed in the PM_1 samples.

Factor 4 was related to the influence of metallurgical industry, with predominance of Fe, Cr and Mn concentrations. Significant correlation was observed between Fe-Mn for winter (ρ = 0.93) and Fe-Cr for summer (ρ = 0.46). Generally the metals are better correlated in winter, as can be seen in Table 2. This is probably related to the metallurgy facilities in the study region and these contributions were higher in winter due to the lower dispersive conditions. The metals correlation in summer may be due to enhanced soil resuspension and also favored by the dispersion conditions, making it difficult to clearly identify the different sources (Minguillón et al., 2012). As reported above, the metals may be associated to mineral material, suggesting presence of metals in soil resuspension. Various authors (Moreno et al., 2010, 2011) have reported that Cr influence in the atmosphere is attributed mostly to industrial metallurgical emissions, likewise was verified for the contributions of Fe and Mn. In the microscopy analysis presented above, the presence of Fe, Cr and Mn was observed, highlighting the contribution of this source. Factor 4 is related to only 2% of the average concentrations observed in the PM_1 samples, i.e. 0.09 $\mu g/m^3$ (Figure 5). No significant seasonal variation in the metals concentrations was observed, with average contributions of 0.11 $\mu g/m^3$ (3%) for summer and 0.07 $\mu g/m^3$ (1%) for winter.

Factor 5 of the source apportionment analysis indicated the association of several anthropogenic metals, such as As, Rb, Sn, Pb, Cd, Zn, Mn, Cr, Cu and K, with the PM_1 samples. Potassium in the fine PM fraction is usually associated with biomass combustion

(Vecchi et al., 2004; Wang et al., 2005; Spindler et al., 2010; Buczynska et al., 2014; Cheng et al., 2014), and the two study sites are influenced by emissions from this activity. In this group of metals there are also anthropogenic metal tracers related to municipal garbage incineration, smelters and oil refining processes. These processes in the study area were evidenced by the presence of As, Cd, Pb, and Zn. The presence of these metals has been reported by several studies with similar sources (Schauer et al., 2006; Wåhlin et al., 2006; Perez et al., 2008; Amato et al., 2011; Moreno et al., 2011; Minguillón et al., 2012; Niu et al., 2015). Furthermore, as indicated before, non-exhaust traffic sources as brakes (Cu, Sn, and Zn) and tires (Cd, Cu, and Pb) (Sanderson et al., 2014) also contributed significantly in this factor. However, metallurgical emissions of Zn, Pb, and Mn associated with other emissions listed above, favors the idea of mixture of atmospheric pollutants and the difficulty of identifying individual sources (Moreno et al., 2011). This was observed in this study, considering that the association of some metals can be emitted by specific source mixed in a factor in the atmosphere or by common emissions sources. Some metals may appear in different factors or metals may be characteristic of a factor with more than one emission source. Significant correlations were observed between As/Cd, Zn/As, Zn/Cu, Cr/Ni, Cr/Zn, Mn/Zn, Mn/Ni, Mn/Cu, and Pb/Cd for winter, while in summer some correlations between these elements do not show much difference. Metal correlations were in agreement with the seasonal variation with an average concentration of 0.37 $\mu g/m^3$ (12%) for summer and 0.86 $\mu g/m^3$ (14%) for winter (Figure 5), revealing a clear seasonal variation.

Factor 6 is related mainly to the contributions of Ca, Cr, Ni, and V. This factor corresponds to 11.4% of the average contributions in the PM_1 samples, and corresponds to cement industry + construction + oil combustion sources. Ca can be probably linked with specific anthropogenic activities, such as construction works, cement factories and building material production plants (Munir and Shaheen, 2008; Perez et al., 2008; Amato et al., 2009; Caggiano et al., 2010; Widory et al., 2010; Crilley et al., 2014). Ni and V can be associated to oil combustion (Arhami et al., 2009; Moreno et al., 2010; Buczynska et al., 2014; Crilley et al., 2014) and this metals are typical tracers of this source (Pandolfi et al., 2011; Cusack et al., 2013b). The study area is mainly influenced by oil combustion that is used by the refineries and steel industry. As reported by some authors (Moreno et al., 2011; Mohiuddin et al., 2014), much of this combustion-derived atmospheric V and Ni were predominantly associated with the finest PM size fraction, and is therefore capable of travelling large distances. Significant

correlations were observed in winter for Ca with V, Cr, and Ni and for Cr/Ni, and in summer between Ca/V and V/Cr. Factor 6 showed seasonal variation, with average concentrations of 0.53 μg/m^3 (17%) for summer and 0.40 μg/m^3 (7%) for winter (Figure 5).

Factor 7 was identified as the contribution due to SO_4^{2-} and NH_4^+, given the relevance of these compounds in the chemical profile (37% and 86%, respectively) (Figure 4). High contributions of this factor to the concentrations of Sb, Pb, Cd, Rb, Ti, Zn, K, Cu (between 10 and 30% of their concentration) were obtained, and most of them are typical tracers of road traffic (Querol et al., 2002; Lin et al., 2005; Pey et al., 2010; Amato et al., 2011; Moreno et al., 2011; Niu et al., 2015). Sulfate concentrations for the winter and summer were 1.21 and 1.26 μg/m^3, respectively, while for ammonium were 1.01 and 0.28 μg/m^3, respectively. The winter/summer sulfate ratios (0.96) indicated a relatively stable seasonal pattern, with slightly higher summer levels, possibly as a result of enhanced photochemistry associated with more intense solar radiation (Cusack et al., 2012). Ammonium showed higher concentration in winter (ratio winter/summer 3.5). Among the constituents of Factor 7 a significantly higher correlation was obtained in winter compared to summer (Table 2). As reported in Factor 5, some metals may appear in different factors, as non-exhaust traffic sources, such as Cu, Sb, Zn and Cd, Cu, Pb, and Cu (Sörme et al., 2001; Kupiainen and Pirjola, 2011; Wiseman et al., 2013; Buczynska et al., 2014; Crilley et al., 2014; Wiseman and Zereini, 2014; Hassavand et al., 2015). Also these elements and compounds can be characterized by anthropogenic activities from industrial sources, traffic and coal combustion. This factor was associated to a mix of anthropogenic sources as its chemical profile is dominated by secondary ammonium sulfate probably from SO_2 emissions from coal fired power plants, smelters and oil refining, but with contributions of tracers of different sources, probably mixed during the atmospheric transport. Factor 7 showed seasonal variation with 0.87 μg/m^3 (14%) in winter and 1.12 μg/m^3 (36%) in summer.

3.5. Back trajectory analysis

Table 3 shows the average concentrations of PM_1, the contributions of each factor of the source apportionment obtained by PMF and the sum of metals for both back trajectory heights. As can be seen, in both cases when air masses from the north of the study area reach the study sites, the PM_1 concentrations were higher. However, after a comparison between means using the non-parametric Mann-Whitney test, it was observed that the mean

differences were not statistically significant. No statistically significant differences were also observed between the mean concentrations of the PMF factors and the sum of metal. This is an indication that both PM_1 and metal concentrations observed in this study correspond mainly to contributions from regional-local sources, as identified by the source apportionment.

In addition, the sensitivity of PM concentrations to the air-flows decreased with increasing arrival-height (Table 3). This result may be due to the fact that polluted air masses at high altitudes have on average a lower impact at the surface PM. Air-flows at higher altitudes are on average characterized by larger path lengths and as a consequence, they are likely more affected by the atmospheric physical and chemical processes occurring during the transport and hence, are less dependent on source properties (Perrone et al., 2013).

In summary, the complex spatial and temporal relationship of the elements measured in this study did not reveal any spatial pattern concerning the origin of the air masses, so studies with more sophisticated techniques are necessary to advance our understanding of the aerosol sources identification from long transport.

Table 3: Proportion of air masses associated air mass origin sectors and the corresponding concentrations of PM_1, PMF factors and sum of the evaluated elements ($\mu g/m^3$).

Trajectory height	Air mass (proportion)	PM_1	Factor 1	Factor 2	Factor 3	Factor 4	Factor 5	Factor 6	Factor 7	Sum of metals
100 m agl	N (4%)	41.3	0.02	0.20	0.96	0.06	0.70	0.34	0.78	3.07
	NE (11%)	12.1	0.87	0.13	0.83	0.13	0.79	0.28	1.82	4.73
	E (4%)	9.36	2.66	0.06	0.81	0.04	1.04	0.42	0.51	5.32
	SE (11%)	8.68	1.77	0.15	0.76	0.16	0.35	0.52	0.89	4.56
	S (18%)	9.93	1.32	0.20	0.62	0.12	0.51	0.58	1.28	4.82
	SW (41%)	14.9	2.05	0.20	0.63	0.06	0.59	0.44	0.70	4.71
	W (0%)									
	NW (8%)	14.9	1.98	0.17	0.79	0.06	0.93	0.58	1.15	5.49
1000 m agl	N (10%)	16.9	2.07	0.10	0.79	0.06	0.53	0.38	0.85	4.68
	NE (10%)	10.6	1.26	0.15	0.90	0.09	0.69	0.30	1.62	4.99
	E (0%)									
	SE (7%)	11.4	3.18	0.10	0.67	0.03	0.61	0.35	1.00	5.83
	S (4%)	9.38	0.00	0.10	0.44	0.18	0.17	0.32	1.51	2.46
	SW (40%)	13.2	2.04	0.25	0.70	0.10	0.48	0.56	0.79	5.05
	W (5%)	15.6	0.56	0.11	0.86	0.07	1.05	0.31	0.75	3.66
	NW (23%)	16.1	1.18	0.16	0.59	0.08	0.88	0.50	1.09	4.47

4. Conclusion

Our study evaluated concentrations of particulate matter <1 μm (PM_1) and metals in two locations in southern Brazil, and revealed a strong anthropogenic influence. The average concentrations of PM_1 for Canoas and Sapucaia do Sul were 12.8 to 15.2 $\mu g/m^3$, respectively, corresponding to levels similar to those reported for several European countries, but much lower than those found in China. Major contributions of PM_1 were secondary pollutants sulfate (SO_4^{2-}) and nitrate (NO_3^-). Trace elements, especially Cu, Pb, Zn, Cd, and Ni also made important contributions being directly associated with anthropogenic contributions. Among these, as verified by the PMF, the major sources correspond to secondary nitrate and sulfate, industrial emissions, especially metallurgical, cement and oil refining processes, in addition to coal, biomass and oil combustion, as well as traffic fuel burning and non-exhaust sources. The crustal contribution was less than 4%, what can be explained because they generally are present in coarser size mode. The analysis for detecting potential long range transport contributions showed no significant influences nor for the PM_1 as for the metal concentrations, which are attributed mostly to contributions from regional-local sources, as identified by the source apportionment. However, in the present study it was observed that the association of some metals in atmospheric particles can be due to emissions from a specific source or by different sources. Some metals may appear in different factors or metals may be characteristic of a factor with more than one emission source. Nevertheless, PMF model was found to be an efficient tool for identifying the main sources responsible for the trace elements. The absence of marker species, such as organic tracers, in the input data sets may be one of the problems of the inability of the model to separate sources.

Acknowledgements

We would like to thank CAPES and CNPq for their financial support. The authors also gratefully acknowledge the NOAA Air Resources Laboratory (ARL) for the provision of the HYSPLIT transport and dispersion model and/or READY website (http://www.ready.noaa.gov) used in this publication.

References

Agudelo-Castañeda, D.M., Teixeira, E.C., 2014. Seasonal changes, identification and source apportionment of PAH in $PM_{1.0}$. Atmos. Environ. 96, 186-200. doi:10.1016/j.atmosenv.2014.07.030

Aldabe J., Elustondo D., Santamaría C., Lasheras E., Pandolfi M., et al., 2011. Chemical characterization and source apportionment of $PM_{2.5}$ and PM_{10} at rural, urban and traffic sites in Navarra (North of Spain). Atmos. Res. 102(1-2), 191-205. doi: 10.1016/j.atmosres.2011.07.003

Almeida, S.M., Pio, C.A., Freitas, M.C., Reis, M.A., Trancoso, M.A., 2006. Approaching $PM_{2.5}$ and $PM_{2.5–10}$ source apportionment by mass balance analysis, principal component analysis and particle size distribution. Sci. Total Environ. 368(2-3), 663–674. doi:10.1016/j.scitotenv.2006.03.031

Amato, F., Pandolfi, M., Escrig, A., Querol, X., Alastuey, A., Pey, J., et al., 2009. Quantifying road dust resuspension in urban environment by Multilinear Engine: a comparison with PMF2. Atmos. Environ. 43(17), 2770–2780. doi:10.1016/j.atmosenv.2009.02.039

Amato, F., Nava, S., Lucarelli, F., Querol, X., Alastuey, A., et al., 2010. A comprehensive assessment of PM emissions from paved roads: Real-world Emission Factors and intense street cleaning trials. Sci. Total Environ. 408(20), 4309-4318. doi:10.1016/j.scitotenv.2010.06.008

Amato, F., Viana, M., Richard, A., Furger, M., Prévôt, A.S.H., et al., 2011. Size and time-resolved roadside enrichment of atmospheric particulate pollutants. Atmos. Chem. Phys. 11, 2917-2931. doi:10.5194/acp-11-2917-2011

Arhami, M., Sillanpää, M., Hu, S., Olson, M.R., Schauer, J.J., et al., 2009. Size-segregated inorganic and organic components of PM in the communities of the Los Angeles Harbor. Aerosol Sci. Technol. 43(2), 145–160. doi: 10.1080/02786820802534757

Birmili, W., Allen, A., Bary, F., Harrison, R., 2006. Trace metal concentrations and water solubility in size-fractionated atmospheric particles and influence of road traffic. Environ. Sci. Technol. 40(4), 1144–1153. doi: 10.1021/es0486925

Buczyńska, A.J., Krata, A., Grieken, R.V., Brown, A., Polezer, G., et al., 2014. Composition of $PM_{2.5}$ and PM_1 on high and low pollution event days and its relation to indoor air quality in a home for the elderly. Sci. Total Environ. 490, 134-143. doi:10.1016/j.scitotenv.2014.04.102

Buonanno, G., Ficco, G., Stabile, L., 2009. Size distribution and number concentration of particles at the stack of a municipal waste incinerator. Waste Manag. 29(2), 749-755. doi:10.1016/j.wasman.2008.06.029

Buonanno, G., Stabile, L., Avino, P., Belluso, E., 2011. Chemical, dimensional and morphological ultrafine particle characterization from a waste-to-energy plant. Waste Manag. 31(11), 2253-2262. doi:10.1016/j.wasman.2011.06.017

Caggiano, R., Macchiato, M., Trippetta, S., 2010. Levels, chemical composition and sources of fi ne aerosol particles (PM_1) in an area of the Mediterranean basin. Sci. Total Environ. 408(4), 884-895. doi:10.1016/j.scitotenv.2009.10.064

Cheng, H., Gong, W., Wang, Z., Zhang, F., Wang, X., et al., 2014. Ionic composition of submicron particles ($PM_{1.0}$) during the long-lasting haze period in January 2013 in Wuhan, central China. J. Environ. Sci. 26(4), 810-817. doi:10.1016/S1001-0742(13)60503-3

Crilley, L.R., Ayoko, G.A., Stelcer, E., Cohen, D.D., Mazaheri, M., et al., 2014. Elemental composition of ambient fine particles in urban schools: sources of children's exposure. Aerosol Air Qual. Res. 14(7), 1906-1916. doi:10.4209/aaqr.2014.04.0077

Cusack, M., Alastuey, A., Péres, N., Pey, J., Querol, X., 2012. Trends of particulate matter ($PM_{2.5}$) and chemical composition at a regional background site in the Western Mediterranean over the last nine years (2002-2010). Atmos. Chem. Phys. 12(18), 8341-8357. doi:10.5194/acp-12-8341-2012

Cusack, M., Alastuey, A., Querol, X., 2013a. Case studies of new particle formation and evaporation processes in the western Mediterranean regional background. Atmos. Environ. 81, 651-659. doi:10.1016/j.atmosenv.2013.09.025

Cusack, M., Pérez, N., Pey, J., Alastuey, A., Querol, X., 2013b. Source apportionment of fine PM and sub-micron particle number concentrations at a regional background site in the western Mediterranean: a 2.5 year study. Atmos. Chem. Phys. 13(10), 5173-5187. doi:10.5194/acp-13-5173-2013

Draxler, R.R., Rolph, G.D., 2003. HYSPLIT (Hybrid Single-Particle Lagrangian Integrated Trajectory) Model access via NOA ARL READY. NOAA Air Resources Laboratory, Silver Spring, MD. (Website) http://ready.arl.noaa.gov/HYSPLIT.php

Drechsler, S., Uhrner, U., Lumpp, R., 2006. Sensitivity of urban and rural ammonium nitrate particulate matter to precursor emissions in Southern Germany. In: Workshop on Contribution of Natural Sources to PM Levels in Europe, JRC ISPRA, 12-13 (Website) http://natsources.jrc.it/

Duan, F.K., Liu, X.D., Yu, T., Cachier, H., 2004. Identification and estimate of biomass burning contribution to the urban aerosol organic carbon concentrations in Beijing. Atmos. Environ. 38(9), 1275–1282. doi:10.1016/j.atmosenv.2003.11.037

Furuta, N., Iijima, A., Kambe, A., Sakai, K., Sato, K., 2005. Concentrations, enrichment and predominant sources of Sb and other trace elements in size classified airborne particulate matter collected in Tokyo from 1995 to 2004. J. Environ. Monitor. 7(12), 1155–1161. doi: 10.1039/B513988K

Gugamsetty, B., Wei, H., Liu, C.N., Awasthi, A., Hsu, S.C., et al., 2012. Source characterization and apportionment of PM_{10}, $PM_{2.5}$ and $PM_{0.1}$ by using Positive Matrix Factorization. Aerosol Air Qual. Res. 12, 476–491. doi:10.4209/aaqr.2012.04.0084

Hassavand, M.H., Naddafi, K., Faridi, S., Nabizadeh, R., Sowlat, M.H., et al., 2015. Characterization of PAHs and metals in indoor/outdoor $PM_{10}/PM_{2.5}/PM_1$. Sci. Total Environ. 527–528, 100–110. doi:10.1016/j.scitotenv.2015.05.001

He, K.B., Yang, F.M., Ma, Y.L., Zhang, Q., Yao, X.H., et al., 2001. The characteristics of $PM_{2.5}$ in Beijing, China. Atmos. Environ. 35(29), 4959–4970. doi:10.1016/S1352-2310(01)00301-6

Helble, J.J., 2000. A model for the air emissions of trace metallic elements from coal combustors equipped with electrostatic precipitators. Fuel Process. Technol. 63(2-3), 125–147. doi:10.1016/S0378-3820(99)00093-4

Hopke, P.K. (Ed.), 1991. Receptor Modeling for Air Quality Management. Elsevier Science Publishers, Amsterdam.

Hopke, P.K., 2003. A guide to Positive Matrix Factorization. Available in: http://www.epa.gov/ttnamti1/files/ambient/pm25/workshop/laymen.pdf

Johansson, C., Norman, M., Burman, L., 2009. Road traffic emission factors for heavy metals. Atmos. Environ. 43(31), 4681–4688. doi:10.1016/j.atmosenv.2008.10.024

Kauppinen, E.I., Pakkanen, T.A., 1990. Coal combustion aerosols: a field study. Environ. Sci. Technol. 24(12), 1811–1818. doi:10.1021/es00082a004

Kupiainen, K.J., Pirjola, L., 2011. Vehicle non-exhaust emissions from the tyre–road interface – effect of stud properties, traction sanding and resuspension. Atmos. Environ. 45, 4141–4146. doi:10.1016/j.atmosenv.2011.05.027

Lin, C.-C., Chen, S.-J., Huang, K.-L., 2005. Characteristics of metals in nano/ultrafine/fine/coarse particles collected beside a heavily trafficked road. Environ. Sci. Technol. 39(21), 8113–8122. doi:10.1021/es048182a

Lough, G.C., Schauer, J.J., Park, J.S., Shafer, M.M., Deminter, J.T., et al., 2005. Emissions of metals associated with motor vehicle roadways. Environ. Sci. Technol. 39(3), 826–836. doi:10.1021/es048715f

Mariani, R.L., Mello, W.Z., 2007. $PM_{2.5-10}$, $PM_{2.5}$ and associated water–soluble inorganic species at coastal urban site in the metropolitan region of Rio de Janeiro. Atmos. Environ. 41(13), 2887–2892. doi:10.1016/j.atmosenv.2006.12.009

Mason, S., 1966. Principles of geochemistry. New York: Wiley.

Mattiuzi, C.D.P., Palagi, A.C., Teixeira, E.C., Wiegand, F., 2012. Poluição Atmosférica do Biodiesel e Estado da Arte. In: Teixera, E.C., Wiegand, F., Tedesco, M. (Eds.), Biodiesel: Impacto Ambiental Agronômico e Atmosférico. Cadernos de Planejamento e Gestão Ambiental Nº 6. FEPAM, Porto Alegre, pp. 43–67.

Migliavacca, D.M., Teixeira, E.C., Gervasonic, F., Conceição, R.V., Rodriguez, M.T.R., 2009. Characterization of wet precipitation by X-ray diffraction (XRD) and scanning electron microscopy (SEM) in the metropolitan area of Porto Alegre, Brazil. J. Hazard. Mater. 171, 230–240. doi:10.1016/j.jhazmat.2009.05.135

Minguillón, M.C., Querol, X., Baltensperger, U., Prévôt, A.S.H., 2012. Fine and coarse PM composition and sources in rural and urban sites in Switzerland: local or regional pollution? Sci. Total Environ. 427–428, 191–202. doi:10.1016/j.scitotenv.2012.04.030

Mohiuddin, K., Strezov, V., Nelson, P.F., Stelcer, E., 2014. Characterisation of trace metals in atmospheric particles in the vicinity of iron and steelmaking industries in Australia. Atmos. Environ. 83, 72-79. doi:10.1016/j.atmosenv.2013.11.011

Moreno, T., Querol, X., Alastuey, A., Amato, F., Pey, J., et al., 2010. Effect of fireworks events on urban background trace metal aerosol concentrations: Is the cocktail worth the show? J. Hazard. Mater. 183(1–3), 945–949. doi:10.1016/j.jhazmat.2010.07.082

Moreno T., Querol X., Alastuey A., Reche C., Cusack M., et al., 2011. Variations in time and space of trace metal aerosol concentrations in urban areas and their surroundings. Atmos. Chem. Phys. 11(17), 9415–9430. doi:10.5194/acp-11-9415-2011

Moreno T., Kojima T., Amato F., Lucarelli F., de la Rosa J., et al., 2013. Daily and hourly chemical impact of springtime transboundary aerosols on Japanese air quality. Atmos. Chem. Phys. 13(3), 1411–1424. doi:10.5194/acp-13-1411-2013

Munir, H.S., Shaheen, N., 2008. Annual and seasonal variations of trace metals in atmospheric suspended particulate matter in Islamabad, Pakistan. Water Air Soil Poll. 190(1), 13–25. doi:10.1007/s11270-007-9575-x

Nazir, R., Shaheen, N., Shah, M.H., 2011. Indoor/outdoor relationship of trace metals in the atmospheric particulate matter of an industrial area. Atmos. Res. 101(3), 765–772. doi:10.1016/j.atmosres.2011.05.003

Ninomiya, Y., Zhang, L., Sato, A., Dong, Z., 2004. Influence of coal particle size on particulate matter emission and its chemical species produced during coal combustion. Fuel Process. Technol. 85(8–10), 1065–1088. doi:10.1016/j.fuproc.2003.10.012

Niu, L., Ye, H., Xu, C., Yao, Y., Liu, W., 2015. Highly time– and size–resolved fingerprint analysis and risk assessment of airborne elements in a megacity in the Yangtze River Delta, China. Chemosphere 119, 112–121. doi:10.1016/j.chemosphere.2014.05.062

Paatero, P., 1997. Least square formulation of robust non–negative factor analysis. Chemometrrics Intell. Lab. Syst. 37(1), 23–35. doi:10.1016/S0169-7439(96)00044-5

Paatero, P., Tapper, U., 1994. Positive matrix factorization: a non–negative factor model with optimal utilization of error estimates of data values. Environmetrics 5, 111–126. doi:10.1002/env.3170050203

Pakkanen, T.A., Kerminen, V.M., Loukkola, K., Hillamo, R.E., Aarnio, P., et al., 2003. Size distributions of mass and chemical components in street–level and rooftop PM_1 particles in Helsinki. Atmos. Environ. 37(12), 1673–1690. doi:10.1016/S1352-2310(03)00011-6

Pandolfi, M., Cusack, M., Alastuey, A., Querol, X., 2011. Variability of aerosol optical properties in the Western Mediterranean Basin. Atmos. Chem. Phys. 11(15), 8189–8203. doi:10.5194/acpd-11-14091-2011

Park, S.S., Kim, Y.J., 2005. Source contributions to fine particulate matter in an urban atmosphere. Chemosphere 59(2), 217–226. doi:10.1016/j.chemosphere.2004.11.001

Parker, J.L., Larson, R.R., Eskelson, E., Wood, E.M., Veranth, J.M., 2008. Particle size distribution and composition in a mechanically ventilated school building during air pollution episodes. Indoor Air 18(5), 386–393. doi:10.1111/j.1600-0668.2008.00539.x

Pérez, N., Pey, J., Querol, X., Alastuey, A., López, J.M., et al., 2008. Partitioning of major and trace components in PM_{10}–$PM_{2.5}$–PM_1 at an urban site in Southern Europe. Atmos. Environ. 42(8), 1677–1691. doi:10.1016/j.atmosenv.2007.11.034

Perrone, M.G., Gualtieri, M., Consonni, V., Ferrero, L., Sangiorgi, G., et al., 2013. Particle size, chemical composition, seasons of the year and urban, rural or remote site origins as determinants of biological effects of particulate matter on pulmonary cells. Environ. Pollut. 176, 215–227. doi:10.1016/j.envpol.2013.01.012

PETROBRAS, 2012. Products and Services. Available in: http://www.petrobras.com.br/pt/produtos/para-voce/nas-ruas/

Pey, J., Querol, X., Alastuey, A., 2009. Variation of levels and composition of PM_{10} and $PM_{2.5}$ at insular site in the Western Mediterranean. Atmos. Res. 94(2), 285–299. doi:10.1016/j.atmosres.2009.06.006

Pey, J., Querol, X., Alastuey, A., 2010. Discriminating the regional and urban contributions in the North–Western Mediterranean: PM levels and composition. Atmos. Environ. 44(13), 1587–1596. doi:10.1016/j.atmosenv.2010.02.005

Querol, X., Alastuey, A., Rodriguez, S., Plana, F., Ruiz, C.R., et al., 2001. PM_{10} and $PM_{2.5}$ source apportionment in Barcelona Metropolitan area, Catalonia, Spain. Atmos. Environ. 35(36), 6407–6419. doi:10.1016/S1352-2310(01)00361-2

Querol, X., Alastuey, A., de la Rosa, J., Sánchez de la Campa, A., Plana, F., et al., 2002. Source apportionment analysis of atmospheric particulates in an industrialised urban site in southwestern Spain. Atmos. Environ. 36(19), 3113–3125. doi:10.1016/S1352-2310(02)00257-1

Querol, X., Viana, M., Alastuey, A., Amato, F., Moreno, T., et al., 2007. Source origin of trace elements in PM from regional background, urban and industrial sites of Spain. Atmos. Environ. 41(34), 7219–7231. doi:10.1016/j.atmosenv.2007.05.022

Ragazzi, M., Tirler, W., Angelucci, G., Zardi, D., Rada, E.C., 2013. Management of atmospheric pollutants from waste incineration processes: the case of Bozen. Waste Manag. Res. 31(3), 235–240. doi:10.1177/0734242X12472707

Saarnio, K., Frey, A., Niemi, J.V., Timonen, H., Rönkkö, T., et al., 2014. Chemical composition and size of particles in emissions of a coal–fired power plant with fuel gas desulfurization. J. Aerosol Sci. 73, 14–26. doi:10.1016/j.jaerosci.2014.03.004

Sánchez de la Campa, A.M., de la Rosa, J.D., González-Castanedo, Y., Fernández-Camacho, R., Alastuey, A., et al., 2010. High concentrations of heavy metal in PM from ceramic factories of Souther Spain. Atmos. Res. 96(4), 633–644. doi:10.1016/j.atmosres.2010.02.011

Sanderson, P., Delgado-Saborit, J.M., Harrison, R.M., 2014. A review of chemical and physical characterisation of atmospheric metallic nanoparticles. Atmos. Environ. 94, 353–365. doi:10.1016/j.atmosenv.2014.05.023

Schauer, J.J., Lough, G.C., Shafer, M.M., Christensen, W.F., Arndt, M.F., et al., 2006. Characterization of Metals Emitted from Motor Vehicles. Health Effects Institute.

Sippula, O., Hokkinen, J., Puustinen, H., Yli-Pirilä, P., Jokiniemi, J., 2009. Comparison of particle emissions from small heavy fuel oil and wood-fired boilers. Atmos. Environ. 43(32), 4855–4864. doi:10.1016/j.atmosenv.2009.07.022

Sörme, L., Bergbäck, B., Lohm, U., 2001. Goods in the anthroposphere as a metal emission source a case study of Stockholm, Sweden. Water Air Soil Pollut. Focus 1(3), 213–227. doi:10.1023/A:1017516523915

Spindler, G., Brüggemann, E., Gnauk, T., Grüner, A., Müller, K., et al., 2010. A four-year size-segregated characterization study of particles PM_{10}, $PM_{2.5}$ and PM_1 depending on air mass origin at Melpitz. Atmos. Environ. 44(2), 164–173. doi:10.1016/j.atmosenv.2009.10.015

Stein, A.F., Draxler, R.R, Rolph, G.D., Stunder, B.J.B., Cohen, M.D., et al., 2015. NOAA's HYSPLIT atmospheric transport and dispersion modeling system. Bull. Amer. Meteor. Soc. 96, 2059–2077. doi:10.1175/BAMS-D-14-00110.1

Tao, J., Shen, Z.X., Zhu, C.S., Yue, J.H., Cao, J.J., et al., 2012. Seasonal variations and chemical characteristics of sub-micrometer particles (PM_1) in Guangzhou, China. Atmos. Res. 118, 222–231. doi:10.1016/j.atmosres.2012.06.025

Teixeira, E.C., Feltes, S., Santana, E., 2008. Study of the emissions from moving sources in the metropolitan area of Porto Alegre – RS – Brazil. Quim. Nova 31, 244–248. doi:10.1590/S0100-40422008000200010

Teixeira, E.C., Santana, R.E., Wiegand, F., 2010. 1st Inventory of Air Emissions from Mobile Sources in the State of Rio Grande Do Sul – Base Year: 2009. Fundação Estadual de Proteção Ambiental Henrique Luis Roessler, Porto Alegre (in Portuguese).

Teixeira, E.C., Mattiuzi, C.D.P., Feltes, S., Wiegand, F., Santana, E.R.R., 2012. Estimated atmospheric emissions from biodiesel and characterization of pollutants in the metropolitan area of Porto Alegre–RS. An. Acad. Bras. Ciências 84(3), 245–261. doi:10.1590/S0001-37652012000300008

Teixeira, E.C., Mattiuzi, C.D.P., Agudelo-Castañeda, D., Garcia, K.O., Wiegand, F., 2013. Polycyclic aromatic hydrocarbons study in atmospheric fine and coarse particles using diagnostic ratios and receptor model in urban/industrial region. Environ. Monit. Assess. 185(11), 9587–9602. doi:10.1007/s10661-013-3276-2

USEPA, 1994. Quality Assurance Handbook for Air Pollution Measurement Systems. In: Ambient Air Specific Methods, vol. II. US Environmental Protection Agency; US Government Printing Office, Washington, DC. Section 2,11; EPA/600/R-94/038a.

Vecchi, R., Marcazzan, G., Valli, G., Ceriani, M., Antoniazzi, C., 2004. The role of atmospheric dispersion in the seasonal variation of PM_1 and $PM_{2.5}$ concentration and composition in the urban area of Milan (Italy). Atmos. Environ. 38(27), 4437–4446. doi:10.1016/j.atmosenv.2004.05.029

Vestenius, M., Leppanen, S., Anttila, P., Kyllonen, K., Hatakka, J., et al., 2011. Background concentrations and source apportionment of polycyclic aromatic hydrocarbons in south-eastern Finland. Atmos. Environ. 45(20), 3391–3399. doi:10.1016/j.atmosenv.2011.03.050

Wåhlin, P., Berkowicz, R., Palmgren F., 2006. Characterization of traffic–generated particulate matter in Copenhagen. Atmos. Environ. 40(12), 2151–2159. doi:10.1016/j.atmosenv.2005.11.049

Wang, Y., Zhuang, G.S., Tang, A.H., Yuan, H., Sun, Y.L., et al., 2005. The ion chemistry and the source of $PM_{2.5}$ aerosol in Beijing. Atmos. Environ. 39(21), 3771–3784. doi:10.1016/j.atmosenv.2005.03.013

WHO, 2013. Review of evidence on health aspects of air pollution – REVIHAAP Project. Technical Report. World Health Organization. Available at: http://www.euro.who.int/__data/assets/pdf_file/0004/193108/REVIHAAP-Final-technical-report-final-version.pdf

Widory, D., Liu, X., Dong, S., 2010. Isotopes as tracers of sources of lead and strontium in aerosols (TSP & $PM_{2.5}$) in Beijing. Atmos. Environ. 44(30), 3679–3687. doi:10.1016/j.atmosenv.2010.06.036

Wiseman, C.L.S., Zereini, F., Püttmann, W., 2013. Traffic–related trace element fate and uptake by plants cultivated in roadside soils in Toronto, Canada. Sci. Total Environ. 442, 86–95. doi:10.1016/j.scitotenv.2012.10.051

Wiseman, C.L.S., Zereini, F., 2014. Characterizing metal(loid) solubility in airborne PM_{10}, $PM_{2.5}$ and PM_1 in Frankfurt, Germany using simulated lung fluids. Atmos. Environ. 89, 282–289. doi:10.1016/j.atmosenv.2014.02.055

Witt, M.L.I., Meheran, N., Mather, T.A., de Hoog, J.C.M., Pyle, D.M., 2010. Aerosol trace metals, particle morphology and total gaseous mercury in the atmosphere of Oxford, UK. Atmos. Environ. 44(12), 1524–1538. doi:10.1016/j.atmosenv.2010.01.008

Wu, G., Xu, B., Yao, T., Zhang, C., Gao, S., 2009. Heavy metals in aerosol samples from the Eastern Pamirs collected 2004–2006. Atmos. Res. 93(4), 784–792. doi:10.1016/j.atmosres.2009.03.011

Yoo, J.-I., Seo, Y.-C., Shinagawa, T., 2005. Particle–size distributions and heavy metal partitioning in emission gas from different coal–fired power plants. Environ. Eng. Sci. 22(2), 272–279. doi:10.1089/ees.2005.22.272

Zheng, N., Liu, J.S., Wang, Q.C., Liang, Z.Z., 2010. Health risk assessment of heavy metal exposure to street dust in the zinc smelting district, Northeast of China. Sci. Total Environ. 408(4), 726–733. doi:10.1016/j.scitotenv.2009.10.075

Zhou, S., Yuan, Q., Li, W., Lu, Y., Zhang, Y., Wang, W., 2014. Trace metals in atmospheric fine particles in one industrial urban city: spatial variations, sources, and health implications. J. Environ. Sci. 26(1), 205–213. doi:10.1016/S1001-0742(13)60399-X

5. RESUMO CONGRESSO: Nanoparticles assessment in Sapiranga city, Southern Brazil

SCHNEIDER, I. L.; TEIXEIRA, E. C.; OLIVEIRA, L. F. S.; VARGAS, M. D.; KRECL, P.; GIDHAGEN, L.. Nanoparticles assessment in Sapiranga city, Southern Brazil. Annals of the 10th International Conference on Air Quality - Science and Application, 2016.

6. CONCLUSÕES

O Material Particulado (MP) atmosférico é um dos poluentes mais importantes quando se refere à Qualidade do Ar e caracteriza-se por uma alta variabilidade tanto no que se refere aos níveis observados como na sua composição. O MP está associado a diversos impactos na saúde e, embora o aumento da sua concentração esteja associado a um aumento da mortalidade e morbidade, ainda não é claro quais componentes específicos devem ser diminuídos para minimizar os efeitos sobre a saúde humana. Também é importante destacar que as nanopartículas atmosféricas, especialmente aquelas com um diâmetro <300 nm, podem causar ainda mais efeitos na saúde, tendo em vista que podem penetrar mais profundamente no sistema respiratório humano e desta maneira aumentar os efeitos toxicológicos prejudiciais. Embora estas partículas sejam emitidas principalmente por veículos, certas condições de combustão de biomassa também podem ser uma importante fonte antropogênica.

Desta forma, vale destacar que esta é a primeira vez em que foram avaliadas as concentrações e a distribuição de nanopartículas atmosféricas na Região Metropolitana de Porto Alegre – RMPA, Brasil. Nesta avaliação foram consideradas tanto fontes de emissão veicular, através do estudo em seis locais de amostragem de Porto Alegre (um background urbano, dois locais a beira de estradas, dois cruzamentos, e um *street canyon*), como também foram avaliadas as concentrações oriundas da queima de biomassa em Sapiranga (Brasil).

Nestes estudos verificou que a ordem decrescente de concentrações de nanopartículas é: cruzamentos de tráfego > *street canyon* > beira de estradas > background urbano. Além disso, vale destacar que os níveis observados foram semelhantes aos de alguns países em desenvolvimento, e bastante superiores aos observados na maioria dos países europeus. Estas

maiores concentrações de nanopartículas observadas na RMPA são causadas principalmente pelo alto teor de enxofre no combustível brasileiro e pela idade da frota em circulação.

No que se refere à distribuição de tamanho das nanopartículas atmosféricas, em geral os resultados apontam para uma distribuição trimodal: moda 1 (nucleação) e moda 2 (Aitken), correspondendo a fontes secundárias e resultantes da conversão gás-partícula, especialmente das exaustões veiculares, e moda 3 (acumulação) decorrente de partículas primárias, ou seja, aquelas emitidas diretamente à atmosfera, ou decorrentes do crescimento das partículas menores. Além disso, verificou-se que os parâmetros meteorológicos também apresentam uma grande influência tanto na concentração de nanopartículas como na sua distribuição de tamanho. Também se constatou que alguns poluentes, tais como NOx e CO, apresentaram grande relação com as concentrações de nanopartículas. Isso decorre do fato de que também são indicadores de emissões provenientes de fontes de combustão.

No estudo realizado em Sapiranga (Brasil) observou-se que o centro da cidade apresentou uma concentração média cerca de 3 vezes maior do que o background local, provavelmente devido às emissões veiculares e à combustão de biomassa. O interessante neste estudo foi constatar que maiores concentrações de nanopartículas foram obtidas durante o final de semana do que durante a semana, o que está relacionado principalmente com a contribuição de combustão de biomassa. Este fato foi confirmado pela avaliação da distribuição de nanopartículas, sendo observadas mais partículas com diâmetros maiores.

Também foram realizados estudos onde se buscou caracterizar poluentes orgânicos (nitro-HPAs) e inorgânicos (metais e íons) em MP_1.

A identificação de grupos funcionais orgânicos em MP_1 foi realizada através de medições de emissividade e transmitância utilizando espectroscopia de infravermelho. Para identificar os nitro-HPAs nas amostras de MP_1 foi realizada uma comparação dos espectros de transmitância e emissividade obtidos com os respectivos espectros em padrões certificados sólidos (1-nitropireno, 2-nitrofluoreno e 6-nitrocriseno). Embora os compostos orgânicos em MP atmosférico sejam pouco estudados utilizando a espectroscopia de infravermelho, o presente estudo ratificou que nitro-HPAs podem ser diferenciados por suas impressões digitais espectrais utilizando os dois métodos descritos: espectros de transmitância e emissividade.

Quanto à avaliação de risco em relação à toxicidade dos nitro-HPAs em MP_1, observou-se que o risco carcinogênico é maior do que o risco mutagênico. Além disso, esses riscos foram maiores durante os períodos frios, o que se deve pelas maiores concentrações de nitro-HPAs observadas nestes períodos. Encontrou-se que os riscos carcinogênico e mutagênico para os nitro-HPAs estudados foram associados a cerca de 99% ao 6-nitrocriseno e 85% ao 1-nitropireno, respectivamente. Os resultados também apontam para a possibilidade de impactos negativos sobre a saúde das pessoas expostas na área de estudo.

Em relação ao estudo que avaliou as concentrações de metais e íons em MP_1 vale destacar que uma forte influência antropogênica foi observada. As concentrações médias de MP_1 para Canoas e Sapucaia do Sul foram 12,8 a 15,2 $\mu g/m^3$, respectivamente, correspondendo a níveis semelhantes aos relatados por vários países europeus, mas muito inferiores a aqueles encontrados na China. As principais contribuições dos elementos avaliados foram decorrentes dos poluentes secundários sulfato (SO_4^{2-}) e nitrato (NO_3^-). Elementos-traço, especialmente Cu, Pb, Zn, Cd e Ni também apresentaram importantes contribuições, sendo diretamente relacionados com contribuições antropogênicas. Entre estas, conforme verificado pelo modelo receptor PMF, as principais fontes correspondem ao nitrato e sulfato secundários, às emissões industriais, especialmente de metalurgia, cimento e processos de refino de petróleo, além de combustão de carvão, biomassa e de óleo, bem como queima de combustíveis fósseis. A contribuição crustal foi inferior a 4%, o que pode ser explicado pelo fato de que esta fonte em geral apresenta maiores contribuições em tamanhos de partícula maiores. A avaliação de potenciais contribuições de longo transporte não apontou influências significativas, nem para os níveis de MP_1 como para as concentrações de metais. Desta forma, as concentrações observadas são atribuídas principalmente às contribuições provenientes de fontes locais, conforme já indicado pelo modelo receptor PMF.

Além disso, observou-se que a associação de alguns metais em partículas atmosféricas pode ser devido às emissões provenientes de uma fonte específica ou de diferentes fontes. Alguns metais podem aparecer em diferentes fatores, por exemplo, ou os metais podem ser característicos de um fator com mais de uma fonte de emissão. No entanto, o modelo PMF verificou-se uma ferramenta eficiente para identificar as principais fontes responsáveis pelos elementos-traço observados neste estudo.

Portanto, considerando todos os resultados obtidos através deste trabalho, recomenda-se, no que se refere à contínua avaliação da Qualidade do Ar na RMPA, a continuidade de estudos abordando a avaliação tanto de poluentes orgânicos como inorgânicos em MP. Além disso, além de avaliar os níveis de poluentes associoados ao MP, uma avaliação da influência da Qualidade do Ar em problemas de saúde, especialmente doenças respiratórias, é fortemente recomendada. Para estes estudos, é de extrema importância que os grupos de risco sejam monitorados, especialmente crianças e idosos.

Também se recomenda a continuidade da avaliação de nanopartículas atmosféricas, tendo em vista sua grande influência em problemas de saúde. Estes estudos futuros devem incluir avaliações das variações diárias e sazonais para melhor compreender os mecanismos de formação de nanopartículas, bem como maneiras de minimizar os níveis observados na atmosfera da RMPA.

7. REFERÊNCIAS BIBLIOGRÁFICAS

ABDUL-KHALEK, I.; KITTELSON, D.; BREAR, F. The influence of dilution conditions on diesel exhaust particle size distribution measurements. *Society of Automotive Engineers (SAE),* Technical Paper v. 011142, 1999.

ABU-ALLABAN, M.; GILLIES J.A.; GERTLER A.W.; et al. Tailpipe, resuspended road dust, and brake-wear emission factors from on-road vehicles. *Atmospheric Environment*, v.37, p. 5283-5293, 2003.

ALDABE, J.; ELUSTONDO D.; SANTAMARIA C.; et al. Chemical characterization and source apportionment of PM2.5 and PM10 at rural, urban and traffic sites in Navarra (North of Spain). *Atmospheric Research*, v. 102, p.191-205, 2011.

ALLEN, D. T.; PALEN, E. J.; HAIMOV M. I.; et al. Fourier Transform Infrared Spectroscopy of Aerosol Collected in a Low Pressure Impactor (LPI/FTIR): Method Development and Field Calibration. *Aerosol Science and Technology*, v. 21, n.4, p. 325-342, 1994.

ALLEN, J. O.; MAYO, P .R.; HUGHES, L.S.; et al. Emissions of size-segregated aerosols from on-road vehicles in the caldecott tunnel. *Environmental Science and Technology*, v. 35, p. 4189-4197, 2001.

AMATO, F.; PANDOLFI, M.; ESCRIG, A.; et al. Quantifying road dust resuspension in urban environment by multilinear engine: A comparison with PMF2. *Atmospheric Environment*, v. 43, p. 2770-2780, 2009.

AMATO, F.; NAVA, S.; LUCARELLI, F.; et al. A comprehensive assessment of PM emissions from paved roads: Real-world Emission Factors and intense street cleaning trials. *Science of the Total Environment*, v. 408, p. 4309-4318, 2010.

ANASTASIO, C.; MARTIN S. T. Atmospheric Nanoparticles. *Mineralogical Society of America*, v. 44, p. 293–349, 2001.

APTE, J. S.; KIRCHSTETTER T. W.; REICH A. H.; et al. Concentrations of fine, ultrafine, and black carbon particles in auto-rick shaws in New Delhi, India. *Atmospheric Environment*, v. 45, p. 4470- 4480, 2011.

BAE, M.S.; SCHWAB, J. J.; HOGREFE, O.; et al. Characteristics of size distributions at urban and rural locations in New York. *Atmospheric Chemistry and Physics*, v. 10, p. 4521-4535, 2010.

BETHA, R.; SPRACKLEN, D. V.; BALASUBRAMANIAN, R. Observations of new aerosol particle formation in a tropical urban atmosphere. *Atmospheric Environment*, v. 71, p. 340-351, 2013.

BECKERMAN, B.; JERRETT, M.; BROOK, J. R.; et al, 2008. Correlation of nitrogen dioxide with other traffic pollutants near a major expressway. *Atmospheric Environment*, v. 42, p. 275-290.

BOURCIER L.; SELLEGRI K.; CHAUSSE P.; et al. Seasonal variation of water-soluble inorganic components in aerosol size segregated at the puy de Dôme station (1465 m.a.s.l.), France. *Journal of Atmospheric Chemistry*, v. 69, p. 47-66, 2012.

BRITTER, R. E.; HANNA, S. R. Flow and dispersion in urban areas. Annual Review of Fluid Mechanics, v. 35, p. 469-96, 2003.

BUONANNO, G.; FUOCO, F. C.; MORAWSKA, L.; et al. Airborne particle concentrations at schools measured at different spatial scales. *Atmospheric Environment*, v. 67, p. 38-45, 2013.

BIRMILI, W.; ALLAVIIPPOLA, B.; HINNEBURG, D.; et al. Dispersion of traffic-related exhaust particles near the Berlin urban motorway – estimation of fleet emission factors. *Atmospheric Chemistry and Physics*, v. 9, p. 2355-2374, 2009.

BIRMILI, W.; TOMSCHE, L.; SONNTAG, A. Variability of aerosol particles in the urban atmosphere of Dresden (Germany): Effects of spatial scale and particle size. *Meteorologische Zeitschrift*, v. 22, p. 195-211, 2013.

BUSECK, P.R.; ADACHI K. Nanoparticles in the atmosphere. *Elements*, v. 4, p. 389-394, 2008.

CARRASCO-FLORES E.A.; CAMPOS VALLETTE M.M.; CLAVIJO E.E.C.; et al. SERS spectrum and DFT calculations of 6-nitrochrysene on silver islands. *Vibrational Spectroscopy*, v. 37, p.153-160, 2005.

CHARRON, A.; HARRISON, R.M. Primary particle formation from vehicle emissions during exhaust dilution in the roadside atmosphere. *Atmospheric Environment*, v. 37, p. 4109-4119, 2003.

CHEN, S. C.; TSAI, C. J.; CHOU, C. C.; et al. Ultrafine particles at three different sampling locations in Taiwan. *Atmospheric Environment*, v. 44, p. 533-540, 2010.

CHENG, T.; LU, D.; CHEN, H.; et al. Physical characteristics of dust aerosol over Hunshan Dake Sandland in Northern China. *Atmospheric Environment*, v. 39, p. 1237-1243, 2005.

CHUEINTA, W.; HOPKE, P. K.; PAATERO, P. Investigation of source of atmospheric aerosol at urban and suburban residential areas in Thailand by positive matrix factorization. *Atmospheric Environment*, v. 34, p. 3319-3329, 2000.

COLVILE, R.N.; HUTCHINSON, E. J.; MINDELL, J. S.; et al. The transport sector as a source of air pollution. *Atmospheric Environment*, v. 35, p. 1537-1565, 2001.

COURY, C.; DILLNER, A.M. A method to quantify organic functional groups and inorganic compounds in ambient aerosols using attenuated total reflectance FTIR spectroscopy and multivariate chemometric techniques. *Atmospheric Environment*, v. 42, p. 5923-5932, 2008.

COZIC, J.; VERHEGGEN, B.; WEINGARTNER, E.; et al. Chemical composition of free tropospheric aerosol for PM1 and coarse mode at the high alpine site Jungfraujoch, *Atmospheric Chemistry and Physics*, v. 8, p. 407-423, 2008.

DALL'OSTO, M.; BEDDOWS, D. C. S; PEY, J.; et al. Urban aerosol size distributions over the Mediterranean city of Barcelona, NE Spain. Atmospheric *Chemistry and Physics*, v. 12, p. 10693-10707, 2012.

DALLAROSA, J. B.; MÔNEGO, G. J.; TEIXEIRA, E. C.; et al. Polycyclic aromatic hydrocarbons in atmospheric particles in the Metropolitan Area of Porto Alegre, Brazil. *Atmospheric Environment*, v. 39, p. 1609-1625, 2005a.

DALLAROSA, J. B.; TEIXEIRA, E. C.; MEIRA, L.; et al. Study of the chemical elements and polycyclic aromatic hydrocarbons in atmospheric particles of PM10 and PM2.5 in the urban and rural areas of South Brazil. *Atmospheric Environment*, v. 39, p. 6587-6596, 2005b.

DI FILIPPO, P.; RICCARDI, C.; POMATA, D.; et al. Concentrations of PAHs, and nitro- and methyl- derivatives associated with a size segregated urban aerosol. *Atmospheric Environment*, v. 44, p. 2742-2749, 2010.

DI SABATINO, S.; KASTNER-KLEIN, P.; BERCOWICZ, R.; et al. The Modelling of Turbulence from Traffic in Urban Dispersion Models – Part I: Theoretical Considerations. *Environmental Fluid Mechanics*, v. 3, p. 129-143, 2003.

DONALDSON, K.; TRAN, L.; ALBERT JIMENEZ, L. A.; et al. Combustion-derived nanoparticles: a review of their toxicology following inhalation exposure. *Particle & Fibre Toxicology*, v. 5, n. 6, p. 553-560, 2005.

EASTER, R. C.; PETERS, L. K.. Binary Homogeneus Nucleation: temperature and relative humidity fluctuations, nonlinearity, and aspects of new particle production in the atmosphere. *Journal of Applied Meteorology*, v. 33, p. 775-784, 1994.

FUJITANI, Y.; KUMAR, P.; TAMURA, K.; et. al. Seasonal differences of the atmospheric particle size distribution in a metropolitan area in Japan. *Science of the Total Environment*, v. 437, p. 339-347, 2012.

GRAMOTNEV, G.; RISTOVKI, Z. Experimental investigation of ultra-fine particle size distribution near a busy road. *Atmospheric Environment*, v. 38, p. 1767-1776, 2004.

GRASKOW, B.; KITTELSON, D. B.; ABDUL-KHALEK, I.; et al. Characterization of exhaust particulate emissions from a spark ignition engine. *SAE Paper* No. 980528, p. 155-165, 1998.

GRAMSCH, E.; GIDHAGEN L.; WAHLIN P.; et al. Predominance of soot-mode ultrafine particles in Santiago de Chile: Possible sources. *Atmospheric Environment*, v. 43, p. 2260-2267, 2009.

HAGLER, G. S. W.; BALDAUF, R. W.; THOMA, E. D.; et al. Ultrafine particles near a major roadway in Raleigh, North Carolina: downwind attenuation and correlation with traffic related pollutants. *Atmospheric Environment*, v. 43, p. 1229-1234, 2009.

HARRIS, S. J.; MARICQ, M. M. Signature size distributions for diesel and gasoline engine exhaust particulate matter. *Aerosol Science*, v. 32, p. 749-764, 2001.

HE, M.; DHANIYALA, S. Vertical and horizontal concentration distributions of ultrafine particles near a highway. *Atmospheric Environment*, v. 46, p. 225-236, 2012.

HINDS, W. C. *Aerosol Technology*: Properties, Behavior, and Measurement of Airborne Particles. New York: Wiley, 1999. 504 p.

HOEK, G.; MELIEFSTE, K.; CYRYS, J.; et al. Spatial variability of fine particle concentrations in three European areas. *Atmospheric Environment*, v. 36, p. 4077-4088, 2002.

HORVATH, H. Atmospheric aerosols, atmospheric optics visibility. *Journal of Aerosol Science*, v. 25, p. S23–S24, 1994.

HUSSEIN, T.; HÄMERI, K.; AALTO P.; et al. Modal structure and spatial–temporal variations of urban and suburban aerosols in Helsinki—Finland. *Atmospheric Environment*, v. 39, p. 1655-1668, 2005.

IPCC - Intergovernmental Panel on Climate Change, 2007. *Climate Change 2007: The Physical Science Basic Summary for Policy- makers, Contribution of Working Group I to the Fourth Assessment Report of the Intergovernmental Panel on Climate Change*. Summary for Policymakers. IPCC Secretariat Geneva, Switzerland, p. 1–21.

JAMRISKA, M.; MORAWSKA, L.; MERGERSEN, K. The effect of temperature and humidity on size segregated traffic exhaust particle emissions. *Atmospheric Environment*, v. 42, p. 2369-2382, 2008.

JOHANSSON, C.; NORMAN, M.; GIDHAGEN, L. Spatial & temporal variations of PM10 and particle number concentrations in urban air. *Environmental Monitoring & Assessment*, v; 127, p. 477-487, 2007.

KASTNER-KLEIN, P.; BERKOWICZ, R.; BRITTER, R. The influence of street architecture on flow and dispersion in street canyons. *Meteorology and Atmospheric Physics*, v. 87, p. 121-131, 2004.

KATSOUYANNI, K.; TOULOUMI, G.; SAMOLI, E.; et al. Confounding and effect modification in the short-term effects of ambient particles on total mortality: results from 29 European cities within the APHEA2 project. Epidemiology, v. 12, p. 521-531, 2001.

KEOGH, D. U.; FERREIRA, L.; MORAWSKA, L. Development of a particle number and particle mass vehicle emissions inventory for an urban fleet. *Environmental Modelling and Software*, v. 24, p. 1323-1331, 2009.

KIM, S.; SHEN, S.; SIOUTAS, C.; et al. Size distribution and diurnal and seasonal trends of ultrafine particles in source and receptor sites of the Los Angeles Basin. *Journal of the Air & Waste Management Association*, v. 52, p. 297-307, 2002.

KIM, E.; HOPKE, P. K.; EDGERTON, E. S. Source identification of Atlanta aerosol by positive matrix factorization. *Journal of the Air & Waste Management Association*, v. 53, p. 731-739, 2003.

KITTELSON, D. B. Engines and nanoparticles: a review. *Journal of Aerosol Science*, v. 29, n. 5/6, p. 575-588, 1998.

KITTELSON, D. B.; WATTS W. F.; JOHNSON, J. P. On-road and laboratory evaluation of combustion aerosols — Part 1: Summary of diesel engine results. *Aerosol Science*, v. 37, p. 913-930, 2006a.

KITTELSON, D.B.; WATTS, W.F.; JOHNSON, J.P., et al. On-road and laboratory evaluation of combustion aerosols — Part 2: Summary of spark ignition engine results. *Aerosol Science*, v. 37, p. 931-949, 2006b.

KORHONEN, P.; KULMALA, M.; LAAKSONEN, A.; et. al. Ternary nucleation of H2SO4, NH3, and H2O in the atmosphere. *Journal of Geophysical Research*, v. 104, p. 349-353, 1999.

KOUSOULIDOU, M.; NTZIACHRISTOS, L.; MELLIOS, G.; et al. Road-transport emission projections to 2020 in European urban environments. *Atmospheric Environment*, v. 42, n. 32, p. 7465-7475, 2008.

KRISTENSSON, A.; JOHANSSON, C.; WESTERHOLM, R.; et al. Real-world traffic emission factors of gases and particles measured in a road tunnel in Stockholm, Sweden. *Atmospheric Environment*, v. 38, p. 657-673, 2004.

KULMALA, M.; VEHKAMÄKI, H.; PETÄJÄ, T.; et al. Formation and growth rates of ultrafine atmospheric particles: a review of observations. *Journal of Aerosol Science*, v. 35, p. 143-176, 2004.

KUMAR. P.; FENNELL, P.; BRITTER, R. Effect of wind direction and speed on the dispersion of nucleation and accumulation mode particles in an urban street canyon. *Science of the Total Environment*, v. 402, p. 82-94, 2008a.

KUMAR, P.; FENNELL P.; BRITTER, R. Measurements of particles in the 5–1000 nm range close to road level in an urban street canyon. *Science of the Total Environment*, v. 390, p. 437-447, 2008b.

KUMAR, P.; FENNELL, P. S.; HAYHURST, A. N.; et al. Street versus rooftop level concentrations of fine particles in a Cambridge Street Canyon. *Boundary-Layer Meteorology*, v. 131, p. 13-18, 2009.

KUMAR, P.; ROBINS, A.; VARDOULAKIS, S.; et al. A review of the characteristics of nanoparticles in the urban atmosphere and the prospects for developing regulatory controls. *Atmospheric Environment*, v. 44, p. 5035-5052, 2010.

KUMAR, P.; KETZEL, M.; VARDOULAKIS, S.; et al. Dynamics and dispersion modeling of nanoparticles from road traffic in the urban atmospheric environment – a review. *Journal of Aerosol Science*, v. 42, p. 580-603, 2011.

KUMAR, P.; MORAWSKA, L.; BIRMILI, W.; et al. Ultrafine particles in cities. *Environment International*, v. 66, p. 1-10, 2014.

LINGARD, J. J. N.; AGUS, E. L.; YOUNG, D. T.; et al. Observations of urban airborne particle number concentrations during rush-hour conditions: analysis of the number based size distributions and modal parameters. *Jornal of Environment Monitoring*, v. 8, p. 1203-1218, 2006.

LI, X. L.; WANG, J. S.; TU, X. D.; et al. Vertical variations of particle number concentration and size distribution in a street canyon in Shanghai, China. *Science of the Total Environment*, v. 378, p. 306-316, 2007.

MARSHALL, T. L.; CHAFFIN, C. T.; HAMMAKER, R. M.; et al. An introduction to open-path FT-IR. *Atmospheric monitoring. Environmental Science &* Technology, v. 28, p. 224A-232A, 1994.

MATHIS, U.; MOHR, M.; ZENOBI, R. Effect of organic compounds on nanoparticle formation in diluted diesel exhaust. *Atmospheric Chemistry and Physics*, v. 4, p. 609-620, 2004.

MEJÍA, J. F.; MORAWSKA, L.; MENGERSEN, K. Spatial variation in particle number size distributions in a large metropolitan area. *Atmospheric Chemistry and Physics*, v. 8, p. 1127-1138, 2008.

METROPLAN. Fundação Estadual de Planejamento Metropolitano e Regional. 2012. Evolução da população na RMPA. Disponível em <http://www.metroplan.rs.gov.br/mapas_estatisticas/ au_rmpa.htm>.

MOHR, M.; LEHMANN, U. Comparison Study of Particle Measurement Systems for Future Type Approval Application, Swiss Contribution to GRPE Particulate Measurement Program (GRPE-PMP CH5*). EMPA Report* No. 202779, 2003.

MORAWSKA, L.; THOMAS, S.; BOFINGER, N.; et al. Comprehensive characterization of aerosols in a subtropical urban atmosphere: Particle size distribution and correlation with gaseous pollutants. *Atmospheric Environment*, v. 32, p. 2467-2478, 1998.

MORAWSKA, L.; RISTOVSKI, Z.; JAYARATNE, E. R.; et al. Ambient nano and ultrafine particles from motor vehicle emissions: Characteristics, ambient processing and implications on human exposure. *Atmospheric Environment*, v. 42, p. 8113-8138, 2008.

MURR, L. E.; GARZA, K. M. Natural and anthropogenic environmental nanoparticulates: their microstructural characterization and respiratory health implications. *Atmospheric Environment,* v. 43, p. 2683-2692, 2009.

NAVARTA, M. D. F.; OJEDA, C. B.; ROJAS, F. S. Aplicación de la Espectroscopia del Infrarrojo Medio. *Química Analítica de Procesos*, v. 2, 93-103, 2008.

NTZIACHRISTOS, L.; NING, Z.; GELLER, M. D. et al. Fine, ultrafine and nanoparticle trace element compositions near a major freeway with a high heavy-duty diesel fraction. *Atmospheric Environment* v. 41, p. 5684-5696, 2007.

ONCHOKE, K. K.; PARKS, M. Experimental and theoretical study of vibrational spectra of 3-nitrofluoranthene. *Journal of Molecular Structure*, v. 999, p. 22–28, 2011.

PAATERO, P. Least square formulation of robust non-negative factor analysis. *Chemometrics and Intelligent Laboratory Systems*, v. 37, p. 23-35, 1997.

PAATERO, P.; AALTO, P.; PICCIOTTO, S.; et al. Estimating time series of aerosol particle number concentrations in the five HEAPSS cities on the basis of measured air pollution and meteorological variables. *Atmospheric Environment* v. 39, p. 2261-2273, 2005.

PEKKANEN, J.; PETERS, A.; HOEK, G.; et al. Particulate air pollution and risk of ST segment depression during repeated submaximal exercise tests among subjects with coronary heart disease: The exposure and risk assessment for fine and ultrafine particles in ambient air (ULTRA) study. *Circulation*, v. 106, n. 8, p. 933-938, 2002.

PETERS, A.; DOCKERY, D. W.; MULLER, J. E.; et al. Increased particulate air pollution and the triggering of myocardial infarction. *Circulation* v. 103, p. 2810-2815, 2001.

PEY, J.; RODRÍGUEZ, S.; QUEROL, X.; et al. Variations of urban aerosols in the western Mediterranean. *Atmospheric Environment*, v. 42, p. 9052-9062, 2008.

PIRJOLA, L.; PAASONEN, P.; PFEIFFER, D.; et al. Dispersion of particles and trace gases nearby a city highway: Mobile laboratory measurements in Finland. *Atmospheric Environment*, v. 40, p. 867-879, 2006.

POPE, C. A.; BURNETT, R. T.; THUN, M. J.; et al. Lung cancer, cardiopulmonary mortality and long-term exposure to fine particulate air pollution. *The Journal of American Medical Association.* v. 287, p. 1132-1141, 2002.

PUTAUD, J. P.; VAN, D. R.; ALASTUEY, A.; et al. A European aerosol phenomenology 3: Physical and chemical characteristics of particulate matter from 60 rural, urban, and kerbside sites across Europe. *Atmospheric Environment*, v. 44, p. 1308-1320, 2010.

QUEROL, X.; VIANA, M.; ALASTUEY, A.; et al. Source origin of trace elements in PM from regional background, urban and industrial sites of Spain. *Atmospheric Environment,* v. 41, p. 7219-7231, 2007.

REPONEN, T.; GRINSHPUN, S. A.; TRAKUMAS, S.; et al. Concentration gradient patterns of aerosol particles near interstate highways in the Greater Cincinnati airshed. *Journal of Environmental Monitoring*, v. 5, p. 557-562, 2003

RICHARD, A.; GIANINI, M. F. D.; MOHR, C. et al. Source apportionment of size and time resolved trace elements and organic aerosols from an urban courtyard site in Switzerland. *Atmospheric Chemistry and Physics*, v. 11, p. 8945-8963, 2011.

RISTOVSKI, Z. D.; JAYARATNE, E. R.; LIM, M.; et al. Influence of Diesel Fuel Sulfur on Nanoparticle Emissions from City Buses. *Environmental Science & Technology*, v. 40, p. 1314-1320, 2006.

ROSENBOHM, E.; VOGT, R.; SCHEER, V.; et al. Particulate size distributions and mass measured at a motorway during the BAB II campaign. *Atmospheric Environment*, v. 39, p. 5696-5709, 2005.

RUUSKANEN, J.; TUCH, T.; BRINK, H. T.; et al. Concentrations of ultrafine, fine and PM2.5 particles in three European cities. *Atmospheric Environment*, v. 35, p. 3729-3738, 2001.

SABALIAUSKAS, K.; JEONG, C. H.; YAO, X.; et al., 2012. Five-year roadside measurements of ultrafine particles in a major Canadian city. *Atmospheric Environment*,v. 49, p. 245-256.

SAKURAI, H.; TOBIAS, H. J.; PARK, K.; et al. On-line measurements of diesel nanoparticle compositionand volatility. *Atmospheric Environment*, v. 37, p. 1199-1210, 2003.

SEINFELD, J. H.; PANDIS, S. N. *Atmospheric chemistry and physics*: from air pollution to climate change. New York: Wiley, John & Sons, Incorporated, 2006. 1203 p.

SHI, J. P.; KHAN, A. A.; HARRISON, R. M. Measurements of ultrafine particle concentration and size distribution in the urban atmosphere. *Science of the Total Environment*, v. 235, p. 51-64, 1999.

SHI, J. P.; EVANS, D. E.; KHAN, A. A.; et al. Sources and concentration of nanoparticles (10 nm diameter) in the urban atmosphere. *Atmospheric Environment*, v. 35, p. 1193-1202, 2001.

SIENRA, M.; ROSAZZA, N.; PRÉNDEZ, M. Polycyclic aromatic hydrocarbons and their molecular diagnostic ratios in urban atmospheric respirable particulate matter. *Atmospheric Research*, v. 75, p. 267-281, 2005.

SOLAZZO, E.; VARDOULAKIS, S.; CAI, X. Evaluation of traffic-producing turbulence schemes within Operational Street Pollution Models using roadside measurements. *Atmospheric Environment*, v. 41, p. 5357-5370, 2007.

STRAWA, A. W.; KIRCHSTETTER, T. W.; HALLAR, A. G.; et al. Optical and physical properties of primary on-road vehicle particle emissions and their implications for climate change. *Journal of Aerosol Science*, v. 41, p. 36-50, 2010.

STURM, P. J.; BALTENSPERGER, U.; BACHER, M.; et al. Road side measurements of particulate matter size distribution. *Atmospheric Environment*, v. 37, p. 5273-5281, 2003.

TEIXEIRA, E. C.; FELTES, S.; SANTANA, E. R. Estudo das emissões de fontes móveis na Região Metropolitana de Porto Alegre, Rio Grande do Sul. *Química Nova*, v. 31, n. 2, p. 244-248, 2008.

TEIXEIRA, E. C.; GARCIA, K. O.; MEINCKE, L.; et al. Study of nitro-polycyclic aromatic hydrocarbons in fine and coarse Atmospheric particles. *Atmospheric Research*, v. 101, p. 631-639, 2011.

TEIXEIRA, E. C.; MATTIUZI, C. D. P.; FELTES, S.; et al. Estimated atmospheric emissions from biodiesel and characterization of pollutants in the Metropolitan Area of Porto Alegre-RS. *Anais da Academia Brasileira de Ciências*, v. 84, n. 3, 245-261, 2012.

TSANG, H.; KWOK, R.; MIGUEL, A. H. Pedestrian exposure to ultrafine particles in Hong Kong under heavy traffic conditions. *Aerosol and Air Quality Research*, v. 8, p. 19-27, 2008.

USEPA - United States Environmental Protection Agency. 2002. *Health Assessment Document for Diesel Engine Exhaust*. Disponível em: http://cfpub.epa.gov/ncea/cfm/recordisplay.cfm?deid¼29060.

VACHON, G.; LOUKA, P.; ROSANT, J. M.; et al. Measurements of traffic-induced turbulence within a street canyon during the NANTES'99 experiment. *Water, Air, and Soil Pollution: Focus*, v. 2, p. 127-140, 2002.

VECCHI, R.; CHIARI, M.; D'ALESSANDRO, A.; et al. A mass closure and PMF source apportionment study on the sub-micron sized aerosol fraction at urban sites in Italy. *Atmospheric Environment*, v. 42, p. 2240-2253, 2008.

WAHLIN, P.; PALMGREN, F.; VAN DINGENEN, R.; et al. Experimental studies of ultrafine particles in streets and the relationship of traffic. *Atmospheric Environment*, v. 35, p. S63–S69, 2001.

WANG, G.; WANG, H.; YU, Y.; et al. Chemical characterization of water-soluble components of PM10 and PM2.5 atmospheric aerosols in five locations of Nanjing, China. *Atmospheric Environment*, v. 37, p. 2893-2903, 2003.

WANG, Y.; ZHU, Y.; SALINAS, R., et al. Roadside measurements of ultrafine particles at a busy urban intersection. *Air and Waste Management Association*, v. 58, p. 1449-1457, 2008.

WEHNER, B.; WIEDENSOHLER, A.; TUCH, T. M.; et al. Variability of the aerosol number size distribution in Beijing, China: New particle formation, dust storms, and high continental background. *Geophysical Research Letters*, v. 31, L22108, 2004.

WEHNER, B.; UHRNER, U.; VON LOWIS, S.; et al. Aerosol number size distributions within the exhaust plume of a diesel and a gasoline passenger car under on-road conditions and determination of emission factors. *Atmospheric Environment*, v. 43, p. 1235-1245, 2009.

WESTERDAHL, D.; FRUIN, S.; SAX, T.. Mobile platform measurements of ultrafine particles and associated pollutant concentrations on freeways and residential streets in Los Angeles. *Atmospheric Environment*, v. 39, p. 3597-3610, 2005

YIN, J.; HARRISON, R. M. Pragmatic mass closure study for PM1, PM2.5 and PM10 at roadside, urban background and rural sites. *Atmospheric Environment*, v. 42, p. 980-988, 2008.

YOUNG, L.; WANG, Y.; HSU, H.; et al. Spatiotemporal variability of submicrometer particle number size distributions in an air quality management district. *Science of the Total Environment*, v. 425, p. 135-145, 2012.

YU, J.; FLAGAN, R. C.; SEINFELD, J. H. Identification of products containing –COOH, -OH, and –C=O in atmospheric oxidation of hydrocarbons. *Environmental Science & Technology*, v. 32, n. 16, p. 2357-2370, 1998.

ZHU, Y.; HINDS, W. C.; KIM, S.; et al. Study of ultrafine particles near a major highway with heavy-duty diesel traffic. *Atmospheric Environment*, v. 36, p. 4323-4335, 2002.

ZHU, Y.; HINDS, W. C.; SHEN, S.; et al. Seasonal trends of concentration and size distribution of ultrafine particles near major highways in Los Angeles Special Issue of Aerosol Science and Technology on Findings from the Fine Particulate Matter Supersites Program. *Aerosol Science and Technology*, v. 38, p. 5-13, 2004.

8. ANEXOS:

8.1. Artigos completos publicados em periódicos como co-autor

- AGUDELO-CASTAÑEDA, D. M.; TEIXEIRA, E. C.; SCHNEIDER, I. L.; PEREIRA, F. N.; OLIVEIRA, M. L.S.; TAFFAREL, S. R.; SEHN, J. L.; RAMOS, C. G.; SILVA, L. F. O.. Potential utilization for the evaluation of particulate and gaseous pollutants at an urban site near a major highway. Science of the Total Environment, 543, 161-170, 2016.

Works of particle number and mass concentration variability have a great importance since they may indicate better the influence of vehicle emissions in an urban region. Moreover, the importance of this work lies in the fact that there are few studies in Brazil, where the fuel used has unique characteristics. Consequently, this paper presents measurements of particle number (size range 0.3-10μm), particle mass (PM_{10}, $PM_{2.5}$, PM_1), O_3 and NO_x (NO, NO_2), in a site near a major highway at the Metropolitan Area of Porto Alegre, south Brazil. Measurements were carried out during two years: 2012 and 2013. Particle number and mass concentrations were measured using an optical counter with a PM_{10} analyzer. Results showed that concentrations of $N_{0.3\text{-}1}$ (0.3-1μm) were the highest, although similar to $N_{1\text{-}2.5}$ (1-2.5μm). Daily variability of the analyzed pollutants followed the traffic pattern. Moreover, NO_2, O_3, and particle number were higher during the day, whereas NO, NO_x, and particle matter showed higher concentrations during nighttime. Traffic influence was evidenced by the mean concentrations of weekends and weekdays, being higher for the latter. Correlation of particles and gases with meteorological variables, together with the application of PCA confirmed the influence of vehicle exhaust discharges.

- AGUDELO-CASTAÑEDA, D. M.; TEIXEIRA, E. C.; SCHNEIDER, I. L.; ROLIM, S. B. A.; BALZARETTI, N.; SILVA, G. S.. Comparison of Emissivity, Transmittance, and Reflectance Infrared Spectra of Polycyclic Aromatic Hydrocarbons with those of Atmospheric Particulates (PM_1). Aerosol and Air Quality Research, 15, 1627-1639, 2015.

Polycyclic Aromatic Hydrocarbons (PAHs) are a group of various complex organic compounds composed of carbon and hydrogen, and two or more condensed benzene rings. They are released into the atmosphere by the incomplete combustion or pyrolysis of organic matter. Some of the major sources of PAHs are burning of coal, wood, oil or gas, vehicle

engines exhaust, and open burning. PAHs are of great concern to human health mainly because of their known carcinogenic and mutagenic properties. Consequently, it is very important to study atmospheric PAHs, especially those associated with ultrafine particles. This study aims to identify the spectral features of PAHs in samples of particulate matter < 1 μm (PM_1) using infrared spectrometry. Emissivity and transmittance spectra of PAHs were obtained by infrared spectroscopy. PAHs standards spectra contributed to effectively identify PAHs in PM_1 samples. Emissivity and transmittance spectra in the range of 680–900 cm^{-1} exhibited the largest number of bands due to C–C out-of-plane angular deformations and C–H out-of-plane angular deformations. Bands of medium intensity in 2900–3050 cm^{-1} region were also observed due to C–H stretching typical of aromatic compounds, although with lower intensity. This study compared the emissivity and transmittance spectra acquired using two different infrared spectrometers in order to identify PAHs in samples of atmospheric particulate matter and analyzed the capability and advantages of each of the infrared spectrometers. In addition, it was confirmed that the PAHs under study can be distinguished by their infrared spectral fingerprints.

8.2. Trabalhos publicados em anais de eventos (resumo)

- AGUDELO-CASTAÑEDA, D. M.; TEIXEIRA, E. C.; SCHNEIDER, I. L.; NORTE, F. P.. A two-year study on urban particle number (0.3-10 μm) and mass concentrations (<10 μm): levels in time and weekly variation. Annals of the 10th International Conference on Air Quality - Science and Application, 2016.

This work presents measurements of particle number (size range 0.3-10 μm) and particle mass (PM_{10}, $PM_{2.5}$, PM_1), in a site near a major highway at the Metropolitan Area of Porto Alegre, south Brazil. Measurements were carried out during two years: 2012 and 2013. Particle number and mass concentrations were measured using an optical counter with a PM_{10} analyzer. Results showed that concentrations of $N_{0.3\text{-}1}$ (0.3-1 μm) were the highest, although similar to $N_{1\text{-}2.5}$ (1-2.5 μm). Daily variability of the analyzed pollutants followed the traffic pattern. Moreover, particle number was higher during the day, whereas particle matter showed higher concentrations during nighttime. Traffic influence was evidenced by the mean concentrations of weekends and weekdays, being higher for the latter.

- SILVA, G. S.; AGUDELO-CASTAÑEDA, D. M.; SCHNEIDER, I. L.; TEIXEIRA, E. C.. Análises de espectros de transmitância na região do infravermelho de amostras de MP_1 e padrões de HPAS. Anais da XI Jornada de Iniciação Científica FZB/FEPAM, 2015.

Os Hidrocarbonetos Policíclicos Aromáticos (HPAs) constituem uma ampla classe de compostos orgânicos. Na atmosfera, eles são emitidos, principalmente, a partir da combustão de combustíveis fósseis, queima florestal ou de madeira e queima de resíduos. Devido as suas conhecidas propriedades carcinogênicas e mutagênicas é necessário realizar o monitoramento e controle desses compostos na natureza. Neste estudo foram obtidos espectros de transmitância na região do infravermelho de quatro padrões de HPAs (Pireno, Fluoranteno, Benzo[*a*]Pireno, Benzo[*a*]Antraceno) e posteriormente estes compostos foram identificados em amostras de material particulado atmosférico < 1μm (MP_1) através da análise dos seus espectros.Os espectros de transmitância foram obtidos em um aparelho BOMEM MB-series FTIR-Hartmann&BraunMichelson equipado com um detector DTGS. Foram utilizados padrões sólidos Sigma-Aldrich com 99% de pureza. A amostragem de MP_1 presentes no ar foi realizada através do amostrador automático sequencial de partículas modelo PM162M construído pela Environnement S.A. utilizando uma vazão volumétrica de 1.0 $m^3 \cdot h^{-1}$. As amostras de MP_1 foram coletadas em filtros de PTFE (politetrafluoretileno) marca Zefluor™ membrane, específicos para amostragem de orgânicos de 47 mm de diâmetro.A identificação das vibrações moleculares foi realizada através de comparação com estudos já publicados. Foram observados nos espectros de transmitância das amostras de MP, coletados em Canoas, a presença de diversos picos correspondentes às vibrações dos anéis aromáticos, os quais também foram identificados nos espectros dos padrões de HPAs. Nos espectros de transmitância das amostras de MP foram observados picos de forte intensidade na região de 1250-1300 cm^{-1} devido à influência do filtro (PTFE), portanto, feições de compostos nesta frequência não puderam ser identificadas sem ambiguidade. A maior parte da intensidade dos picos observados nos espectros de transmitância das amostras de MP_1 foi fraca possivelmente pelas baixas concentrações destes compostos orgânicos, especialmente HPAs, na ordem de ng/m^3.Os resultados obtidos com os espectros de transmitância foram consistentes com os estudos prévios de HPAs. Análises por transmitância na região do infravermelho são técnicas úteis para a análise de amostras de material particulado de uma maneira simples. Os resultados de padrões permitirão contribuir de forma mais embasada na identificação dos HPAs em material particulado atmosférico.

- FEISTAUER, H.; SCHNEIDER, I. L.; TEIXEIRA, E. C.. Estudo de nanopartículas em Canoas, Região Metropolitana de Porto Alegre. Anais da XI Jornada de Iniciação Científica FZB/FEPAM, 2015.

As nanopartículas com diâmetro ≤300nm possuem como principal fonte a queima de combustível fóssil, especialmente fontes móveis. Estas partículas acarretam diversos problemas de saúde, pois elas possuem a capacidade de se depositaremnos pulmões, especialmente nos alvéolos e bronquíolos, assim maximizando os efeitos adversos. No presente trabalhofoi determinada a concentração em número e a distribuição de tamanho das nanopartículas entre 6 e 225 nm, na cidade de Canoas, RS. A amostragem e a determinação de nanopartículas foi realizada utilizando o classificador de partículas SMPS modelo 3936 (TSI Inc.). O período de amostragem foi entre dezembro de 2014 e janeiro de 2015. Neste período também foram consideradas as concentrações de O_3 e NO_x (NO + NO_2) e variáveis meteorológicas. Os resultados mostraram que a concentração média de nanopartículas durante o período de estudo foi de 1.32 ±1.18 x 10^4 partículas/cm³. A variação diária apontou concentraçõesmáximasem dois períodos: durante o rush, entre 6h e 9h e entre 17h e 20h, e em alguns dias, às 12h, decorrente a processos de nucleação fotoquímica.Durante este processofoi observado que a distribuição de tamanho das partículas apresentou uma moda centrada em 10 nm,se deslocando até 40nm indicandoum crescimento das partículas. Os dados também apresentaram nos períodos relativos à influência do tráfego uma distribuição trimodal, com modas centradas em 5 nm, entre 15-20 nm e entre 100-110 nm. As correlações entre as concentrações médias de nanopartículas, de gases e as variáveis meteorológicas mostraram que radiação (+0.24) e O_3 (+0.20) influenciaram as partículas <30 nm, formadas principalmente através dos eventos de nucleação fotoquímica. NOx e NO_2 apresentaram maiores correlações com partículas entre 30 e 100 nm e >100 nm, respectivamente. A velocidade do vento influenciou apenas as partículas >30 nm (-0.24) indicando que a concentração aumentou com a diminuição da velocidade. A direção do vento indicou que as maiores concentrações foram observadas quando o local de amostragem recebia influência da BR-116. Estes sãoresultadospreliminares de um estudo que continua em andamento.

- LAWALL, V.; SCHNEIDER, I. L.; TEIXEIRA, E. C.. Avaliação da concentração em número e da distribuição de tamanho de nanopartículas em Porto Alegre. Anais da XI Jornada de Iniciação Científica FZB/FEPAM, 2015.

As nanopartículas constituem um importante poluente para a qualidade do ar. Essas partículas, especialmente as <300 nm, possuem uma concentração em número que corresponde a mais de 99% da concentração total presente na atmosfera. Em um ambiente urbano, geralmente as emissões veiculares apresentam uma predominância em relação às outras fontes. Este trabalho avalia o número e a distribuição de tamanho das nanopartículas em dois locais de Porto Alegre. Além disso, as concentrações obtidas são correlacionadas com parâmetros meteorológicos e com o fluxo de veículos. Os locais de amostragem selecionados foram: 1 - cruzamento entre as avenidas Farrapos e Sertório, e 2 - Av. Borges de Medeiros. O equipamento utilizado para amostragem foi o NanoScan modelo 3910 (TSI Inc.), que considera partículas entre 10 e 420 nm. As amostragens foram realizadas por 7 dias no local 1 e 6 dias no local 2, ao longo de 2014. Para cada local de amostragem, foram calculadas médias horárias do número e de distribuição de partículas. As concentrações médias horárias em número de partículas foram: $1.51 \pm 0.68 \times 10^5$ e $1.00 \pm 0.39 \times 10^5$, respectivamente para os locais 1 e 2. Para a distribuição de partículas, os locais 1 e 2 apresentaram contribuições similares nos modos: nucleação, Aitken e acumulação. Ambos os locais apresentam uma distribuição de tamanho trimodal, com o local 1 apresentando modas centradas em 14.1, 31.0 e 103 nm, e o local 2 em 13.9, 32.1 e 104 nm. Essa distribuição é típica de emissões veiculares, já que os veículos a diesel emitem preferencialmente partículas com diâmetro entre 20 e 120 nm e os movidos a gasolina entre 20 e 60 nm. Para o local 1, as correlações foram significativas entre as concentrações de nanopartículas e temperatura (-0.74), umidade (0.83), radiação (-0.77), velocidade (-0.69) e direção do vento (-0.54). Isso indica um aumento no número de partículas com a diminuição da temperatura, da radiação, e da velocidade do vento. Para o local 2, não foram observadas correlações significativas indicando a forte influência da arquitetura local. As concentrações de nanopartículas observadas no presente estudo são elevadas quando comparadas aos níveis de boa parte dos países europeus. Mais estudos serão desenvolvidos para melhor compreender a influência dos parâmetros meteorológicos e da variação sazonal.

- SCHNEIDER, I. L., TEIXEIRA, E. C., NORTE, F. P., AGUDELO-CASTANEDA, D. M., OLIVEIRA, L. F. S. Nanoparticles number concentration and size distribution near a highway in South Brazil In: 9th International Conference on Air Quality – Science and Application, 2014, Garmisch-Partenkirchen. Annals of the 9th International Conference on Air Quality – Science and Application, 2014.

The aim of this study was to evaluate the nanoparticles number concentration and size distribution at the BR-116 highway roadside, one of the main roads of south Brazil. SMPS was used to obtain the particles number concentrations (PNC) with sizes between 10 and 420 nm, with average concentration of $1.33 \times 10^5 \pm 0.84 \times 10^5$ particles/cm³. Correlation between PNC and NO_x ($NO + NO_2$) occurred because they have similar sources, that is vehicular emissions. Moreover, a negative correlation with ozone was obtained, indicating their contribution to the particles formation, especially in the Aitken and accumulation modes. The influence of engine exhaust may be also noted in the particle size distribution with modes at 13.9, 28.3 and 110.4 nm, typical for diesel and petrol engines. 1-h average data showed the highest PNC concentrations at 9 a.m.

- MASETTO, J. M., OLIVEIRA, L. F. S., SCHNEIDER, I. L., TEIXEIRA, E. C. Avaliação da concentração em número e distribuição de nanopartículas em Canoas, Região Metropolitana de Porto Alegre (RMPA). Anais da X Jornada de Iniciação Científica FZB/FEPAM, 2014.

O crescente aumento de veículos tem causado uma grande preocupação com a qualidade do ar, especialmente quanto à emissão de nanopartículas. Estas partículas, especialmente as com tamanho <300 nm, correspondem a 99% da concentração em número de partículas e podem causar diversos efeitos nocivos à saúde. Podem ser subdivididas conforme seu tamanho em diferentes modos: nucleação (<25 nm), Aitken (25 a 100 nm) e acumulação (100 a 1000 nm). O objetivo deste estudo é avaliar a concentração e a distribuição do número de nanopartículas em Canoas, na RMPA, junto a BR-116, local sob influência veicular. Na RMPA há cerca de 2 milhões de veículos (14% diesel e 86% gasolina) e um fluxo diário de aproximadamente 150 mil veículos na BR-116. Foram avaliadas as nanopartículas de 10 a 420 nm entre 8 e 10 de outubro de 2013 em Canoas (6 m do solo e a 70 m da BR-116), utilizando o classificador de partículas SMPS modelo 3910, da TSI Inc.

Também foram consideradas as concentrações de NO_x (NO + NO_2) e O_3, medidas por analisadores de quimiluminescência e radiação UV, respectivamente, além das variáveis meteorológicas (velocidade e direção do vento, umidade, radiação e temperatura). A concentração total média para o período avaliado foi de 5.21 ±2.21 x 10^4 cm^{-3}, atingindo uma concentração máxima de 17.3 x 10^4 cm^{-3} às 6:00 h, explicado pelo rush da manhã. Obteve-se uma distribuição trimodal com as modas definidas em 13.6 nm (nucleação), 33 nm (Aitken) e 110 nm (acumulação). A análise estatística mostrou que a concentração total de nanopartículas apresentou uma correlação significativa com NO e NO_x de 0.44 e 0.47, respectivamente, desta forma, confirmando a mesma origem, as fontes móveis. Para avaliar o efeito da temperatura sobre a concentração total foram estabelecidas correlações para o período de dia e noite, com médias de 21.9 e 16.6 ºC, respectivamente. Durante o dia, observa-se uma correlação negativa (-0.24), indicando que maiores temperaturas correspondem a menores concentrações de nanopartículas. Já durante o período noturno, com menores temperaturas, se observa um efeito contrário (correlação de 0.45). A concentração total não apresentou correlações significativas com os demais parâmetros. A direção do vento predominante foi de 100º, indicando que o local de amostragem estava à jusante da BR-116. É importante destacar que este é um estudo preliminar nesta região e para uma melhor compreensão dos resultados é necessária uma avaliação durante um período maior.

- SCHILD, L. B., SCHNEIDER, I. L., TEIXEIRA, E. C. Concentração em número e distribuição de tamanho de nanopartículas atmosféricas em Porto Alegre In: X Jornada de Iniciação Científica FZB/FEPAM, 2014, Porto Alegre. Anais da X Jornada de Iniciação Científica FZB/FEPAM, 2014.

Um dos grandes problemas da qualidade do ar em áreas urbanas é a alta concentração de partículas atmosféricas, especialmente as nanopartículas de tamanho <300 nm. Estas nanopartículas provêm, em sua maioria, de atividades antropogênicas, principalmente veículos automotores e estão relacionadas com questões de saúde, como doenças respiratórias. As nanopartículas são subdivididas conforme o seu tamanho em modo nucleação (<25 nm), modo Aitken (25 a 100 nm) e modo acumulação (100 a 1000 nm). Este trabalho visa avaliar a concentração em número e distribuição de tamanho das nanopartículas atmosféricas em dois locais de Porto Alegre: 1 - Parque Jardim Botânico (background) e 2 - cruzamento entre as

avenidas Assis Brasil e Sertório (alto fluxo de veículos). As amostragens foram realizadas pela manhã com o *Scanning Mobility Particle Sizer* (SMPS) modelo 3910 da TSI Inc. por três dias, para cada local, em janeiro de 2014. As concentrações de nanopartículas foram relacionadas com parâmetros meteorológicos (temperatura, umidade, radiação, velocidade e direção do vento) e com fluxo de veículos. As concentrações médias encontradas para o local 1 e 2 foram de $2.96 \pm 0.95 \times 10^4$ cm^{-3} e $14.6 \pm 6.3 \times 10^4$ cm^{-3}. Para este local foram encontradas correlações significativas para a velocidade do vento (-0.52), temperatura (-0.32) e radiação (-0.62). Isso indica que quanto maior a velocidade do vento, maior será a dispersão das partículas, reduzindo a concentração. A resultante da direção do vento foi 79º. As correlações também apontam uma diminuição do número de partículas com o aumento de temperatura e radiação. Como não houve grande variação do fluxo de veículos nesta área, não foi verificada correlação entre a concentração total e o número de veículos. O fluxo médio foi de 99 veículos/minuto, sendo composto por 15% de veículos a diesel, 76% a gasolina e 9% de motocicletas. Para o local 1, não foram observadas correlações significativas com nenhum dos parâmetros meteorológicos considerados, mas foi verificada a mesma tendência quanto à influência da temperatura. Este estudo é uma avaliação preliminar da concentração de nanopartículas em Porto Alegre e estudos futuros são necessários para analisar os padrões sazonais nesta região.

- SILVA, G. S., SCHNEIDER, I. L., AGUDELO-CASTANEDA, D. M., TEIXEIRA, E. C. Identificação em padrões sólidos de HPA's por espectroscopia no infravermelho In: X Jornada de Iniciação Científica FZB/FEPAM, 2014, Porto Alegre. Anais da X Jornada de Iniciação Científica FZB/FEPAM, 2014.

Os HPAs são um grupo de diversos compostos orgânicos complexos, constituídos por carbono e hidrogênio junto com dois ou mais anéis benzênicos condensados. Na atmosfera eles são emitidos a partir da combustão incompleta ou pirólise do material orgânico. Dentre as fontes de emissão de HPA's estão, principalmente, a combustão de combustíveis fósseis, queima florestal ou de madeira e queima de resíduos. Os HPAs são de grande preocupação à saúde humana, principalmente devido as suas conhecidas propriedades carcinogênicas e mutagênicas. Sendo assim, fazer o monitoramento da presença desses compostos no meio ambiente é de extrema importância. O objetivo do trabalho foi estudar os diferentes padrões

sólidos de HPA's para identificação de feições espectrais características aplicando espectrometria de infravermelho. Foram realizadas análises de espectros de transmitância de Pireno, Fluoranteno, Benzo[a]Pireno e Benzo[a]Antraceno, obtidos através da espectroscopia no infravermelho. Os padrões foram preparados em pastilhas de KBr. Os espectros de transmitância foram obtidos em espectrômetro BOMEM MB-series FTIR-Hartmann & Braun Michelson equipado com detector DTGS, com uma resolução de 4 cm^{-1}. A faixa espectral medida foi de 350 até 4000 cm^{-1}. A identificação das vibrações moleculares dos espectros foi realizada através da comparação com trabalhos científicos previamente publicados. Os resultados mostram que o maior número de bandas de fortes intensidades ocorre na região espectral de 680-900 cm^{-1}, devido às deformações angulares CC fora do plano e deformações angulares CH fora do plano. Bandas na região espectral de 900-2000 cm^{-1} foram observadas, porém, com menor intensidade. Na região de 3000-3050 cm^{-1}, também foram observadas bandas, devido ao estiramento CH, característico de compostos aromáticos. Os resultados obtidos com os espectros de transmitância foram consistentes com os estudos prévios de HPA's. Este estudo confirma que esses HPA's podem ser diferenciados pelas suas assinaturas espectrais no infravermelho. Os resultados de padrões permitirão contribuir de forma mais embasada na identificação dos HPAs em material particulado atmosférico.

- CAMPANA, H. A., SCHNEIDER, I. L., TEIXEIRA, E. C. Identificação de HPAs e NHPAs em MP_1 por espectroscopia de infravermelho. Anais da IX Jornada de Iniciação Científica – Meio Ambiente FZB/FEPAM, 2013.

A queima incompleta de combustíveis fósseis, principalmente do diesel e da gasolina, libera na atmosfera gases, vapores e material particulado. Entre os compostos liberados estão os Hidrocarbonetos Policíclicos Aromáticos (HPA´s) e os Nitro Hidrocarbonetos Policíclicos Aromáticos (NHPA´s), os quais podem estar adsorvidos nas partículas ultrafinas presentes na atmosfera. Este material particulado (MP), com diâmetro <1μm, representa um potencial dano à saúde humana, já que atinge os alvéolos pulmonares, maximizando, assim, problemas respiratórios. O presente trabalho teve por objetivo identificar HPAs e NHPAs, através de espectroscopia de infravermelho, em amostras de MP 1 μm coletadas na Região Metropolitana de Porto Alegre (RMPA). Para tal, foi elaborado um banco de dados a partir de trabalhos científicos publicados, na forma de tabela, apontando a localização das vibrações das ligações químicas dos diferentes compostos considerados neste estudo. A espectroscopia

vibracional mede diferentes tipos de vibrações entre átomos de acordo com a alteração que suas ligações interatômicas sofrem ao serem expostas a radiação infravermelha. Destas vibrações destacam-se as provenientes de estiramentos e torções. Os espectros vibracionais de transmitância e emissividade das amostras foram obtidos na faixa do infravermelho, de 3 a 16 μm, com um espectrômetro de infravermelho com transformada de Fourier. Os resultados foram expressos na forma de gráficos comprimento de onda versus percentual de transmitância ou emissividade. Os espectros gerados foram comparados com o banco de dados elaborado e os HPAs e NHPAs de interesse foram identificados nas amostras analisadas. Destacam-se as vibrações características de CH_4 em 3.40 μm, de CO_2 em 4.25 μm e de H_2O em 4.43 μm. Picos múltiplos de fraca a média intensidade, provenientes do estiramento das ligações C-H dos anéis aromáticos ocorrem na região entre 5.6 a 7.2 μm. Também foram observadas as vibrações de estiramento C-C e de inclinação fora do eixo C-H na região entre 9 e 13 μm. As vibrações decorrentes de estiramento NO_2 ocorrem entre 6.4 e 7.6 μm. Os resultados também apontaram influência da temperatura da amostra sobre a resposta espectral de emissividade.

8.3. Trabalhos publicados em anais de eventos (resumo expandido)

- AGUDELO-CASTAÑEDA, D. M.; TEIXEIRA, E. C.; SCHNEIDER, I. L.. Assessing environmental carcinogenic risk for polycyclic aromatic hydrocarbons in $PM_{1.0}$, $PM_{2.5}$ and $PM_{2.5-10}$ at an urban area at South Brazil. International Journal of Chemical and Environmental Engineering, 2016.

Particulate matter (PM) is considered as one of the major pollutants that affect the health of humans, especially for the fine and ultrafine fraction, which can adsorb greater concentrations of toxic compounds, e.g., polycyclic aromatic hydrocarbons (PAHs). PAHs are a group of several complex organic compounds consisting of carbon and hydrogen, and two or more condensed benzene rings and represent one of the most stable families of organic compounds known. The known carcinogens isomers are primarily associated with particulate material and, usually, the highest concentrations are in the respirable fraction <5 μm. High PAHs levels in ambient air of large metropolitan areas are usually associated with vehicular emissions, including diesel and gasoline vehicles. Particle-bound PAHs in the fine and ultrafine fraction present a higher risk because they can deposit in the respiratory tract, hence

aggravating the potentially negative health effects. In addition, some PAHs are possibly or probably carcinogenic to humans (benzo[a]anthracene, benzo[b]fluoranthene, benzo[k] fluoranthene, benzo[a]pyrene, dibenzo[a,h] anthracene, and indeno[1,2,3-cd]pyrene). Thus, there is considerable concern about the relationship between PAHs exposure in the ambient air and the potential to contribute to human cancer incidence. The objective of this study was to conduct an assessment of carcinogenic and mutagenic risks of the studied PAHs in the $PM_{1.0}$, $PM_{2.5}$ and $PM_{2.5-10}$ samples. The toxic equivalent factors were calculated to characterize more accurately the risk of cancer from PAH exposure in the PM samples. This was based on the contribution of the carcinogenic potency of benzo[a]pyrene. The ambient concentrations of 12 PAHs, beginning from fluorene, and their toxic equivalence factor (TEF) were used in the calculation. The carcinogenic risk for five carcinogenic PAHs (Chr, BaA, BaP, Ind, and DahA) in the $PM_{2.5}$ and $PM_{2.5–10}$ fractions ranged from 44.9% to 56.8%, of DahA ranged from 35.12% to 44.63%, and of Ind ranged from 5.24% to 6.65% of the total carcinogenic activity in the study area. For $PM_{1.0}$ fraction, BaP and DahA dominated the BaP_{eq} levels. The carcinogenicity activity contribution of BaP was in the range of 27.1% (Canoas summer) up to 44.0% (Sapucaia winter); and the contribution of DahA was of 22.7% (Sapucaia winter) up to 45.3% (Canoas summer). The contribution of Ind for the BaPeq levels was of 15.0% (Sapucaia summer) up to 17.8% (Sapucaia winter). Since 2006 to 2013, the highest BaP_{eq} levels were observed in winter in the study, and there has not been an increase in the contribution in the BaP_{eq} levels of potentially carcinogenic PAHs, except for Ind. The recent established air quality limit of the European Parliament, the scientific publication of the IARC and the carcinogenic risk demonstrate the importance that these pollutants require maximum reduction and their study. These results may help the environmental agency and government to have tools to control PAHs in ambient air.

- MASETTO, J. M., OLIVEIRA, L. F. S., SCHNEIDER, I. L., TEIXEIRA, E. C. Avaliação da concentração em número e distribuição de tamanho de nanopartículas em Canoas, Brasil. Anais do 1° International Symposium: Environmental Toxicity, 2014. p.106 – 110

Concentrações em número e distribuição de tamanho de partículas atmosféricas entre 10 e 420 nm foram estudadas no município de Canoas, sul do Brasil. Este município

apresenta influência do tráfego da rodovia BR-116. O presente estudo foi realizado de 8 a 10 de outubro de 2013, utilizando o classificador de partículas SMPS modelo 3910, da TSI Inc. Os gases NO_x (NO + NO_2) e O_3, e as variáveis meteorológicas (velocidade e direção do vento, umidade, radiação e temperatura) foram também consideradas. Os resultados parciais mostraram que a concentração total média para o período avaliado foi de 5.21 ±2.21 x 10^4 partículas/cm^3, atingindo uma concentração máxima de 17.3 x 10^4 partículas/cm^3 às 6 h. Nestes resultados foram observados uma distribuição tri modal, com modas centradas em 13.6, 33.0 e 110 nm. A análise estatística revelou que a concentração total de nanopartículas apresentou uma correlação significativa com NO, NO_2 e NO_x, desta forma, confirmando a mesma origem, as fontes móveis. A temperatura apresentou correlação negativa com a concentração total de nanopartículas durante o dia e durante a noite a correlação foi contrária, ou seja, positiva. Os demais parâmetros considerados, não apresentaram correlações significativas. A resultante da direção do vento foi de 100º, indicando que o local de amostragem considerado estava à jusante da BR-116, ou seja, sob influência das emissões veiculares.

- SCHILD, L. B., SCHNEIDER, I. L., TEIXEIRA, E. C. Concentração em número e distribuição de tamanho de nanopartículas atmosféricas em Porto Alegre. Anais do 1° International Symposium: Environmental Toxicity, 2014. p.137 – 141

No presente estudo foram determinadas a concentração em número e a distribuição de tamanho das nanopartículas atmosféricas (10-420 nm) em dois locais de Porto Alegre: local 1 - Parque Jardim Botânico (background) e local 2 - cruzamento entre as avenidas Assis Brasil e Sertório (alto fluxo veicular). O estudo foi realizado em janeiro de 2014, utilizando o classificador de partículas SMPS modelo 3910, da TSI Inc., e as concentrações foram relacionadas com parâmetros meteorológicos e com o fluxo de veículos. As concentrações médias encontradas para os locais1 e 2 foram de 2.96 ±0.95 x10^4 #/cm^3 e 14.6 ±6.3 x10^4 #/cm^3, respectivamente. O local 2 apresentou correlações significativas entre a concentração de nanopartículas e a velocidade do vento (-0.52), temperatura (-0.32) e radiação (-0.62). Como não houve grande variação do fluxo de veículos nesta área (média de 99 veículos/min), não foi verificada correlação entre a concentração total e o número de veículos. Para o local 1,

não foram observadas correlações significativas com nenhum dos parâmetros meteorológicos considerados.

- SILVA, G. S., SCHNEIDER, I. L., AGUDELO-CASTANEDA, D. M., TEIXEIRA, E. C. Identificação de HPAs em amostras de $MP_{1.0}$ por espectroscopia no infravermelho. Anais do 1° International Symposium: Environmental Toxicity, 2014. p.69 – 72

Os Hidrocarbonetos Policíclicos Aromáticos (HPAs) são um grupo de diversos compostos orgânicos complexos e são de grande preocupação à saúde humana, devido as suas conhecidas propriedades carcinogênicas e mutagênicas. Na atmosfera eles são emitidos a partir da combustão incompleta ou pirólise do material orgânico. Sendo assim, fazer o monitoramento da presença desses compostos no meio ambiente é de extrema importância. Neste estudo foram identificadas as feições espectrais características dos HPAs, através de análises de padrões, e posteriormente estes compostos foram identificados em amostras de $MP_{1.0}$ utilizando espectrometria no infravermelho. Este estudo confirma que esses HPAs (Pireno, Benzo[a]Pireno, Fluoranteo e Benzo[a]Antraceno) podem ser diferenciados pelas suas assinaturas espectrais no infravermelho.